

mgr inż. Aleksandra Majewska

**Rola PTEN w hipoksyjnym mikrośrodowisku
raka nerki i czerniaka**

**Rozprawa na stopień doktora nauk medycznych i nauk o zdrowiu
w dyscyplinie nauki medyczne**

Promotor: prof. dr hab. Claudine Kieda

Promotor pomocniczy: dr Klaudia Brodaczewska

Laboratorium Onkologii Molekularnej i Terapii Innowacyjnych
Wojskowy Instytut Medyczny – Państwowy Instytut Badawczy



Obrona rozprawy doktorskiej przed Radą Dyscypliny Nauk Medycznych

Warszawskiego Uniwersytetu Medycznego

Warszawa, 2023

Słowa kluczowe: angiogeneza, czerniak, hipoksja, mikroRNA, PTEN, rak nerki,

Key words: angiogenesis, hypoxia, kidney cancer, melanoma, microRNA, PTEN

Badania realizowane w ramach rozprawy doktorskiej były częścią projektów badawczych finansowanych przez:

- Narodowe Centrum Nauki, grant OPUS 12, numer: 2016/23/B/NZ1/03211; kierownik projektu: prof. dr hab. Claudine Kieda,
- Narodowe Centrum Nauki, grant Preludium 19, numer: 2020/37/N/NZ5/04024; kierownik projektu: mgr inż. Aleksandra Majewska,
- Ministerstwo Edukacji i Nauki, projekt statutowy Wojskowego Instytutu Medycznego – Państwowego Instytutu Badawczego, numer: 1/8974 (519); kierownik projektu: dr Klaudia Brodaczewska.

Pragnę złożyć serdeczne podziękowania:

*prof. dr hab. Claudine Kieda za zaangażowanie, profesjonalizm i cenne wskazówki
w realizacji pracy naukowej.*

*dr Klaudii Brodaczewskiej za nieocenioną pomoc merytoryczną, wsparcie
i nieustającą wiarę w moje możliwości.*

*Dziękuję wszystkim Pracownikom
Laboratorium Onkologii Molekularnej i Terapii Innowacyjnych
Wojskowego Instytutu Medycznego – Państwowego Instytutu Badawczego,
za pomoc i rodzinną atmosferę.*

Wykaz prac stanowiących rozprawę doktorską:

- **Majewska, A.** Brodaczevska K, Filipiak-Duliban A, Kieda C. Comparative analysis of the effect of hypoxia in two different tumor cell models shows the differential involvement of PTEN control of proangiogenic pathways. *Biochem Cell Biol.* 2023 Jul 17. doi: 10.1139/bcb-2023-0047. Epub ahead of print. PMID: 37459649.
IF: 2.9
MEiN: 70
- Brodaczevska, K.*, **Majewska A.***, Filipiak-Duliban A, Kieda C. Pten knockout affects drug resistance differently in melanoma and kidney cancer. *Pharmacol Rep.* 2023 Oct;75(5):1187-1199. doi: 10.1007/s43440-023-00523-y. Epub 2023 Sep 6. PMID: 37673853; PMCID: PMC10539195
* These authors contributed equally to this work
IF: 4.4
MEiN: 140
- **Majewska, A.** Brodaczevska K, Filipiak-Duliban A, Kajdasz A, Kieda C. miRNA Pattern in Hypoxic Microenvironment of Kidney Cancer-Role of PTEN. *Biomolecules.* 2022 May 11;12(5):686. doi: 10.3390/biom12050686. PMID: 35625614; PMCID: PMC9138332.
IF: 5.5
MEiN: 100

Sumaryczny IF: 12.8

Sumaryczny MEiN: 310

SPIS TREŚCI

Wykaz skrótów	11
Streszczenie	13
Abstract	15
1 Wstęp.....	17
1.1 Mikrośrodowisko guza	17
1.1.1 Hipoksja	18
1.1.2 Unaczynienie w nowotworach.....	20
1.1.3 Terapie celujące w angiogenezę guza	23
1.1.4 Trispirofosforan mio-inozytolu ITPP.....	25
1.2 PTEN	26
1.2.1 Struktura PTEN	26
1.2.2 Regulacja ekspresji i aktywności PTEN	26
1.2.3 Molekularne funkcje PTEN.....	27
1.2.4 Znaczenie kliniczne PTEN	29
1.3 MikroRNA	31
1.3.1 Definicja, biogeneza, funkcja	31
1.3.2 Ekspresja miRNA w nowotworach.....	32
1.3.3 Sygnatura miRNA w hipoksji.....	34
1.3.4 miRNA w regulacji ekspresji PTEN.....	35
2 Cel i założenia pracy	36
3 Kopie opublikowanych prac	38
3.1 Publikacja 1.....	38
3.2 Publikacja 2.....	53
3.3 Publikacja 3.....	72
4 Podsumowania i wnioski.....	98
5 Opinia komisji etycznej.....	100
6 Oświadczenia Współautorów.....	102
7 Dorobek naukowy	112
8 Referencje.....	114

WYKAZ SKRÓTÓW

3D	Trójwymiarowy	Three-dimensional
AGO	-	Argonaute
AKT / PKB	Kinaza białkowa B	Protein kinase B
ANG	Angiopoetyna	Angiopoietin
BAD	-	Bcl-2 associated agonist of cell death
Bcl-2	-	B-cell leukemia/lymphoma 2
BRAF	-	V-Raf murine sarcoma viral oncogene homolog B1
CCL	-	C-C motif chemokine ligand
COSMIC	Katalog mutacji somatycznych w nowotworach	Catalogue of somatic mutations in cancer
CSCs	Nowotworowe komórki macierzyste	Cancer stem cells
DALY	Lata życia skorygowane niesprawnością	Disability adjusted life-years
DGCR8	-	DiGeorge syndrome critical region 8
ECs	Komórki śródbłónka	Endothelial cells
ECM	Macierz zewnątrzkomórkowa	Extracellular matrix
EMT	Przejście epithelialno-mezenchymalne / Przejście nabłonkowo-mezenchymalne	Epithelial-mesenchymal transition
EPCs	Progenitory komórek śródbłónka	Endothelial progenitor cells
EVs	Pęcherzyki zewnątrzkomórkowe	Extracellular vesicles
FAK	Ogniskowa kinaza adhezyjna	Focal adhesion kinase
FDA	Agencja Żywności i Leków	Food and Drug Administration
FGF	Czynnik wzrostu fibroblastów	Fibroblast growth factor
HIFs	Czynniki indukowane niedotlenieniem	Hypoxia inducible factors
HRE	Element odpowiedzi na niedotlenienie	Hypoxia response element
IL	Interleukina	Interleukin
ITPP	Trispirofosforan mio-inozytolu	Myo-inositol trispyrophosphate
MDM2	-	Murine double minute 2
MMP	Metaloproteinaza macierzy	Matrix metalloproteinase
MREs	Miejsca odpowiedzi na miRNA	MiRNA response elements
mTOR	Ssaczy cel rapamycyny	Mammalian target of rapamycin

mRNA	Informacyjny RNA	Messenger RNA
miRNA miR	MikroRNA	MicroRNA
NF-κB	-	Nuclear factor kappa-light-chain-enhancer of activated B cells
NK	Komórki naturalnej cytotoxyczości	Natural killer cells
NH₂	Grupa aminowa	Amino group
NSCLC	Niedrobnokomórkowy rak płuca	Non-small-cell lung cancer
PAI-1	Inhibitor aktywatora plazminogenu	Plasminogen activator inhibitor
PBD	Domena wiążąca PIP2	PIP2 binding domain
PD	Domena fosfatazy	Phosphatase domain
PDGF	Płytkowy czynnik wzrostu	Platelet derived growth factor
PDGFR	Receptor płytkowego czynnika wzrostu	Platelet derived growth factor receptor
PD-L1	Ligand receptora programowej śmierci 1	Programmed death ligand 1
PDCD4	Gen programowanej śmierci komórki 4	Programmed cell death 4
PHD2	Białko zawierające domenę hydroksylazy proliowej 2	Prolyl hydroxylase domain-containing protein 2
PHTS	Zespół guzów hamartomatycznych związanych z mutacjami PTEN	PTEN hamartoma tumor syndromes
PIP2	-	Phosphatidylinositol-3, 4, 5-triphosphate
PIP3	-	Phosphatidylinositol 4, 5-triphosphate
PIGF	Łożyskowy czynnik wzrostu	Placenta growth factor
PTEN		Phosphatase and tensin homolog
Pre-miRNA	Pekursorowe miRNA	Precursor miRNA
Pri-miRNA	Pierwotne miRNA	Primary miRNA
RISC	-	RNA-induced silencing complex
SDF-1	Czynnik 1 pochodzący z komórek zrębu	Stromal cell-derived factor 1
TKI	Inhibitory kinaz tyrozynowych	Tyrosine kinase inhibitors
TME	Mikrośrodowisko guza	Tumor microenvironment
TNF-α	Czynnik martwicy nowotworów alfa	Tumor necrosis factor alpha
VEGF	Czynnik wzrostu śródbłonna naczyniowego	Vascular endothelial growth factor
VEGFR	Receptor czynnika wzrostu śródbłonna naczyniowego	Vascular endothelial growth factor receptor
VHL	-	von Hippel-Lindau

STRESZCZENIE

Zrozumienie mechanizmów molekularnych, związanych z progresją nowotworów i kompleksowe podejście do całości mikrośrodowiska guza (TME, ang. *tumor microenvironment*), ma kluczowe znaczenie w poszukiwaniu skutecznych terapii przeciwnowotworowych. Jedną z krytycznych cech TME guzów litych jest niedotlenienie – niski, niefizjologiczny poziom tlenu (hipoksja). Hipoksja jest głównym czynnikiem powodującym patologiczne unaczynienie w guzach, a nieprawidłowości naczyń mają istotny wpływ na progresję choroby i determinują skuteczność leczenia. Normalizacja naczyń, za pośrednictwem allosterycznego efektora hemoglobiny – ITPP (ang. *myo-inositol trispyrophosphate*), wydaje się obiecującym podejściem terapeutycznym, co wykazano m.in. w modelu czerniaka. Oprócz kompensacji niedotlenienia ITPP może również aktywować supresor nowotworu PTEN (ang. *phosphatase and tensin homolog*). PTEN pełni istotne funkcje w wielu procesach biologicznych m.in. proliferacji czy metabolizmie komórek. Mutacje *PTEN* lub utrata jego funkcji są obserwowane w wielu typach nowotworów. Celem niniejszej pracy było sprawdzenie skuteczności działania ITPP w mysim modelu raka nerki i określenie roli PTEN w hipoksyjnym mikrośrodowisku guzów.

Badania przeprowadzono z wykorzystaniem mysich modeli nowotworów: raka nerki (Renca) i czerniaka (B16 F10). *In vivo* zbadano skuteczność stosowania ITPP w raku nerki – jednak nie wykazano pozytywnych efektów terapii, obserwowanych wcześniej w modelu czerniaka. Wykonano zatem szereg doświadczeń mających na celu określenie roli PTEN w obu modelach cechujących się odmienną odpowiedzią na leczenie ITPP. Eksperymenty miały na celu zbadanie aktywności i funkcji PTEN w komórkach nowotworowych w warunkach niedotlenienia z uwzględnieniem jego wpływu na proces angiogenezy (*in vitro*). Dodatkowo z zastosowaniem edycji genomu metodą CRISPR/Cas9 uzyskano mysie linie komórkowe czerniaka i raka nerki z nokautem *Pten*, co pozwoliło bezpośrednio określić rolę PTEN zarówno w progresji guzów (*in vivo, in vitro*), jak i w odpowiedzi na standardowe leki przeciwnowotworowe (*in vitro*). Ponadto w modelu raka nerki, z wykorzystaniem sekwencjonowania nowej generacji (NGS, ang. *next generation sequencing*), określono wpływ hipoksji i mutacji *Pten* na zmiany ekspresji miRNA (*in vivo, in vitro*).

Zarówno w czerniaku jak i raku nerki wykazano zależny od hipoksji spadek poziomu PTEN i dominację fosforylowanej formy (pPTEN). Tylko w komórkach Renca w niedotlenieniu obserwowano równocześnie zmiany aktywności ścieżki p53/MDM2 przy braku akumulacji pAKT. Z kolei w modelu czerniaka spadek poziomu PTEN skutkował klasyczną aktywacją PI3K/AKT. Jednocześnie, hipoksja silnie stymulowała wydzielanie czynników pro-angiogennych w modelu raka nerki, co skutkowało zmianami aktywności i funkcji komórek śródbłonna. Badania prowadzone z wykorzystaniem ustalonych linii komórkowych z nokautem *Pten* nie wykazały istotnego wpływu dysfunkcji PTEN na wzrost guzów (*in vivo*) i proliferację komórek (*in vitro*). Badane modele różniły się jednak opornością na cisplatynę. Komórki Renca z nokautem *Pten* (*Pten/KO*) cechowała większa oporność na leczenie niż komórki *Pten/WT*. Z kolei w modelu czerniaka komórki B16 F10 *Pten/KO* były bardziej wrażliwe na leczenie cisplatyną niż komórki *Pten/WT*. Obserwowane różnice mogą wynikać z odmiennych efektów nokaut *Pten* m. in. na ekspresję p53 i wydzielanie PAI-1 (ang. *plasminogen activator inhibitor 1*) w obu testowanych modelach. Co więcej, w komórkach Renca nokaut *Pten* powodował zmiany poziomu markerów charakterystycznych dla przejścia nabłonkowo-mezenchymalnego (EMT, ang. *epithelial to mesenchymal transition*). W modelu raka nerki obserwowano również istotny wpływ hipoksji i nokautu *Pten* na zmiany ekspresji miRNA. Głównym miRNA ulegającym zwiększonej ekspresji w hipoksji był miR-210, natomiast wzrost ekspresji miR-221 może być związany ze spadkiem poziomu PTEN w hipoksji. Wśród miRNA ulegających destabilizacji w modelach mutacji *Pten* wyróżnia się onkomir miR-155 oraz miR-100.

Podsumowując niedotlenienie jest istotnym czynnikiem regulującym aktywność PTEN w czerniaku i raku nerki, jednak funkcja PTEN istotnie różni w obu badanych modelach. Różnice te mogą odgrywać kluczową rolę w odpowiedzi komórek na standardowe terapie przeciwnowotworowe, a wraz z różnicami potencjału proangiogennego mogą determinować odpowiedź związaną z normalizacją naczyń za pośrednictwem ITPP. Deregulacja PTEN może również istotnie modyfikować mikrośrodowisko guza poprzez zmiany ekspresji miRNA.

ABSTRACT

The role of PTEN in the hypoxic microenvironment of kidney cancer and melanoma

Understanding the molecular mechanisms involved in cancer progression and a comprehensive approach taking into account the entire tumor microenvironment (TME) is crucial for the search of effective anticancer treatment. One of the critical features of the TME of solid tumors is hypoxia - low, non-physiological oxygen tension. Hypoxia is the main factor causing pathological angiogenesis in tumors. Vessels abnormalities have a significant impact on cancer progression and determine the effectiveness of treatment. Normalization of vessels via the allosteric effector of hemoglobin – ITPP (myo-inositol trispyrophosphate), seems to be a promising therapeutic approach, as demonstrated, among others, in a melanoma model. In addition to compensation of tumor hypoxia, ITPP can also activate the tumor suppressor PTEN (phosphatase and tensin homolog). PTEN plays an important role in different cellular processes, including cell proliferation and metabolism. PTEN mutations or loss of PTEN function are observed in many types of cancer. The aim of this study was to verify the effectiveness of ITPP treatment in a murine model of kidney cancer and to determine the role of PTEN in the hypoxic tumor microenvironment.

Experiments were performed using murine models of kidney cancer (Renca) and melanoma (B16 F10). The effectiveness of ITPP in kidney cancer was tested *in vivo* – however, the positive effects of therapy, previously observed in melanoma, were not demonstrated. Therefore, research was conducted to determine the role of PTEN in both models characterized by a different response to ITPP treatment. The experiments aimed to assess the activity and function of PTEN in cancer cells in hypoxia, taking into account their effect on angiogenesis (*in vitro*). Additionally, using CRISPR/Cas9 mediated genome editing, murine melanoma and kidney cancer cell lines with *Pten* knockout were established, which allowed direct determination of the role of PTEN in tumor progression (*in vivo*, *in vitro*), as well as in response to standard anticancer treatment (*in vitro*). Moreover, in a kidney cancer model, the impact of hypoxia and *Pten* mutations on changes in miRNA expression were determined (by next-generation sequencing, NGS), *in vivo* and *in vitro*.

Both in melanoma and kidney cancer cells we observed hypoxia-dependent decrease in PTEN levels and a domination of the phosphorylated form (pPTEN). However, only in Renca hypoxia caused changes in p53/MDM2 pathway in the absence of pAKT accumulation, while in melanoma, a decrease in PTEN levels resulted in classic PI3K/AKT activation. Hypoxia also strongly stimulated the secretion of pro-angiogenic factors in the kidney cancer model, which resulted in changes in the activity and function of endothelial cells. Experiments performed using established *Pten* knockout cell lines showed no significant impact of PTEN dysfunction on tumor growth (*in vivo*) and cell proliferation (*in vitro*). However, both tested models showed different resistance to cisplatin treatment. Renca cells with *Pten* knockout (*Pten/KO*) were more resistant to treatment than *Pten/WT* cells. In turn, B16 F10 *Pten/KO* cells were more sensitive to cisplatin than *Pten/WT* cells. The observed differences may be related to the different effects of *Pten* knockdown on p53 expression and PAI-1 secretion in both tested models. Moreover, in Renca cells, *Pten* knockdown caused changes in the levels of markers characteristic for epithelial to mesenchymal transition (EMT). In kidney cancer model, a significant effect of hypoxia and *Pten* knockout on changes in miRNA expression were also observed. The main miRNA upregulated by hypoxia was miR-210, while the increase in miR-221 expression may be associated with hypoxia-dependent decrease of PTEN level. Among the miRNAs destabilized in *Pten* mutant cells, the oncomir miR-155 and miR-100 were upregulated.

To conclude, hypoxia is an important factor regulating PTEN activity in melanoma and renal cell carcinoma, but the outcome of PTEN modulation differs significantly in both tested models. These differences may play a key role in the response of cancer cells to standard anticancer treatment, and together with differences in pro-angiogenic potential, they may determine the ITPP-dependent vessels normalization. Deregulation of PTEN may also significantly modify the tumor microenvironment through changes in miRNA expression.

1 WSTĘP

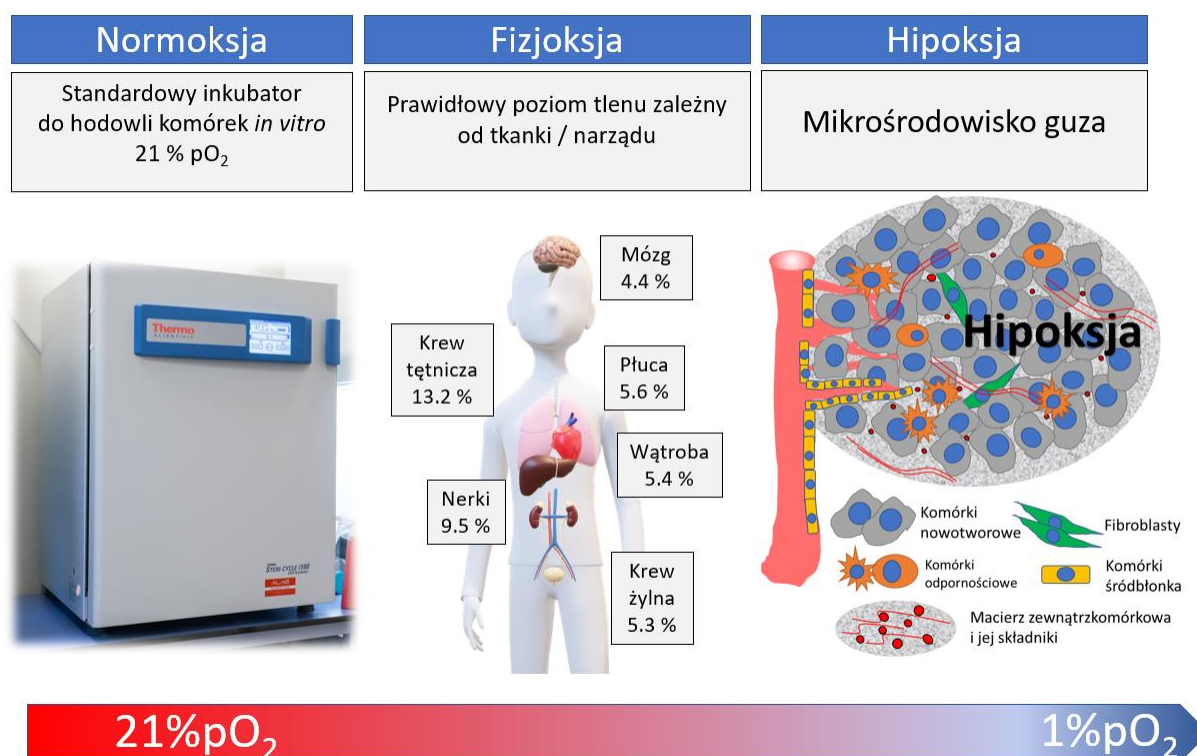
Nowotwory stanowią poważny problem zdrowotny społeczeństwa na całym świecie. W 2019 roku na świecie odnotowano 23,6 mln nowych przypadków oraz 10 mln zgonów spowodowanych nowotworami [1]. W tej samej analizie wykazano, że wskaźnik DALY („lata życia skorygowane niesprawnością”, ang. *disability adjusted life-years*) wyrażający łącznie lata życia utracone wskutek przedwczesnej śmierci bądź uszczerbku na zdrowiu; dla nowotworów wynosi 250 milionów lat [1], co również stanowi istotny problem społeczny. Prezentowane dane wskazują tendencję wzrostową w porównaniu z rokiem 2010, a prognozy zakładają, że ten trend utrzyma się przez kolejne 20 lat [2]. W świetle tych perspektyw niezbędne są intensywne badania mające na celu rozwój profilaktyki, diagnostyki i terapii przeciwnowotworowej.

1.1 MIKROŚRODOWISKO GUZA

Zrozumienie mechanizmów molekularnych związanych z progresją nowotworów jest kluczowe dla poszukiwania nowych celów terapii przeciwnowotworowej. Kompleksowe badania patofizjologii nowotworów skupiają się nie tylko na komórkach nowotworowych, ale również całym mikrośrodowisku guza (TME, ang. *tumor microenvironment*). Wśród komponentów komórkowych, oprócz komórek nowotworowych w TME wyróżnia się głównie: komórki śródbłonna (ECs, ang. *endothelial cells*), komórki układu odpornościowego oraz fibroblasty [3]. W TME znajduje się macierz zewnątrzkomórkowa (ECM, ang. *extracellular matrix*) czyli sieć makrocząsteczek, które zapewniają wsparcie strukturalne i biochemiczne otaczającym ją komórkom. W ECM obecne są m.in.: kolageny, lamininy, elastyny i włókna elastyczne, glikoproteiny i proteoglikany; jednak zarówno skład, jak i funkcja ECM w nowotworach istotnie różni się od macierzy w prawidłowych tkankach [4, 5]. Komunikację między składnikami mikrośrodowiska guza zapewniają cząsteczki sygnałowe (cytokiny, chemokiny, czynniki wzrostu) oraz pęcherzyki zewnątrzkomórkowe [6]. Do krytycznych cech TME zalicza się również fizykochemiczne właściwości: niskie pH, wysokie ciśnienie śródmiąższowe oraz niedotlenienie [7]. Interakcje pomiędzy wszystkimi elementami i cechami fizykochemicznymi TME wpływają na progresję choroby, a także determinują skuteczność leczenia. Kluczowe szlaki sygnałowe w TME mogą stanowić cel terapeutyczny, co daje duże nadzieje na skuteczne, celowane terapie przeciwnowotworowe.

1.1.1 Hipoksja

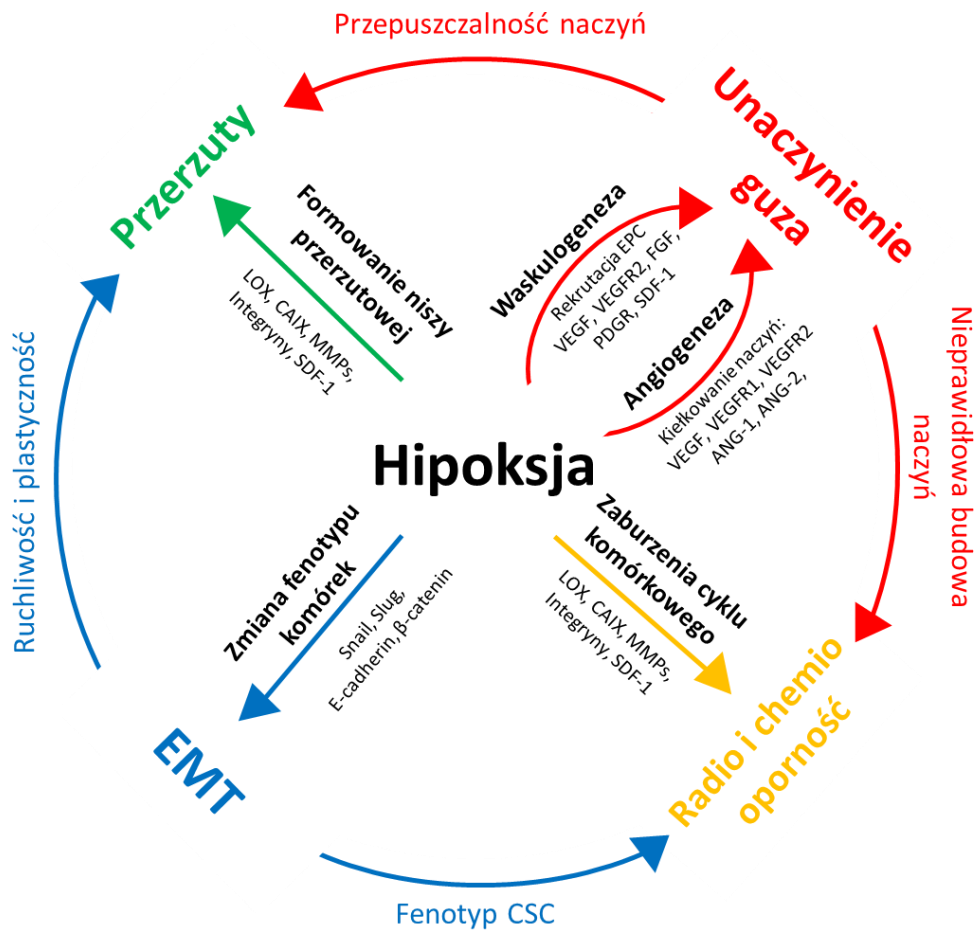
Niedotlenienie (hipoksja) – niskie, niefizjologiczne ciśnienie parcjalne tlenu jest charakterystycznym zjawiskiem występującym w wielu guzach litych. Intensywnie proliferujące komórki nowotworowe powodują rozrost guza i zwiększają odległość od istniejących naczyń krwionośnych, co ogranicza dyfuzję tlenu i prowadzi do hipoksji. Przyjmuje się, że poziom tlenu w niedotlenionych tkankach nowotworu wynosi ok. 1 % pO_2 , jednak może różnić się pomiędzy heterogennymi obszarami guza [8]. Warto podkreślić, że fizjologiczne (występujące w zdrowych tkankach) ciśnienie parcjalne tlenu (fizjoksja) różni się między tkankami czy narządami [9, 10] i jest przeważnie niższe niż wykorzystywany standardowo w badaniach *in vitro*, atmosferyczny poziom tlenu (21% pO_2), co zobrazowano na Rycinie 1.



Rycina 1. Poziom tlenu w doświadczeniach *in vitro*, prawidłowych tkankach i w mikrośrodowisku guza.

Niedotlenienie indukuje liczne zmiany w mikrośrodowisku guza [11] – najważniejsze z nich przedstawiono na Rycinie 2. Pokrótce: hipoksja promuje unaczynienie guzów, które jest jednak nieprawidłowe (patologiczne) i umożliwia przerzutowanie i jednocześnie obniża skuteczność radio i chemioterapii. Powstawanie przerzutów jest również związane z dynamicznymi zmianami – przejściem z fenotypu

nabłonkowego do mezenchymalnego, co określa się również terminem przejścia eptelialno-mezenchymalnego (EMT, ang. *epithelial-mesenchymal transition*). Zmiany te zwiększają plastyczność, mobilność i agresywność komórek nowotworowych. Regulowane przez niedotlenienie zaburzenia cyklu komórkowego czy indukcja komórek o fenotypie nowotworowych komórek macierzystych (CSCs, ang. *Cancer stem cells*) mogą przyczynić się do zmniejszenia efektywności leczenia. Wszystkie te aspekty omówiono szczegółowo w kolejnych rozdziałach tej pracy.



Rycina 2. Rola niedotlenienia w progresji nowotworów, angiogenezie, przerzutach i oporności na leczenie. Na podstawie [11], zmienione.

Odpowiedź komórki na hipoksję jest głównie kontrolowana przez rodzinę czynników indukowanych niedotlenieniem (HIFs, ang. *hypoxia inducible factors*). W fizjologicznych warunkach tlenowych podjednostki HIF- α są enzymatycznie hydroksylowane, a następnie kierowane do ubiquitynacji za pośrednictwem białka von Hippel-Lindau (VHL). W warunkach niedotlenienia, hydroksylacja podjednostek HIF- α zostaje zatrzymana, białko ulega stabilizacji, wiąże się z podjednostką HIF- β i jest transportowane do jądra komórkowego. Powstały dimer przyłącza się do sekwencji DNA

w miejscu odpowiedzi na niedotlenienie (HRE, ang. *hypoxia response element*) i rozpoczyna proces transkrypcji genów związanych z hipoksją [12]. Do tej pory odkryto trzy izoformy HIF- α : HIF-1 α , HIF-2 α oraz HIF-3 α [13]. Poziom HIF-1 α wzrasta podczas ostrej odpowiedzi na niedotlenienie, osiągając szczyt po 4-8 godzinach, podczas gdy HIF-2 α gromadzi się w celu regulacji odpowiedzi komórkowej w długotrwałym niedotlenieniu (24-72 h) [14]. Z kolei HIF-3 α jest negatywnym regulatorem podjednostki HIF-1 α i hamuje wiązanie HIF-1 z DNA [13]. HIF-1 α może być stabilizowany także niezależnie od poziomu tlenu; poprzez mutacje genu *VHL*, których efektem jest zaburzenie degradacji HIF- α i wywołanie stanu „pseudohipoksji” [15]. Mutacje *VHL* są często spotykane w nowotworach nerki, gdzie stanowią, według różnych źródeł, do 60 % przypadków [16, 17].

Niezależnie czy stabilizacja HIF- α odbywa się w sposób zależny czy niezależny od niedotlenienia, to powoduje aktywację transkrypcji wielu genów. Do tej pory potwierdzono ponad 100 genów docelowych dla HIFs, w tym głównie regulujących angiogenezę, ale też istotnych dla przemian metabolicznych, proliferacji i apoptozy, migracji czy przerzutowania [18]. Zatem szlaki sygnałowe indukowane za pośrednictwem HIFs mają istotne znaczenie w progresji nowotworów i regulacji wielu komponentów mikrośrodowiska guza.

1.1.2 Unaczynienie w nowotworach

Rozwój naczyń krwionośnych w TME umożliwia dostarczanie składników odżywczych i tlenu, a także usuwanie metabolitów – co jest niezbędne do wzrostu guzów. Wyróżnia się kilka sposobów rozwoju układu naczyniowego w nowotworach, najważniejsze to: angiogeneza, waskulogeneza i mimikra naczyniowa.

Angiogeneza, czyli wzrost nowych naczyń z wcześniej istniejących, występuje najczęściej i jest ściśle związana z odpowiedzią na niedotlenienie. Krytycznym czynnikiem angiogenezy jest regulowana m.in. przez HIFs rodzina czynników wzrostu śródbłonna naczyniowego VEGF (ang. *vascular endothelial growth factor*), w której wyróżniamy: VEGF-A, VEGF-B, VEGF-C, VEGF-D i łożyskowy czynnik wzrostu (PIGF, ang. *placenta growth factor*). Kluczowym czynnikiem stymulującym unaczynienie w nowotworach jest VEGF-A, który działa poprzez receptory VEGFR1 i VEGFR2 (ang. *vascular endothelial growth factor receptor*) obecne głównie na komórkach śródbłonna. Sygnalizacja VEGF-VEGFR zwiększa aktywność i migrację EC,

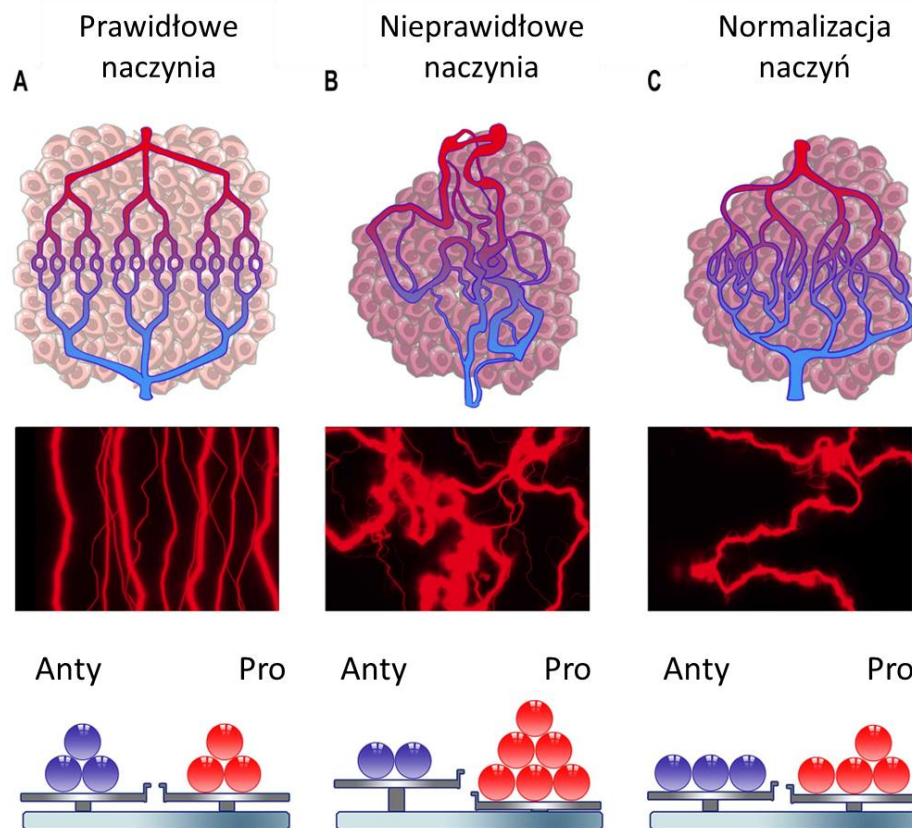
a także promuje powstawanie tzw. komórek wierzchołkowych (ang. *tip cells*), które odgrywają istotną rolę w kiełkowaniu nowych naczyń krwionośnych. Wśród innych ważnych czynników proangiogennych można wyróżnić również: czynnik wzrostu fibroblastów-2 (FGF2, ang. *fibroblast growth factor-2*), płytkopochodny czynnik wzrostu (PDGF, ang. *platelet derived growth factor*) czy angiopoetyny: ANG-1 ANG-2 (ang. *angiopoietin*) [19].

Unaczynienie guza może powstawać w procesie waskulogenezy, czyli tworzenia naczyń *de novo*, w którym uczestniczą progenitory komórek śródbłonna (EPCs, ang. *endothelial progenitor cells*). Proces ten wymaga mobilizacji i rekrutacji EPCs ze szpiku kostnego do guza, co jest regulowane m.in. przez: VEGF, SDF-1 (czynnik 1 pochodzący z komórek zrębu, ang. *stromal cell-derived factor 1*), czy chemokiny CCL2 i CCL5 (ang. *C-C motif chemokine ligand*) [20]. EPCs tworzą nowe naczynia krwionośne i różnicują się w dojrzałe ECs. Wzmoczoną migrację EPCs, a także możliwość wbudowywania się w struktury naczyniopodobne tworzone przez dojrzałe ECs, obserwowano w modelu 3D czerniaka *in vitro* [21]. Co ciekawe, EPCs zapewniają nie tylko wsparcie strukturalne powstającym naczyniom, ale także wydzielają szereg czynników regulujących angiogenezę [22]. Istotna rola EPCs w tworzeniu naczyń, może być również wykorzystana jako cel terapeutyczny – prowadzone są liczne badania mające na celu wykorzystanie EPCs w terapii chorób związanych z niedotlenieniem, w tym w nowotworach [23], ale również w chorobach kardiologicznych [24], chorobach płuc [25] czy w chorobach neurodegeneracyjnych – co wykazał nasz zespół również w modelu Alzheimerera [26].

Rozwój unaczynienia guza może być związany także z procesem zwanym mimikrą naczyniową. Jest to zdolność komórek nowotworowych do tworzenia struktur przypominających naczynia, bez udziału komórek śródbłonna. Struktury te stanowią alternatywną drogę dostarczania krwi i składników odżywczych do guza, jednocześnie promując przerzuty [27]. Mimikrę naczyniową zaobserwowano w wielu typach nowotworów, w tym: czerniaku [28], glejaku [29] czy nowotworach płuc [30].

W prawidłowych tkankach proces tworzenia naczyń jest regulowany poprzez homeostazę czynników pro i antyangiogennych (Rycina 3A). W nowotworach balans pomiędzy czynnikami stymulującymi i hamującymi tworzenie nowych naczyń zostaje zaburzony (Rycina 3B) [31]. Istotną rolę odgrywa również macierz zewnątrzkomórkowa,

stanowiąca rezerwuuar czynników proangiogennych, które są uwalniane z macierzy m.in. przez plazminę czy metaloproteinazy (MMPs, ang. *matrix metalloproteinases*) [32]. Tworzone w warunkach ciągłej stymulacji proangiogennej naczynia krwionośne są niefunkcjonalne. Patologiczne unaczynienie guzów charakteryzuje się brakiem hierarchicznej organizacji i pozbawione jest podziału na tętniczki, naczynia włosowate i żyłki [33]. Naczynia guza mają nieregularny kształt i wykazują wysoką heterogenność w obrębie TME, co powoduje nieprawidłowy przepływ krwi oraz wzrost ciśnienia płynu śródmiąższowego. Komórki śródbłonna w naczyniach krwionośnych guza nie tworzą ciasnych połączeń (ang. „*tight junctions*”), co wzmacnia przepuszczalność naczyń [34]. Udowodniono, że ECs izolowane z nowotworu piersi istotnie różnią się fenotypowo i funkcjonalnie od ECs zdrowej tkanki tej samej pacjentki [35]. W TME obserwuje się również zaburzenia komórek okołonaczyniowych; perycytów czy komórek mięśni gładkich naczyń, a także defekty błony podstawnej [36, 37]. Z patologicznym unaczynieniem związane są również nieprawidłowości macierzy zewnątrzkomórkowej – zwiększenie sztywności ECM charakterystyczne dla nowotworów może zaburzać tworzenie regularnych naczyń i szczelność połączeń między ECs [38, 39]. Wadliwe funkcjonowanie naczyń w guzie promuje obszary hipoksyjne, utrudnia transport leków – co powoduje nieskuteczność terapii; zaburza także rekrutację komórek układu odpornościowego i umożliwia ucieczkę komórek nowotworowych do krwiobiegu, co prowadzi do powstawania przerzutów [19].



Rycina 3. Schematyczne porównanie unaczynienia. Prawidłowe tkanki z zachowaniem równowagi pomiędzy czynnikami pro i antyangiogennymi (A), nieprawidłowe unaczynienie w nowotworach – dominacja czynników proangiogennych (B) koncepcja normalizacji naczyń w nowotworach i przywrócenie balansu między czynnikami pro i antyangiogennymi (C) Na podstawie [31], zmienione.

1.1.3 Terapie celujące w angiogenezę guza

Badania skupiające się na angiogenezie jako potencjalnym celu terapii przeciwnowotworowej zostały zapoczątkowane w latach 70-tych XX wieku. Wtedy, Judah Folkman zaobserwował, że przy braku unaczynienia guzy nie mogą rosnąć więcej niż do 2-3 mm i zaproponował, że inhibicja tworzenia naczyń spowoduje zahamowanie wzrostu guzów [40]. Dało to początek terapii przeciwiangiogennej zwanej również terapią antyangiogenną, prężnie rozwijającej się przez kolejne lata. Pierwszym, zatwierdzonym w 2004 roku przez Agencję Żywności i Leków (FDA, ang. *Food and Drug Administration*) antyangiogennym lekiem był bewacyzumab, humanizowane przeciwciało monoklonalne, które wiążąc krążący VEGF-A zapobiega jego interakcji z receptorem i hamuje szlak proangiogeny [41, 42]. Od tego czasu opracowano szereg inhibitorów angiogenezy, stosowanych w badaniach klinicznych i zatwierdzonych do stosowania w leczeniu wielu nowotworów. Leki te różnią się mechanizmem działania, jednak zdecydowana większość z nich skupia się na sygnalizacji przez VEGF [43]. Przykładowo aflibercept to rekombinowane białko fuzyjne, które blokuje interakcję

VEGF (VEGF-A i VEGF-B) oraz PlGF z ich receptorami, działając na zasadzie pułapki wiążącej białka [44]. Z kolei inhibitory kinaz tyrozynowych (TKIs, ang. *tyrosine kinase inhibitors*) hamują wewnątrzkomórkowe szlaki sygnałowe poprzez blokowanie receptorów odgrywających istotną rolę w procesie angiogenezy. Wśród TKIs wyróżniamy m.in.: sorafenib, celujący w VEGFR2 i 3, PDGFR-b, Flt-3 i c-Kit, sunitynib ukierunkowany na VEGFR1 i 3, PDGFR, Flt-3 i c-Kit, a także aksytynib charakteryzujący się dużą selektywnością wobec VEGFR [45, 46]. Warto zaznaczyć, że wśród TKI są również leki skierowane na inne szlaki sygnałowe np. wemurafenib czyli wysoce selektywny inhibitor kinazy BRAF, stosowany z leczeniu czerniaka z mutacją genu *BRAF* [47].

Leki celujące w angiogenezę mogą być stosowane w monoterapii lub w połączeniu z radio i chemioterapią – w zależności od typu nowotworu czy mechanizmu działania leku. Przykładowo, bewacyzumab stosowany w raku okrężnicy daje pozytywne efekty z chemioterapeutykami, ale nie w monoterapii [42, 48]. Z kolei w nowotworach płuc wykazano, że kombinacja bewacyzumab z chemioterapią istotnie zmniejsza perfuzję leku do guza, co przekłada się na nieskuteczność terapii mieszanej [49]. Stosowanie TKIs w monoterapii wykazało pozytywny efekt u pacjentów z rakiem wątrobowo-komórkowym (sorafenib [50]) czy rakiem nerki (sorafenib [51, 52], sunitynib [53]).

Niestety skuteczność terapii antyangiogennej jest ograniczona. Do najważniejszych czynników decydujących o wytworzeniu oporności na leczenie zalicza się promowanie niedotlenienia, indukcję komórek o fenotypie CSCs oraz zwiększenie agresywności komórek i promowanie przerzutów [54]. Nowym podejściem w terapii celującej w unaczynienie jest kontrolowanie angiogenezy i przywrócenie równowagi między czynnikami pro i antyangiogennymi, czego efektem jest normalizacja naczyń w guzie (Rycina 3C). Wykazano, że submaksymalne dawki leków antyangiogennych mogą normalizować naczynia krwionośne i zwiększać skuteczność terapii skojarzonej (z chemioterapią lub radioterapią) [55]. Wyzwaniem jest jednak określenie „okna terapeutycznego”, kiedy normalizacja następuje; i dostosowanie harmonogramu leczenia do konkretnych typów nowotworów i mechanizmu działania leku [56]. W związku z tym coraz częściej poszukuje się alternatywnych metod promujących normalizację naczyń. W modelu mysim wykazano, że białko Semaforyna 3A może być skutecznym regulatorem angiogenezy, umożliwiając normalizację naczyń, także poprzez poprawę funkcji perycytów [57]. Z kolei wazohibina, będąca regulatorem

ujemnego sprzężenia zwrotnego angiogenezy [58], promuje dojrzewanie naczyń hamując kiełkowanie ECs w modelu czerniaka [59]. Normalizację naczyń w guzie osiągnięto również u myszy z niedoborem PHD2 (ang. *prolyl hydroxylase domain-containing protein 2*), co skutkowało zmniejszeniem inwazyjności i przerzutów [60]. Jednak dalsze badania nad terapiami pozwalającymi osiągać stabilną, długotrwałą normalizację naczyń są wciąż konieczne i mogą istotnie przyczynić się do poprawy skuteczności leczenia nowotworów.

1.1.4 Trispirofosforan mio-inozytolu ITPP

Trispirofosforan mio-inozytolu (ITPP, ang. *Myo-inositol trispyrophosphate*) to cząsteczka o obiecujących właściwościach pozwalających na kompensację niedotlenienia w guzie i uzyskanie stabilnej normalizacji naczyń. Działa jako allosteryczny efektor hemoglobiny, indukując przesunięcie krzywej równowagi tlen-hemoglobina w czerwonych krwinkach [61], co może mieć kluczowe znaczenie w regulacji angiogenezy. *In vitro* w badaniu prowadzonym w dynamicznym modelu przepływów obecność erytrocytów traktowanych ITPP hamowała zdolność ECs do tworzenia naczyń w niedotlenieniu, przy jednoczesnym obniżeniu ekspresji HIF i VEGF [62]. ITPP wykazuje aktywność w niskim pH, czyli warunkach charakteryzujących TME [63]. Cząsteczka ta została z powodzeniem przetestowana w kilku zwierzęcych modelach nowotworów, a także chorób kardiologicznych [64]. Stosowanie ITPP spowodowało redukcję wielkości guzów i zmniejszenie rejonów nekrotycznych w modelu czerniaka, redukując także przerzuty do płuc i poprawiając przeżywalność zwierząt [65]. Podobne efekty obserwowano w modelu nowotworu wątroby – hamowanie wzrostu guza, zwiększone przeżycie zwierząt przy jednoczesnej zmniejszonej aktywności HIF i spadku poziomu VEGF [66]. W modelu nowotworu głowy i szyi nie odnotowano wpływu ITPP na wielkość guzów, jednak wykazano pozytywny efekt w terapii mieszanej: lepsze utlenowanie guza związane z działaniem ITPP zwiększyło skuteczność radioterapii [67]. Z kolei w glejakach nie obserwowano pozytywnych efektów stosowania ITPP, również w połączeniu z radioterapią [68, 69]. Pośrednio ITPP może regulować także inne elementy mikrośrodowiska guza – podniesienie poziomu tlenu na skutek stosowania ITPP moduluje fenotyp i właściwości odpowiedzi immunologicznej [70]. W modelu czerniaka wykazano, że ITPP może aktywować jeden z głównych supresorów nowotworu – PTEN (ang. *phosphatase and tensin homolog*) w komórkach śródbłonna, co ma kluczowe znaczenie w kontrolowaniu

wzrostu guza i regulacji angiogenezy. Specyficzność aktywacji PTEN przez ITPP potwierdzono również w badaniach *in vitro* z wykorzystaniem techniki powierzchniowego rezonansu plazmonowego [71]. Wszystkie powyższe właściwości ITPP są obiecujące w kontekście osiągnięcia stabilnej normalizacji naczyń i terapeutycznej modyfikacji mikrośrodowiska guza, jednak niespójność wyników w różnych typach nowotworów wymaga dalszych badań, również w kontekście aktywacji PTEN.

1.2 PTEN

PTEN, supresor nowotworu, został po raz pierwszy opisany w 1997 roku [72, 73]. Początkowo PTEN uważano za białko cytoplazmatyczne, jednak obecnie wiadomo, że jest obecne też w jądrze komórkowym, retikulum endoplazmatycznym, mitochondriach, a także przestrzeni międzykomórkowej, przez co wpływa na modulację komponentów TME [74, 75]. Ze względu na różnorodność biologicznych funkcji (związanych ściśle z lokalizacją śródkomórkową) oraz wiele poziomów regulacji ekspresji i aktywności, potencjał diagnostyczny i terapeutyczny PTEN wciąż pozostaje niejednoznaczny.

1.2.1 Struktura PTEN

Gen *PTEN* zlokalizowany jest na chromosomie 10q23 i koduje białko złożone z 403 aminokwasów, w którym wyróżnia się 5 domen funkcyjnych. Przy końcu NH₂ znajduje się domena wiążąca fosfatydyloinozitol-4,5-bisfosforan (PBD ang. *PIP2 binding domain*) oraz domena fosfatazy (PD ang. *phosphatase domain*), która jest odpowiedzialna za aktywność enzymatyczną supresoru guza. Dalej wyróżnia się domenę wiążącą błonę lipidową, która uczestniczy w wiązaniu PTEN do błony plazmatycznej oraz C-końcowy ogon i domeny wiążące białka PDZ, regulujące aktywność i stabilność białka PTEN [76].

1.2.2 Regulacja ekspresji i aktywności PTEN

Utrata funkcji PTEN może być następstwem wielu zdarzeń molekularnych, zarówno genetycznych, jak i epigenetycznych. Szacuje się, że ok 13,5 % ludzkich nowotworów ma mutację lub zmienioną funkcję PTEN [77]. Co więcej, PTEN jest uważany za gen haploniewystarczalny – mutacja tylko w jednym allelu jest wystarczająca do promowania progresji guza, co udowodniono w mysim modelu raka prostaty [78].

Mutacje zarodkowe genu *PTEN* powodują występowanie zespołów guzów hamartomatycznych (PHTS, ang. *PTEN hamartoma tumor syndromes*), obejmujących szereg autosomalnych dominujących zespołów klinicznych, takich jak: zespół Cowdena, zespół Bannayana-Rileya-Ruvalcaby czy zespół Prometeusza [79]. PHTS wiąże się z dużą podatnością na występowanie nowotworów, w tym nowotworu: piersi, jelita grubego, tarczycy, endometrium, nerki czy czerniaka [80].

W wielu typach nowotworów występują somatyczne mutacje *PTEN*, których, według katalogu mutacji COSMIC, wykryto ponad 1900, w tym: delecje, insercje czy mutacje zmiany sensu [81]. Mutacje te występują w miejscach kodujących wszystkie 5 domen funkcyjnych, dlatego też efekt biologiczny poszczególnych mutacji może być różny. Ekspresja *PTEN* jest związana z regulacją transkrypcji, w tym zmian epigenetycznych lub zmian aktywności czynników transkrypcyjnych [76, 82]. Kluczową rolę w regulacji potranskrypcyjnej *PTEN* odgrywa również mikroRNA, co szerzej opisano w Rozdziale 1.3.4. Funkcjonalność *PTEN* zależy także od modyfikacji potranslacyjnych (w tym fosforylacji, ubikwitynacji czy acetylacji), które determinują aktywność *PTEN*, a także wpływają na jego subkomórkową lokalizację [76]. Co więcej, interakcje z innymi białkami również wpływają na funkcje *PTEN* [82]. Istotną rolę w regulacji ekspresji i aktywności *PTEN* może również odgrywać niedotlenienie – w modelu nowotworów płuc wykazano, że hipoksja zmniejsza poziom *PTEN*, promując jego mniej aktywną formę – fosforylowany *PTEN* (p*PTEN*) [83].

1.2.3 Molekularne funkcje *PTEN*

Główna rola *PTEN* w komórce jest związana z aktywnością fosfatazy lipidowej. *PTEN* jest negatywnym regulatorem ścieżki PI3K/AKT/mTOR – defosforylując PIP3 do PIP2 hamuje aktywność serynowo-treoninowej kinazy białkowej AKT, zwanej także kinazą białkową B (PKB, ang. *Protein kinase B*) [84]. Kluczowym efektem AKT jest ssaczy cel rapamycyny, mTOR (ang. *mammalian target of rapamycin kinase*), pełniący istotne funkcje w procesach związanych z proliferacją, wzrostem i metabolizmem komórek [85]. Oprócz mTOR kinaza AKT reguluje również inne białka, w tym MDM2 (ang. *murine double minute 2*) – inhibitor supresora nowotworu p53 [86], czy BAD (ang. *Bcl-2 associated agonist of cell death*) – białko regulujące apoptozę [87]. Sygnalizacja PI3K/AKT jest jedną z najczęściej aktywowanych ścieżek w wielu typach nowotworów i uczestniczy w regulacji wielu podstawowych procesów komórkowych, istotnych

w progresji guza, jak: wzrost, proliferacja, przeżycie, metabolizm, a także odpowiedź immunologiczna [88, 89]. Co więcej, nieprawidłowości sygnalizacji PI3K/AKT mają istotne znaczenie dla skuteczności stosowanych terapii przeciwnowotworowych [84]. Oprócz kanonicznej funkcji fosfatazy lipidowej, PTEN wykazuje także aktywność fosfatazy białkowej, np. defosforylując białko FAK (ang. *focal adhesion kinase*) i białko Shc może regulować migrację komórek [90, 91]. Funkcja PTEN w regulacji adhezji komórek jest związana z bezpośrednią defosforylacją białka β -catenin i pośrednią regulacją kompleksu adhezyjnego β -catenin/E-cadherin [92]. W modelu nowotworu płuc wykazano, że utrata PTEN powodowała spadek ekspresji β -catenin, a także indukowała zmiany charakterystyczne dla EMT: zmniejszenie poziomu E-cadherin przy jednoczesnym wzroście ekspresji białek Vimentin i MMP2, a także nagromadzenie w jądrze czynników transkrypcyjnych Snail i Slug [93]. Funkcje PTEN niezwiązane z aktywnością fosfatazy są szczególnie istotne w jądrze komórkowym. Wykazano, że PTEN odgrywa istotną rolę w utrzymaniu stabilności genomu poprzez interakcje z cząsteczkami zaangażowanymi w replikację DNA, a utrata jądrowego PTEN prowadzi do rozległych pęknięć centromeru i translokacji chromosomów [94]. PTEN jest również istotnym elementem mechanizmów naprawy DNA [95] i pełni kluczowe funkcje w regulacji cyklu komórkowego [96, 97]. PTEN uczestniczy również w utrzymaniu prawidłowej kondensacji chromatyny poprzez wiązanie histonu H1 [98].

Wiele funkcji PTEN jest ściśle związane z mikrośrodowiskiem guza. Wykazano, że może być wydzielany w postaci rozpuszczalnej (PTEN-long) i transportowany za pośrednictwem egzosomów, co przyczynia się do modulacji innych komponentów TME [99]. W badaniach na myszach wykazano, że dootrzewnowe podanie PTEN-long powodowało regresję guza w modelu nowotworu jelita grubego [100]. Co ciekawe, także mikrośrodowisko może regulować jego wydzielanie – obserwowano zmniejszenie wydzielania PTEN-long w hipoksji [101]. Z kolei rola PTEN w modulacji odpowiedzi immunologicznej jest dwójaka – zmiany PTEN w komórkach nowotworowych modulują sygnały wysyłane do TME, a z drugiej strony dysfunkcja PTEN w komórkach układu odpornościowego wpływa na ich aktywność [102]. Utrata PTEN zwiększa ekspresję ligandu programowanej śmierci komórki PD-L1 (ang. *programmed death ligand 1*), który jest negatywnym regulatorem odporności przeciwnowotworowej [103, 104]. Poziom PTEN wpływa również na potencjał wydzielniczy komórek nowotworowych; przykładowo w nowotworze prostaty wykazano korelację między utratą PTEN

a zwiększeniem poziomu wydzielanej interleukiny 8 (IL, ang. *Interleukin*) [105]. W modelach przedklinicznych czerniaka utrata PTEN w komórkach nowotworowych zwiększyła wydzielanie cytokin immunosupresyjnych, powodując zmniejszenie infiltracji limfocytów T w guzach [106]. Dodatkowo zmiany aktywności PTEN w komórkach odpornościowych: komórkach dendrytycznych, makrofagach czy limfocytach również skutkują zmniejszeniem skuteczności odpowiedzi przeciwnowotworowej [107]. PTEN pełni również istotne funkcje w angiogenezie [75]. Wyciszenie ekspresji *PTEN* w komórkach nowotworowych zwiększa wydzielanie VEGF, co w kokulturze z komórkami śródbłonna promuje ich proliferację, migrację, a także indukcję angiogenezy *in vitro* [108]. Dodatkowo delecja PTEN w komórkach śródbłonna, także powoduje rozrost naczyń związany z brakiem pośrednictwa w zatrzymaniu proliferacji wywołanym przez Notch [109].

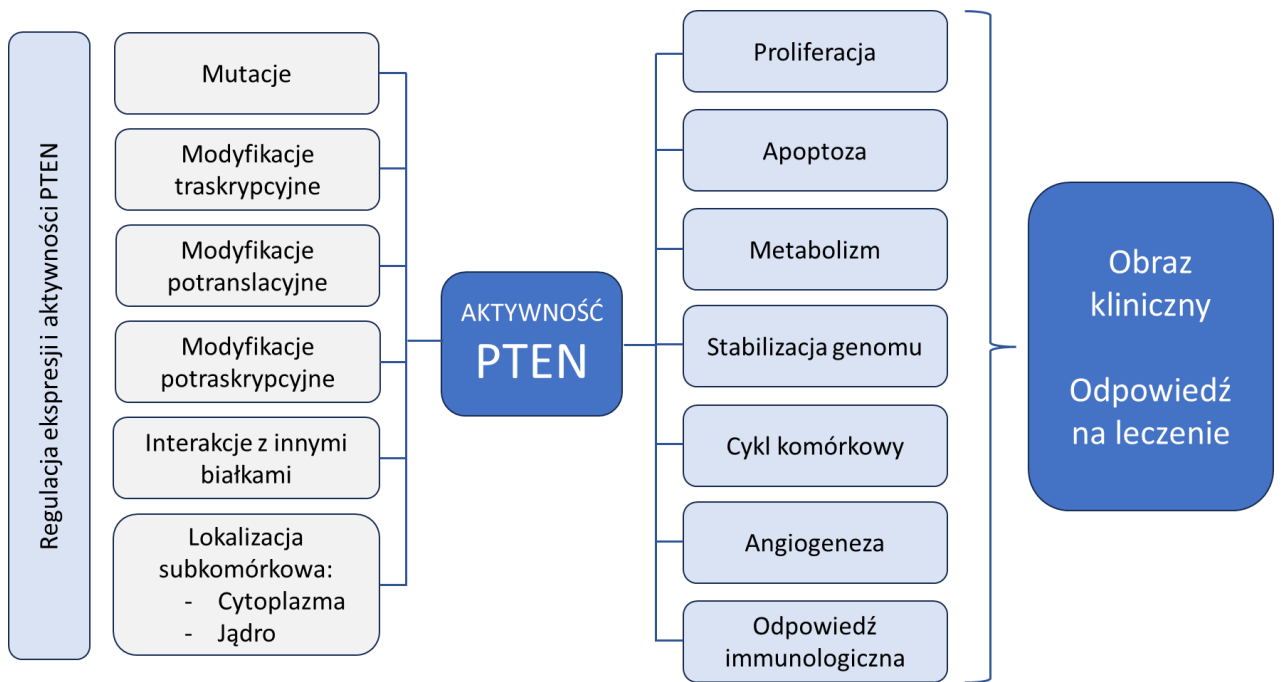
1.2.4 Znaczenie kliniczne PTEN

W wielu nowotworach wykazuje się korelację poziomu PTEN z obserwacjami klinicznymi. U pacjentów z rakiem prostaty obniżony poziom PTEN był związany z wyższym stopniem agresywności, a także zwiększonym występowaniem przerzutów i ryzykiem zgonu [110]. Zmniejszone przeżycie pacjentów, wzrost agresywności guzów i występowanie przerzutów korelowało ze zmniejszoną ekspresją PTEN również w innych typach nowotworów, w tym: w raku piersi, wątroby, jajnika czy w glejakach [111-113]. W przypadku czerniaka obniżony poziom PTEN korelował ze zmniejszonym czasem przeżycia pacjentów, a także krótszym czasem wystąpienia przerzutów do mózgu [114]. Niewiele jednak wiadomo na temat molekularnych aspektów utraty PTEN – w analizie 92 próbek pierwotnych czerniaków 33% charakteryzowało się obniżonym poziomem cytoplazmatycznego białka PTEN, natomiast w 91% próbek wykazano brak lub obniżony poziom ekspresji jądrowego PTEN [115]. Utrata jądrowego PTEN korelowała z anatomiczną lokalizacją przerzutów i indeksem mitotycznym w badanych próbkach, jednak utraty cytoplazmatycznego białka nie udało się połączyć z obserwacjami klinicznymi [115]. Szczegółowa analiza ekspresji PTEN w lokalizacjach subkomórkowych jest rzadkością w badaniach prowadzonych na dużej grupie pacjentów. Jednocześnie w wielu typach nowotworów wartość prognostyczna PTEN pozostaje kontrowersyjna i publikowane dane prowadzą do rozbieżnych wniosków. Przykładowo w raku nerki dwie niezależne metaanalizy wskazują jednocześnie na istotne znaczenie

poziomu PTEN w progresji choroby [116], jak i brak korelacji poziomu PTEN z cechami kliniczno-patologicznymi [117].

W wielu typach nowotworów wykazano zależność między poziomem PTEN a odpowiedzią na stosowane terapie przeciwnowotworowe. Kontrola wielu procesów biologicznych przez PTEN sprawia, że modulacja oporności na leczenie odbywa się za pośrednictwem wielu mechanizmów i dotyczy terapii o różnym mechanizmie działania. Mutacje PTEN indukują oporność na standardowe terapie (chemio i radioterapia) poprzez hiperaktywację szlaku AKT [118]. Zwiększoną oporność na radioterapię obserwowano w komórkach z mutacją PTEN (indukowaną za pośrednictwem edycji genomu z użyciem systemu CRISPR/Cas9) w modelu nowotworu płuc [119]. Poziom PTEN ma również istotne znaczenie w odpowiedzi na klasyczne chemioterapeutyki. W modelu nowotworu jajnika wyciszenie PTEN spowodowało wzrost oporności na cisplatynę – chemioterapeutyk zaburzający replikację DNA i podział komórek, a także indukujący apoptozę komórek [120]. Z kolei w raku endometrium mutacje PTEN powodują zwiększenie oporności na docetaksel – lek zakłócający podziały komórkowe poprzez wiązanie i stabilizację mikrotubul [121]. Ekspresja PTEN wpływa również na wrażliwość na doksorubicynę, której działanie opiera się na hamowaniu topoizomeras i interkalację w DNA, czego skutkiem jest zahamowanie proliferacji komórek. W modelach ostrej białaczki limfoblastycznej niska ekspresja PTEN skutkowała mniejszą wrażliwością na leczenie doksorubicyną, a mechanizm tej oporności był związany z aktywacją mechanizmów antyapoptotycznych za pośrednictwem MDM2 [122]. Poziom PTEN odgrywa również istotną rolę w odpowiedzi na terapie celowane. W raku nerki wykazano, że zmniejsza skuteczność leczenia sunitynibem i sorafenibem – lekami o właściwościach antyangiogennych. Co istotne, zależność tę wykazano *in vitro* indukując mutacje PTEN metodą CRISPR/Cas9 w liniach komórkowych raka nerki, ale również potwierdziły to obserwacje kliniczne – w grupie pacjentów leczonych sorafenibem lub sunitynibem o niskim poziomie PTEN, czas przeżycia wolny od progresji był znacząco niższy, niż w grupie o wysokim poziomie PTEN [123]. Z kolei w modelu czerniaka wykazano, że spadek poziomu PTEN indukuje oporność na inhibitory BRAF, poprzez hamowanie apoptozy [124]. Istotna rola PTEN w modulacji odpowiedzi immunologicznej w TME przekłada się także na niższą skuteczność immunoterapii nowotworów – co wykazano m.in. w modelu czerniaka czy raka prostaty [106, 125].

Podsumowanie rozważań dotyczących mechanizmów regulacji i funkcji PTEN w nowotworach zaprezentowano na Rycinie 4. Pomimo niekwestionowanej roli PTEN w progresji nowotworów, modulacji ich mikrośrodowiska, a także odpowiedzi na terapię przeciwnowotworowe, zarówno wartość prognostyczna, jak i terapeutyczna tego supresora guza wymaga dalszych badań i zrozumienia aktywności PTEN unikalnej dla różnych typów nowotworów.



Rycina 4. Schemat przedstawiający złożoność mechanizmów regulacji i lokalizacji PTEN w nowotworach wpływających na różnorodność funkcji i znaczenie kliniczne.

1.3 MIKRORNA

1.3.1 Definicja, biogeneza, funkcja

MikroRNA (miRNA, miR, ang. *Micro-RNA*) to małe, jednoniciowe, niekodujące cząsteczki RNA uczestniczące w regulacji ekspresji genów. Po raz pierwszy miRNA opisano w 1993 roku u nicienia *Caenorhabditis elegans* [126]. Kanoniczna biogeneza miRNA rozpoczyna się w jądrze komórkowym, gdzie sekwencje kodujące miRNA ulegają transkrypcji przez polimerazę II tworząc długie pierwotne miRNA (pri-miRNA, ang. *primary miRNA*) [127]. Pri-miRNA następnie jest przetwarzany na krótsze (70-120 nukleotydowe) prekursorowe miRNA (pre-miRNA, ang. *Precursor miRNA*) przez kompleks katalityczny (zwany mikroprocesorem) złożony z RNazy III Drosha i białek wiążących RNA, DGCR8 (ang. *DiGeorge syndrome critical region 8*) [128, 129]. Pre-miRNA jest transportowany do cytoplazmy, gdzie ulega rozdzieleniu na mniejsze

(19-24 nukleotydowe), dwuniciowe fragmenty przy udziale endonukleazy Dicer [130]. Dupleks miRNA jest następnie przekazywany do białek AGO (ang. *Argonaute*) – zostaje wytworzona dojrzała, jednoniciowa cząsteczka miRNA, i tworzony jest kompleks RISC (ang. *RNA-induced silencing complex*), który pośredniczy w rozpoznawaniu docelowych dla miRNA informacyjnych RNA (mRNA, ang. *messenger RNA*) [131]. Mechanizmy regulacji ekspresji miRNA obejmują zarówno zmiany transkrypcyjne (zmiany ekspresji genów i hipermetylacji promotora), potranskrypcyjne (zmiany w przetwarzaniu miRNA), jak i wpływ związków endogennych (np. hormony, cytokiny) i egzogennych (np. ksenobiotyki) [132]. Główny mechanizm działania miRNA polega na przyłączaniu się na zasadzie komplementarności do miejsc odpowiedzi na miRNA (MREs ang. *miRNA response elements*). MREs zlokalizowane są głównie obrębie regionu 3'UTR docelowego transkryptu, co prowadzi do degradacji mRNA lub zahamowania translacji [133]. Istnieją również dowody wykazujące, że miRNA może wpływać stymulująco na ekspresję niektórych genów [134]. Szacuje się, że ekspresja ok 30 % ludzkich genów może być regulowana przez miRNA – co czyni je ważnymi regulatorami wielu istotnych procesów biologicznych [134]. Jedna cząsteczka miRNA może regulować ekspresję wielu mRNA, a z drugiej strony każde mRNA może być regulowane przez wiele miRNA, dlatego sieć powiązań miRNA-mRNA jest bardzo rozbudowana. Liczne badania poświęcone ilościowej i jakościowej ocenie ekspresji miRNA wykazały znaczne zmiany w ich profilach ekspresji w różnych stanach patologicznych, w tym w nowotworach [135, 136].

1.3.2 Ekspresja miRNA w nowotworach

Nieprawidłowa ekspresja miRNA w nowotworach jest spowodowana zmianami genetycznymi i epigenetycznymi [137]. Zmniejszona ekspresja Dicer w raku płuc korelowała z gorszym rokowaniem, co może być związane z zaburzeniem syntezy miRNA [138]. Również deregulacje ekspresji białek AGO mogą odgrywać istotną rolę w progresji m.in.: raka jajnika, piersi czy okrężnicy [139]. Kluczową rolę w zaburzeniach ekspresji miRNA odgrywa również mikrośrodowisko guza (w tym niedotlenienie, co szerzej opisano w Rozdziale 1.3.3.) [139]. MiRNA są wydzielane do przestrzeni około komórkowej i odgrywają istotną rolę w komunikacji między komponentami TME [140]. Transport miRNA odbywa się za pośrednictwem zewnątrzkomórkowych pęcherzyków (EVs, ang. *extracellular vesicles*), które ze względu na rozmiar klasyfikuje się jako: egzosomy (<100 nm), mikropęcherzyki (<1000 nm), ciała apoptotyczne: 1-4 μm [141]. MiRNA może przemieszczać się również w formie swobodnie pływających kompleksów

miRNA z białkami AGO [142]. Wiele miRNA jest ściśle zaangażowanych w patogenezę raka, w tym proliferację komórek, przeżycie czy inwazję komórek nowotworowych. MiRNA ulegają destabilizacji również w innych niż nowotworowe komórkach TME. Wykazaliśmy, że profil miRNA istotnie różni się w komórkach śródbłonna izolowanych z nowotworu piersi w porównaniu do ECs izolowanych ze zdrowej tkanki tej samej pacjentki [143]. Kontrolowanie zmienionych miRNA ma duży potencjał jako nowa strategia terapeutyczna w leczeniu nowotworów, jednak potrzebne są dalsze badania określające profil miRNA w konkretnych nowotworach i mechanizmy pośredniczące w zmianie ich ekspresji.

Wśród miRNA istotnych w progresji nowotworów można wyróżnić onkomiry, czyli miRNA których ekspresja jest silnie podwyższona w nowotworach. Do najważniejszych onkomirów zalicza się miR-21, którego nadekspresję wykazano w nowotworach piersi, płuc, okrężnicy, prostaty, trzustki czy nerki [144]. MiR-21 bezpośrednio reguluje ekspresję genów związanych z przeżyciem komórek nowotworowych: programowana śmierć komórki 4 (*PDCD4*, ang. *programmed cell death 4*) genu *Bcl-2* kodującego antyapoptotyczne białko o tej samej nazwie [145, 146], czy genu *PTEN*, (co opisano w Rozdziale 1.3.1). Udowodniono, że zmniejszenie ekspresji tego miRNA wykazuje działanie przeciwnowotworowe hamując proliferację, migrację i wzrost guzów w mysim modelu raka piersi [147]. Innym istotnym onkomirem, o nieprawidłowej ekspresji w wielu typach nowotworów, jest miR-155, kontrolujący ekspresję genów związanych z odpowiedzią na uszkodzenia DNA, niedotlenienie czy reakcją układu odpornościowego. W kontekście angiogenezy wykazano, że miR-155 może bezpośrednio regulować ekspresję VHL aktywując HIF-1 α i stymulując angiogenezę, co potwierdzono w modelu mysim i *in vitro* z wykorzystaniem komórek HUVEC [148]. Wysoki poziom miR-155 moduluje odpowiedź immunologiczną i napływ komórek NK (ang. *natural killer*) poprzez hamowanie ekspresji negatywnych regulatorów odpornościowych, w tym inozytol-polifosforan-5-fosfatazy-1 (SHIP-1), a także zwiększa produkcję cytokin prozapalnych takich jak TNF- α (ang. *tumor necrosis factor alpha*) i IL-1 β [149, 150]. Nadekspresja miR-155 jest również związana z opornością na chemio i radioterapię, a także na gefitinib, lek z grupy inhibitorów kinaz tyrozynowych [151].

W przeciwieństwie do onkomirów grupę miRNA, których ekspresja jest obniżona w nowotworach określa się jako miRNA supresorowe guza. Przykładem może być

rodzina miRNA let-7, które fizjologicznie odpowiadają za różnicowanie komórek, a ich nieprawidłowa ekspresja jest związana z inicjacją i progresją nowotworów [151]. Niskie poziomy miRNA let-7, porównując do zdrowej tkanki, obserwowane są w wielu typach nowotworów m.in.: czerniaku, nowotworze płuc, prostaty czy jajnika [152]. Z kolei spadek ekspresji miR-15a i miR16 w modelu przewlekłej białaczki limfocytowa przyczynia się do wzrostu ekspresji Bcl-2 i zahamowaniu apoptozy [153]. Obniżoną ekspresję miR15b i miR-16 oraz zwiększenie poziomu Bcl-2 obserwowano w aktywowanych komórkach gwiaździstych trzustki (PSC, ang. *pancreatic stellate cells*), które odgrywają kluczową rolę w rozwoju nowotworu trzustki. W tym modelu przywrócenie prawidłowych poziomów miR-15b i miR-16 znacznie zmniejszyło poziom białka Bcl-2, co zaindukowało apoptozę w aktywowanych PSC [154]. Innym przykładem miRNA supresorowego jest miR-146a, który reguluje aktywność ważnego czynnika transkrypcyjnego NF- κ B (ang. *nuclear factor kappa-light-chain-enhancer of activated B cells*) – wykazano, że obniżony poziom tego miRNA jest skorelowany ze wzrostem guzów [155]. Obniżony poziom miR-340 obserwowano w wielu typach nowotworów. W niedrobnokomórkowym raku płuca (NSCLC, ang. *non-small-cell lung cancer*) wykazano, że spadek miR-340 koreluje z gorszym obrazem klinicznym pacjentów, za sprawą deregulacji szlaków związanych z p27 [156]. Z kolei w raku piersi obniżona ekspresja miR-340 przyczynia się do zwiększenia migracji i inwazji poprzez bezpośrednie celowanie w c-MET i pośrednią regulację metaloproteinaz MMP2 i MMP9 [157]. Klinicznie obniżony poziom miR-340 zwiększa przerzuty do węzłów chłonnych, co przekłada się na krótszy czas przeżycia pacjentów [157].

1.3.3 Sygnatura miRNA w hipoksji

Hipoksyjne mikrośrodowisko nowotworu ma kluczowe znaczenie dla regulacji poziomu wielu miRNA, a grupę miRNA o zmienionej ekspresji w odpowiedzi na niskie pO₂ określa się hipoksymirami (ang. *hypoxymirs*). W wielu badaniach wykazano, że niedotlenienie odgrywa znaczącą rolę zarówno w regulacji transkrypcji miRNA, ale również w późniejszych etapach ich biogenezy. HIF-1 α , główny czynnik transkrypcyjny indukowany przez niedotlenienie, reguluje ekspresję miRNA poprzez bezpośrednie wiązanie się z HREs w ich promotorach. Przykładem może być miR-210, jeden z najważniejszych i najlepiej zbadanych hipoksyjnych miRNA; ale również miR-103 czy miR-213, miR-382 [158-160]. Co ciekawe, miR-210 ulega również zwiększonej ekspresji w stanie pseudohipoksji, spowodowanym nieprawidłową funkcją

VHL – u pacjentów z nowotworem nerki z mutacją *VHL* poziom miR-210 był wyższy niż u pacjentów z prawidłowym *VHL* [161]. Inne czynniki transkrypcyjne, których ekspresja jest regulowana przez hipoksję, również wpływają na zmiany ekspresji miRNA. Na przykład p53, którego poziom może być modyfikowany przez niedotlenienie, indukuje transkrypcję miR-34, zaangażowanego w regulację cyklu komórkowego [162]; a także kontroluje transkrypcję miRNA z rodziny miR-200, odpowiedzialnych za regulację EMT i powstawanie przerzutów [163]. Oprócz modulacji ekspresji miRNA na poziomie transkrypcji, hipoksja modyfikuje również aktywność innych białek związanych z biogenezą miRNA. Indukowane niedotlenieniem obniżenie poziomu Drosha i Dicer związane jest ze zmniejszonym poziomem miR-21, -22, -30c i let7f w modelu fibroblastów płucnych [164]. W raku jajnika wykazano, że hipoksja reguluje spadek poziomu Drosha i Dicer poprzez deregulację czynników transkrypcyjnych ETS1/ELK1 i metylację promotora, co przyczynia się do zmian poziomu miRNA [165]. Niedotlenienie może również modyfikować dojrzewanie miRNA w następstwie potranslacyjnych modyfikacji białka AGO [166]. Podsumowując, hipoksyjne mikrośrodowisko guzów może mieć istotne znaczenie w zmianach sygnatury miRNA obserwowanych w nowotworach.

1.3.4 miRNA w regulacji ekspresji PTEN

MiRNA odkrywają znaczącą rolę w regulacji ekspresji PTEN, zarówno bezpośrednio poprzez interakcję z jego mRNA, jak i pośrednio regulując ekspresję innych czynników istotnych w modulacji poziomu PTEN [82, 167]. W wielu typach nowotworów wykazano, że nadekspresja onkomiru miR-21 bezpośrednio wpływa na obniżenie ekspresji PTEN, powodując progresję guza czy determinując odpowiedź na leczenie [167]. Na przykład w modelu *in vitro* gruczolaka płuc zwiększenie poziomu miR-21 (za pomocą miR-21 mimic) spowodowało spadek poziomu PTEN, a odwrotną zależność obserwowano po zastosowaniu inhibitora tego miRNA [168]. Co więcej, wzrost ekspresji miR-21 i spadek poziomu PTEN powodowały zmniejszenie apoptozy i nekrozy po leczeniu 5-fluorouracylem, natomiast po zastosowaniu inhibitora miR-21 komórki były bardziej odporne na leczenie [168]. Podobną zależność pomiędzy miR-21 i poziomem PTEN obserwowano w raku jajnika [169], prostaty [170] czy wątroby [171]. Wśród innych miRNA powodujących spadek ekspresji PTEN wyróżnia się również miR-221/222 – w modelu raka piersi obserwowano, że ta regulacja sprzyja proliferacji, inwazji i migracji komórek, a także promuje fenotyp CSCs [171]. MiR-221

odgrywa również kluczową rolę w regulacji EMT poprzez celowanie w PTEN [172]. Rodzina miR-130 również uczestniczy w regulacji poziomu PTEN. W raku piersi nadekspresja miR-130 spowodowała spadek ekspresji PTEN, czego następstwem było zwiększenie proliferacji komórek i wzrost guzów [173]. W próbkach klinicznych raka pęcherza moczowego stwierdzono, że spadek poziomu PTEN jest ściśle skorelowany z poziomami ekspresji rodziny miR-130, a w modelu *in vitro* wykazano, że nadekspresja tych miRNA sprzyja migracji i inwazji komórek [174]. Odmienne obserwacje dotyczyły nowotworu płuc – obniżona ekspresja miR-130 wiązała się z agresywnymi cechami kliniczno-patologicznymi i złym rokowaniem pacjentów z NSCLC [175]. Doświadczenia *in vitro*, z wykorzystaniem linii komórkowych nowotworu płuc wykazały, że nadekspresja miR-130 powoduje zwiększenie poziomu PTEN, jednak nie wskazano potencjalnych mechanizmów takiej regulacji [175]. Podobnie zwiększona ekspresja miR-451 powoduje wzrost poziomu PTEN indukując wrażliwość na radioterapię, co także obserwowano w nowotworze płuc [176]. Ekspresja miR-29, miR-101 czy miR195 jest również związana ze wzrostem poziomu PTEN poprzez indukcję hipometylacji promotora PTEN [177].

Regulacja ekspresji PTEN za pośrednictwem miRNA jest wielokierunkowa i zależna od typu nowotworu, co powoduje, że określenie molekularnych i klinicznych skutków tych interakcji jest skomplikowane. Interesująca jest również odwrotna zależność – wpływ mutacji PTEN na modyfikacje ekspresji miRNA. Do tej pory przeprowadzono nieliczne badania mające na celu identyfikacji tych zmian. W raku prostaty wykazano, że utrata PTEN powoduje m.in. wzrost ekspresji onkomiru miR-155 [178], co stawia nowe wyzwania w określeniu zależności miRNA-PTEN w progresji nowotworów.

2 CEL I ZAŁOŻENIA PRACY

Poszukiwanie skutecznych terapii przeciwnowotworowych jest wciąż wielkim wyzwaniem i wymaga kompleksowego podejścia uwzględniającego całość mikrośrodowiska guza, w tym charakterystycznych dla TME warunków tlenowych – hipoksji. Strategia normalizacji naczyń w nowotworach za pośrednictwem ITPP, wydaje się obiecującym podejściem terapeutycznym, również z uwagi na wielokierunkowy mechanizm działania tej cząsteczki (kompensacja niedotlenienia i aktywacja PTEN). Jednak niejednoznaczność wyników stosowania ITPP w różnych typach nowotworów

wskazuje na konieczność pogłębienia wiedzy dotyczącej mechanizmów molekularnych odpowiedzialnych za te różnice. PTEN, jako supresor guza, pełni istotną funkcję w regulacji podstawowych procesów komórkowych, mimo to jego znaczenie prognostyczne oraz jako potencjalny cel terapeutyczny wymaga dalszych badań.

Punktem wyjścia do przedstawienia celów i hipotezy pracy było sprawdzenie skuteczności stosowania ITPP w mysim modelu nowotworu nerki (Renca) *in vivo*. W badaniach wstępnych obserwowano brak pozytywnych efektów leczenia w tym modelu; guzy z komórek Renca nie zmieniały się pod wpływem ITPP. Dlatego dalsze badania prowadzono z wykorzystaniem dwóch modeli: czerniaka B16 F10 (jako typ nowotworu, w którym leczenie ITPP spowodowało zmniejszenie guzów i redukcję obszaru nekrotycznego [65]) i nowotworu nerki Renca – jak przykład nowotworu nie reagującego na ITPP. Jako, że aktywacja PTEN jest jednym ze skutków działania ITPP, a poziom i aktywność PTEN odgrywa znaczącą rolę w progresji wielu typów nowotworów w niniejszej pracy skupiono się na określeniu funkcji PTEN w badanych modelach, również w kontekście hipoksyjnego mikrośrodowiska guza.

Hipoteza pracy: aktywność PTEN istotnie różni się w modelu raka nerki i czerniaka, co może modyfikować mikrośrodowisko guza i wpływać na odpowiedź na terapię przeciwnowotworowe.

W celu weryfikacji tej hipotezy zrealizowano następujące cele badawcze:

- 1) określenie wpływu niedotlenienia na poziom i aktywność PTEN oraz potencjał proangiogeny testowanych modeli (*in vitro*),
- 2) zbadanie roli PTEN w raku nerki i czerniaku, z wykorzystaniem edycji genomu metodą CRIPSR/Cas9 do wytworzenia linii z mutacją PTEN – charakterystyka komórek z nokautem PTEN, określenie ich wrażliwości na leczenie *in vitro* oraz wpływ na progresję guzów *in vivo*,
- 3) sprawdzenie wpływu mutacji PTEN i niedotlenienia na modyfikację mikrośrodowiska guza poprzez regulację ekspresji miRNA w modelu raka nerki (*in vitro* i *in vivo*).

3.1 PUBLIKACJA 1

Comparative analysis of the effect of hypoxia in two different tumor cell models shows the differential involvement of PTEN control of proangiogenic pathways

Aleksandra Majewska^{a,b}, Klaudia Brodaczevska^a, Aleksandra Filipiak-Duliban^{a,b}, and Claudine Kieda^{a,c}

^aMilitary Institute of Medicine—National Research Institute, Laboratory of Molecular Oncology and Innovative Therapies, Szaserów 128, 01-141 Warsaw, Poland; ^bPostgraduate School of Molecular Medicine (Medical University of Warsaw), Żwirki i Wigury 61, 02-091 Warsaw, Poland; ^cCenter for Molecular Biophysics UPR 4301 CNRS, 45071 Orleans, France

Corresponding author: Aleksandra Majewska (email: amajewska1@wim.mil.pl)

Abstract

Hypoxia, low, non-physiological oxygen tension is a key regulator of tumor microenvironment, determining the pathological tumor vascularization. Alleviation of hypoxia through vessel normalization may be a promising therapeutic approach. We aimed to assess the role of low oxygen tension in PTEN-related pathways and proangiogenic response, in vitro, in two different tumor cell lines, focusing on potential therapeutic targets for tumor vessel normalization. Downregulation of PTEN in hypoxia mediates the activation of distinct mechanisms: cytoplasmic pAKT activation in melanoma and pMDM2 modulation in kidney cancer. We show that hypoxia-induced proangiogenic potential was stronger in Renca cells than B16 F10—confirmed by a distinct secretory potential and different ability to affect endothelial cells functions. Therefore, the impact of hypoxia on PTEN-mediated regulation may determine the therapeutic targets and effectiveness of vessel normalization and intrinsic characteristics of cancer cell have to be taken into account when designing treatment.

Key words: angiogenesis, hypoxia, melanoma, PTEN, renal cell carcinoma

Introduction

The incidence of renal cell carcinoma (RCC) is estimated at about 430 000 cases per year worldwide (Global Cancer Observatory n.d.), making it the sixth most commonly diagnosed cancer in men and ninth in women (Siegel et al. 2023). RCC is highly resistant to radiotherapy and chemotherapy (Makhov et al. 2018), what prompted the development of targeted therapies and immunotherapies.

Tumor hypoxia is one of the major factors determining tumor progression. The mechanisms associated with low pO₂ upregulate hypoxia-inducible factors (HIFs), resulting in the stimulation of proangiogenic response (Liao and Johnson 2007). In RCC, deregulation of HIF-1 α is also due to frequent VHL (*von Hippel-Lindau*) mutations—approximately 60% of RCC tumors show an inactivated VHL (50% through somatic mutations or 10% through promoter methylation) (Rini and Small 2005; Bratslavsky et al. 2007). Non-functional VHL (causing pseudohypoxic state), as well as tumor hypoxia, lead to stabilization of HIF-1 α and its accumulation and heterodimerization with HIF-1 β . Resulting HIF-1, upon translocation in the nucleus, binds to hypoxia response element (HRE), which activates the transcription of downstream genes, namely *Vegf-a* (vascular endothelial growth factor a), which turns on angiogenesis (Hayashi et al. 2019). Under the constant proangiogenic signaling state in tumors, the

newly formed tumor vasculature is pathological and non-functional. Vessel disorders cause disturbances of the blood flow, which deepens the hypoxic state (Baluk et al. 2005; McDonald and Baluk 2005). In pathological vessels, endothelial cell (EC) junctions are leaky, which worsens the drug delivery and allows tumor cells to escape into the bloodstream and metastasize (Hashizume et al. 2000; Folkman 2002). The concept of controlling tumor angiogenesis, as a therapeutic target, was introduced by Judah Folkman and colleagues in the 1970s (Folkman 1971). Since then, several antiangiogenic therapies have been developed that target the VEGF signaling pathway, including anti-VEGF antibody (Bevacizumab) and tyrosine kinase inhibitors (TKI), Sorafenib and Sunitinib, also used in RCC (Lugano et al. 2020; Sekino et al. 2020). As antiangiogenic strategies aimed at destroying the tumor vessels, they are poorly effective and deleterious—by increasing the tumor hypoxia, they lead to the selection of drug-resistant, aggressive, cancer-stem-like cells (Paez-Ribes et al. 2009). Currently, much hope is placed on another approach to control tumor angiogenesis—namely, normalization of tumor vessels (Goel et al. 2012). Submaximal doses of antiangiogenic drugs might normalize blood vessels and increase the effectiveness of combinational therapy (with chemotherapy or radiotherapy) (Jain 2001). In mouse model, improving tumor vascular perfusion and oxygenation by vessel normal-

ization increases the efficacy of conventional therapies, such as radiotherapy, chemotherapy, and immunotherapy, and reduces metastatic spread (Mazzone et al. 2009). The challenge of such therapies is to define the therapeutic window when the vessels are normalized—therefore, it is necessary to find new molecules that induce a stable, long-lasting normalization of the vessels (Sato 2011).

PTEN (phosphatase and tensin homolog deleted on chromosome 10) is a tumor suppressor molecule that affects PI3K/AKT/mTOR pathway, regulating basic cellular processes, namely, growth control (Milella et al. 2015). Its loss promotes tumor development in melanoma (Stahl et al. 2003) and affects the outcome of RCC treatments (Sekino et al. 2020). The role of PTEN in hypoxia-related pathways was already assessed in lung cancer (Kohnoh et al. 2016), glioblastoma (Rong et al. 2005), head, and neck squamous cell carcinoma (Nascimento-Filho et al. 2019), but is poorly documented in RCC. In addition to the canonical PI3K/AKT pathway regulatory function, PTEN, as a phosphatase, is involved in controlling the other tumor suppressor—p53, by antagonizing Akt-Mdm2 pathway (Mayo and Donner 2001) or in a phosphatase-independent manner PTEN by complexing p300 and interacting with p53 in the nucleus (Li et al. 2006). PTEN also modulates angiogenesis through VEGFA regulation (Huang and Kontos 2002). In hepatocellular carcinoma, the angiogenic function of PTEN is modulated by both phosphatase activity and in phosphatase-independent manner (Tian et al. 2010). In ECs, PTEN mediates the Notch-dependent tip cell/stalk cell crossstalk and growth arrest (Serra et al. 2015).

As RCC is known to be a highly angiogenic tumor, due to both VHL-mediated pseudohypoxic state and the hypoxic microenvironment (Hayashi et al. 2019), the knowledge of PTEN/hypoxia-regulated pathways may help to better understand the molecular aspects and reveal new targets for adjuvant therapies. Molecule with promising properties to compensate tumor hypoxia and activate PTEN is myo-inositol trispyrophosphate (ITPP). In vivo ITPP treatment reduced tumor size and necrotic area, inhibited lung metastasis formation, and improved survival of mice with melanoma (Kieda et al. 2013). ITPP activates PTEN in the endothelium, which has particular importance in the context of stabilization of normalized vessels (Kieda et al. 2013) and which mechanism has been proven recently in vitro (Grzymajlo et al. 2023). Elevating pO₂ upon ITPP treatment also affects other components of the tumor microenvironment by modulating the phenotype and properties of the immune infiltrate, reducing the tumor immunosuppressive properties (El Hafny-Rahbi et al. 2021). The multifaceted action of ITPP may contribute to a more comprehensive approach to vessel normalization than therapies focused on a single pathway.

The aim of the present study was to identify hypoxia-mediated changes in PTEN-related pathways in melanoma and kidney cancer models in vitro, searching for potential therapeutic targets to compensate hypoxia in RCC. Simultaneously, we aimed to uncover the differences in the proangiogenic potential upon hypoxia by their ability to modulate EC properties related to the secreted component properties. We compared kidney cancer cells with melanoma that previously positively responded to ITPP treatment compensating tumor

hypoxia, stably normalizing vessels and activating PTEN in tumor microenvironment (Kieda et al. 2013). We could evidence the differential activation of PTEN-mediated pathways regulating angiogenesis in both cancer models and by their distinct reaction in hypoxia.

Materials and methods

Cell lines

Murine kidney cancer cells Renca were purchased from ATCC (Cat No. CRL-2947, LOT No. 63226315 ATCC, USA), while murine melanoma cells B16 F10 were given by prof. Dulak from the Department of Medical Biotechnology, Faculty of Biochemistry, Biophysics and Biotechnology, Jagiellonian University, Cracow, Poland (authenticated by ATCC Cell Authentication Service in 2021). Eighteen mouse short tandem repeat (STR) loci and two human markers: D8 and D4 were analyzed to screen for the presence of human or African green monkey species in tested cells. The profile of B16 F10 samples were the same in 97% to the reference profile ATCC MUSA0830.

Cancer cell lines were cultured in RPMI-1640 GlutaMaxTM medium (ThermoFisher Scientific, USA), with 10% FBS (ThermoFisher Scientific, USA). Murine brain derived mature ECs (MBr MEC FVB) (Bizouarne et al. 1993) (CNRS Patent Number CN12/9916169) and MAgEC 11.5 (Collet et al. 2016; Klimkiewicz et al. 2017) (Patent Number US9631178B2) were cultured in OPTI MEM medium (ThermoFisher Scientific, USA), with 2% Fetal Bovine Serum—FBS (ThermoFisher Scientific, USA). All cell lines were Mycoplasma-free (Biomedica, Poland) and did not exceed 15th passage. Cells were passaged at 80% confluence by detaching with Accutase solution (Biogend, USA).

Animals

BALB/c mice were obtained from the Medical University of Białystok. Animal care and experimental procedures were approved by the Second Warsaw Local Ethics Committee for Animal Experimentation (No. WAW2/76/2017) and performed following Directive 2010/63/EU regulations. Mice were housed in a controlled environment (12 h light/12 h dark cycle, ad libitum access to tap water, and full-fledged diet). Before starting the experiments, the mice were acclimatized for a week.

In vivo ITPP treatment of renca tumors

Renca cells were implanted in mice leg as subcutaneous tumors by injection of a plug constituted by 10⁵ cells in 100 μL MatrigelTM (Corning, USA) diluted in 1:1 in phosphate-buffered saline (PBS). The treatment consisted of an intraperitoneal injection of ITPP in saline at a dose of 1.5 g per kg of body weight for 2 consecutive days, every 5 days. Treatment was performed in two groups—ITPP 1 mice received the first dose on day 5 after tumor cell injection, while ITPP 2 mice received the first dose of treatment only when tumors were visible (after 10 days). Corresponding controls (Control 1, Control 2) received an injection of saline without ITPP every 5 days. After 22 days, the experiment was stopped due to the large size

of the tumors, which negatively affected the welfare of the animals. Tumor weight was measured in the control groups and after ITPP treatment. The experimental groups consisted of four mice, each with a tumor on the right and left legs.

Cancer cell cultures in normoxia and hypoxia

7000 cancer cells (Renca, B16 F10) per cm^2 were seeded on standard tissue culture-treated flasks (VWR International, USA) and allowed to adhere to the culture surface for 24 h. At the same time, fresh RPMI 10% FBS was left under normoxic and hypoxic conditions for 24 h. Next medium was exchanged to pre-equilibrated normoxic or hypoxic medium and cells were cultured in standard cell culture incubator (21% pO_2 ; 5% CO_2) or XVivo X3 workstation (Biospherix, USA) in 1% pO_2 and 5% CO_2 , respectively. When the cultures were subconfluent (after 48 h for B16 F10 and 72 h for Renca), culture supernatants were collected, centrifuged to remove cell contaminants, and frozen at -20°C , while the cells were washed in PBS and harvested using Accutase (Biolegend, USA). Cells were used for flow cytometry staining or protein and RNA isolation.

Conditioned medium for experiments with EC cells

To assess the effect of conditioned medium (CM) from cancer cells on ECs, B16 F10 and Renca cells were cultured as described above, but the medium used was OPTI MEM (ThermoFisher Scientific, USA) 2% FBS. Cancer cells were previously adapted by gradual change of medium over 2 weeks. Conditioned media were obtained after centrifugation to remove cell contaminants and further cleaned using $0.2\ \mu\text{mol/L}$ cellulose acetate filters (VWR International, USA).

Endothelial cells culture

MBr MEC FVB (3000 cells/ cm^2) were seeded on tissue culture-treated flasks (VWR International, USA) and allowed to adhere to the culture surface for 24 h (protocol of the experiment is represented as scheme on Fig. 1B). Media were exchanged with normoxic or hypoxic medium or mixed (1:1) with CM from Renca cells maintained in appropriate aerobic conditions and further cultured in normoxia and hypoxia for 48 h. Cells were washed by PBS, harvested using Accutase (Biolegend, USA), and used for protein isolation.

Western blotting

RIPA buffer, containing inhibitors Cocktail (both ThermoFisher Scientific, USA) was used to lyse cells. Twelve microgram of total protein, measured by BCA assay, was solubilized in Laemmli sample buffer (AlfaAesar, USA). Samples were separated on 12% polyacrylamide gel and then transferred onto nitrocellulose membranes (BioRad, USA). Non-specific binding was reduced by a blocking step in 5% skimmed milk (2 h at RT—room temperature). Membranes were incubated overnight at 4°C in the presence of a solution containing primary antibodies (Table 1), then membranes were incubated for 2 h with the relevant secondary antibody diluted 1:10 000 (Goat Anti-Rabbit IgG Antibody or Horse Anti-Mouse IgG Antibody conjugated with horseradish

peroxidase (HRP)—both from Vector Laboratories, USA). Reactive bands were revealed by reaction with enhanced chemiluminescence substrate (Santa Cruz Biotechnology, USA) and visualized using X-ray films (Carestream Health USA). Quantification of the integrated optical density (IOD) of the bands was performed using analysis software ImageJ. In quantitative analysis, the relative IOD of target proteins was normalized to IOD of Vinculin. Due to the different levels of proteins, the membranes were cut horizontally, what allowed to adjust the incubation time with the substrate to the expression level of particular protein.

Real-time PCR

Total RNA was extracted from Renca and B16 F10 cells cultured in normoxia and hypoxia using RNeasy Mini Kit (Qiagen, Germany). The samples were freed from DNA using TURBO DNA-free kit (ThermoFisher Scientific, USA) and RNA quality and concentrations were assessed by measuring the absorbance at 230 nm, 260 nm, and 280 nm using the μDrop plate in Multiskan™ GO microplate spectrophotometer (ThermoFisher Scientific USA). For cDNA synthesis, $2\ \mu\text{g}$ of total RNA was used for reverse transcription reaction (High-Capacity cDNA Reverse Transcription Kit; ThermoFisher Scientific, USA) and the product was diluted 3 \times . Real-time PCR was performed using TaqMan™ Gene Expression Master Mix (Thermo Fisher Scientific, USA) with TaqMan probes (all from ThermoFisher Scientific: *Vegf-a*: Mm00437306, *Hif-1 α* : Mm00468869, *Pten*: Mm00477208, *Akt*: Mm00437306, *Actin β* : Mm02619580). Reactions were run on Bio-Rad CFX384 qPCR System or CFX Connect qPCR System (BioRad). The relative mRNA level was calculated with $2^{-\Delta\Delta\text{CT}}$ method, with normalization to the expression of *Actin β* as a house-keeping gene.

Flow cytometric detection of PTEN

Renca cells, after culture in normoxia or in hypoxia were washed and stained for 20 min at RT (room temperature) using LIVE/DEAD™ Fixable Green Dead Cell Stain Kit, for 488 nm excitation (ThermoFisher Scientific, USA), which reacts with free amines both in the cell interior and on the cell surface in dead cells, yielding intense fluorescent staining. In viable cells, the dye's reactivity is restricted to the cell-surface amines, resulting in less intense fluorescence. After washing steps cells were fixed using Fixation Buffer (1:1, v/v) for 10 min on ice, then permeabilized using ice-cold Permeabilization Buffer (both from Millipore's Muse™ Dual Detection kits, Merck Millipore, USA) for 10 min on ice. Intracellular staining was performed using PE-labeled monoclonal mouse anti-PTEN IgG antibody (Cat No. 560002, BD Bioscience, Switzerland; diluted 1:25). All samples were analyzed using CytoFLEX Flow Cytometer (Beckman Coulter, USA).

PTEN immunofluorescent staining

Renca cells were cultured on glass coverslips as described in *Cell cultures in normoxia and hypoxia*. Next, cells were fixed by 4% (w/v) paraformaldehyde solution in PBS for 10 min, permeabilized with Permeabilization Buffer (Millipore's Muse™ Dual Detection kits, Merck Millipore, USA) blocked with 5% BSA in PBS/0.01% Triton X-100 for 1 h at RT, and incubated

Fig. 1. Effect of hypoxia on PTEN expression in B16 F10 and Renca cells. (A) Relative to Actin β expression of PTEN gene ($n > 3$; t Student test for B16 F10; Mann–Whitney test for Renca). (B) PTEN and pPTEN detection by Western blots with Vinculin as loading control in Renca and B16 F10 cells cultured in normoxia and hypoxia. (C) Quantification of the PTEN expression relative to Vinculin level $*P < 0.05$, $**P < 0.01$ ($n > 3$; Mann–Whitney test). (D) Quantification of ratio pPTEN to PTEN $*P < 0.05$, $**P < 0.01$ ($n > 3$; t Student test for B16 F10; Mann–Whitney test for Renca). (E) Representative flow cytometry histograms of PTEN detected in Renca cells cultured in normoxia and hypoxia. (F) Detection of PTEN by immunofluorescence staining in Renca cells cultured in hypoxia (right panel) as compared to normoxia (left panel) (scale bar: 20 μ m).

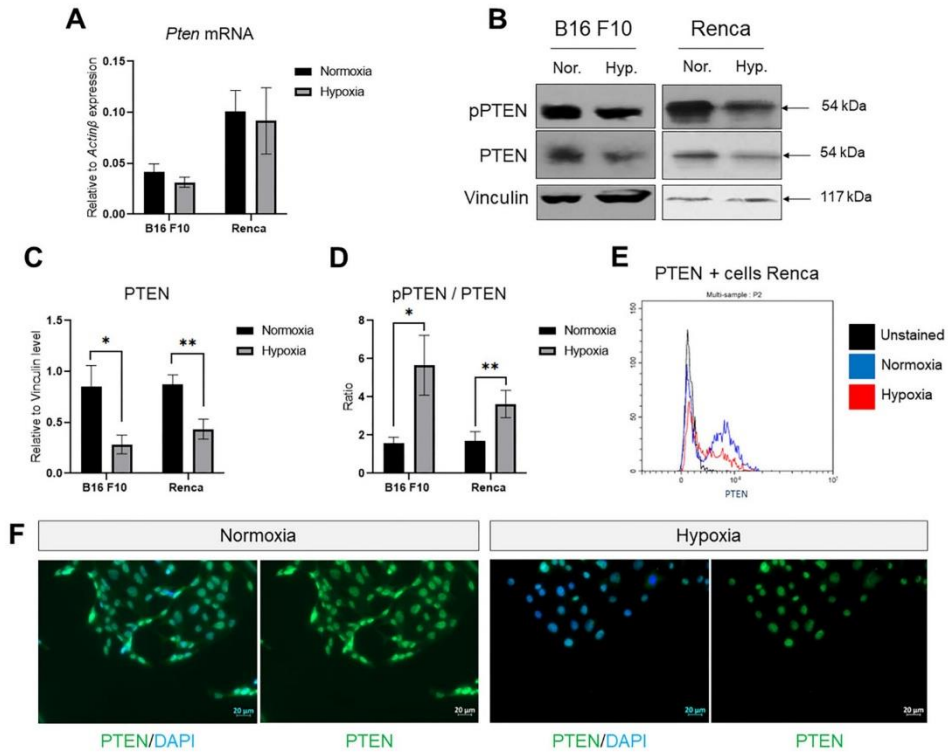


Table 1. Primary antibodies used in Western Blot.

Target	Dilution	Cat No.	Company
PTEN	1:750	9556	Cell Signalling Technology
AKT	1:700	sc-5298	Santa Cruz Biotechnology
p53	1:1000	2524	Cell Signalling Technology
MDM2	1:1000	MA1-24755	ThermoFisher Scientific
Vinculin	1:1000	sc-59803	Santa Cruz Biotechnology
Histone H3	1:1000	4499	Cell Signalling Technology
pPTEN (Ser380/Thr382/383)	1:1000	9549	Cell Signalling Technology
pAKT (Ser473)	1:1000	MAB887	R&D System
PI3K	1:1000	sc-365404	Santa Cruz Biotechnology
pMDM2 (Ser166)	1:1000	3521	Cell Signalling Technology
Claudin1	1:1000	13255	Cell Signalling Technology

with a primary mouse monoclonal anti-PTEN IgG (Cat No. 9556, Cell Signaling Technology, USA; diluted 1:200 in blocking solution) at 4 °C overnight in a humidified chamber. Then cells were incubated with secondary Alexa-Fluor (AF) 488-conjugated goat antimouse IgG (1:200) (Jackson ImmunoResearch, United Kingdom) for 1 h at RT. Negative controls were obtained by using the secondary antibodies only. Nuclei were stained with DAPI using EverBrite™ Hardset Mounting Medium (Biotium, USA). Images were acquired using a Zeiss AxioObserver.7 fluorescence and inverted microscope (20× magnification) and analysis performed with the Zen 2.6 blue edition software (Zeiss, Germany).

Isolation of cytoplasmic and nuclear protein fractions

Renca cells after culture in normoxia or in hypoxia were washed with PBS; cytoplasmic and nuclear fractions were isolated using Nuclear and Cytoplasmic Extraction Reagents (ThermoFisher Scientific), according to the manufacturer's protocol. Lysed fractions were used for PTEN detection by Western Blot. Ponceau staining and specific loading controls for the fractions—Vinculin for total sample and cytoplasmic fraction and Histone H3 for nuclear fraction—were used to calculate IOD.

Pseudo tube formation for angiogenesis activity assessment

A total of 96-well plates were coated with 60 µL per well of Growth Factor Reduced Matrigel (Merc, Sigma-Aldrich, USA). 20 000 MBr MEC FVB (calcein stained) or 25 000 MAgEC 11.5 cells per well were seeded in basal medium OPTI MEM 2% FBS (control) or medium OPTI MEM 2% FBS mixed with CM from Renca cells cultured in normoxia or hypoxia (1:1). The formation of tube-like structures was observed by video microscopy, using an inverted Microscope Zeiss AxioObserver.7 (Zeiss, Germany), in real time. After 4 h, photographs were taken of each well. Number of nodes and junctions were examined using ImageJ Angiogenesis software (in cooperation with dr Maria Paprocka, Ludwik Hirsfeld Institute of Immunology and Experimental Therapy, Polish Academy of Sciences, Wrocław, Poland).

VEGF quantification by ELISA

Level of VEGF was measured in supernatants from cells cultured in normoxic and hypoxic conditions using commercially available enzyme-linked immunosorbent assay, specific for natural and recombinant mouse VEGF (ELISA, R&D Systems, USA). The test was carried out according to the supplier's guidelines. The results were normalized to 10⁶ cells.

Mbr MEC FVB monolayer permeability assessment

MBr MEC FVB monolayer permeability was assessed in the presence of CM from Renca cells cultured in normoxia and hypoxia. A model of the blood brain barrier and a permeability test was performed according to Wilhelm et al. (Wilhelm et al. 2011). Briefly, MBr MEC FVB were seeded on collagen IV and Fibronectin-coated 0.4 µmol/L Transwell filters. After

reaching confluence, factors increasing the barrier tightness (hydrocortisone, cAMP, RO) were added for 5 h with or without CM from Renca cells. Then sodium fluorescein was added to the upper layer of the filter and fluorescence measurements were made in the lower layer after 1 h and 5 h using FLUOstar Omega (BMG LabTech, Germany).

Cytokine secretion measurement by membrane protein array

The secretory potential of Renca and B16 F10 cells was measured in cell culture supernatants using Proteome Profiler Mouse XL Cytokine Array (R&D Systems, USA) according to the manufacturer's instructions. Briefly, membranes were blocked with Array Buffer 6 for 1 h, the CM was added to membranes (1 mL CM with 0.5 mL Array Buffer4) and incubated overnight at 4 °C. After the washing, step membranes were incubated in Detection Biotin-labeled-antibody Cocktail diluted in the Array Buffer 4/6 for a 1 h incubation. Washing was repeated, and then streptavidin-horseradish peroxidase was incubated for 30 min and further allowed to react with the ChemiReagent Mix. The chemiluminescent signal on the membranes was detected using X-ray films (Carestream Health, Rochester). Quantification of the IOD of the spots was performed using analysis software ImageJ. The results were normalized to references spots and 10⁶ cells.

Statistical analysis

Each experiment was performed at least 3 times in independent biological replicates. The results are shown as a mean ± SEM, where appropriate results are presented as fold change as compared to normoxia. All statistical analyses were performed using GraphPad Prism 9.0 software. Statistical test was chosen dependent on the Gaussian distribution and is indicated in the figure captions.

Results

Hypoxia inhibits PTEN expression and activation in both melanoma and RCC models

Beneficial results of ITPP treatment shown previously in melanoma (Kieda et al. 2013) were not achieved in the kidney cancer model (Supplementary Figs. S1A–S1C), using the same dose and treatment scheme. Therefore, a comparison of B16 F10 cells and Renca cells at the level of hypoxia-regulated PTEN changes and pro-angiogenic potential was assessed in vitro to identify the molecular background of different response to treatment. Due to the diversity of PTEN functions related to different signaling pathways and subcellular localization (Fusco et al. 2020), its status and activity in tumor cells in response to hypoxia was comprehensively determined.

PTEN mRNA in both melanoma and RCC was not significantly changed after exposure to hypoxia (Fig. 1A), while both cell lines were characterized by a lower total amount of PTEN protein in low pO₂ (what we showed previously in Renca cells (Majewska et al. 2022) resulting in the relative predominance of the inactive phosphorylated form—pPTEN (Figs. 1B–1D). Hypoxic Renca cells displayed also a lower relative fluorescence intensity corresponding to PTEN expres-

sion when assessed by microscopy (Fig. 1F); localization was cytoplasmic and nuclear in normoxia and appeared mostly nuclear in hypoxic cells. This was confirmed when cytosolic and nuclear fractions were checked separately by Western blot (Supplementary Figs. S2A and S2B). PTEN downregulation in hypoxia was also confirmed by flow cytometry analysis (Fig. 1E). PTEN + cells in normoxia were estimated at about 56.87% ($\pm 0.78\%$) and in hypoxia 45.54% ($\pm 1.1\%$). As a permeabilization kit for cytoplasmic staining was used, it cannot be excluded that the unstained population may contain PTEN + cells with nuclear localization only.

Hypoxia-induced PTEN downregulation distinctly affects the PI3K/AKT pathway in melanoma and the MDM2/p53 axis in RCC cells

Despite a similar response to low pO₂ in terms of regulating PTEN level and activity, significant differences were observed in the hypoxia-dependent regulation of PTEN-related pathways between melanoma and kidney cancer models. As the phosphatase activity of PTEN is the direct negative regulator of PI3K signaling, a main modulator for cell growth, metabolism, and survival, the levels of PI3K and AKT in hypoxic cells were evaluated. pAKT accumulation upon hypoxia-induced PTEN inactivation was observed only in melanoma cells (Figs. 2A, 2B). RCC cells did not express detectable pAKT in both tested oxygen conditions (Figs. 2A, 2B), despite the strong upregulation of pAKT in *Pten* knock-out Renca cells (Majewska et al. 2022). This may indicate that the remaining PTEN activity in the AKT pathway is sufficient regardless of the downregulation due to hypoxia. *Akt* transcript level was decreased in both cell lines in response to low pO₂ (Fig. 2D); however, only RCC cells showed a strong tendency to decrease the AKT protein level as well (Figs. 2A, 2C). The downregulation of the *Akt* transcript suggests a different pathway regulating *Akt* expression in hypoxia, independently of PTEN activity. At the same time, as the total level of PI3K protein decreased under hypoxia in both models (Fig. 2E), it implies that the activity is here more significant than gene expression.

As PTEN was shown to protect p53 from degradation, the activation of this pathway was checked. Indeed, in PTEN-reduced hypoxic cells, the downregulation of *p53* mRNA was observed (Fig. 2G), but no change in p53 inhibitor—*Mdm2*—was displayed (Fig. 2H). However, as both the transcript and protein levels of p53 were reduced, an additional transcriptional regulation of p53 by low pO₂ apart from PTEN-p53 direct interaction might be involved. Additionally, in Renca cells, the pMDM2 active form of the molecule dominated over the total MDM2, which tended to be reduced in hypoxia; this explains the downregulation of p53 activity in addition to the simultaneous decrease of the p53 protein level (Figs. 2E, 2I). This effect was not observed in B16 F10 as pMDM2 was not detected in these cells.

Hypoxia strongly influences the proangiogenic potential of RCC cells

The differential modulation of the PTEN versus MDM2 and p53 activity in tested cell lines prompted us to test proangiogenic

potential of cancer cells in response to hypoxic condition. In response to low pO₂, the increase of *Hif-1 α* expression was not visible after a prolonged exposure to hypoxia (Fig. 3A), but one of its downstream genes—*Vegf-a*—was upregulated in both cell lines (Fig. 3B). Accordingly, the level of the VEGF-A secreted protein was elevated (Fig. 3C). The proangiogenic potential of cancer cells was assessed using the endothelial progenitor cells (EPCs)—MAGEC11.5—that were not spontaneously forming pseudo-vessels in tube formation assay. The factors contained in CM from RCC cells stimulated the MAGEC11.5 to form pseudo-vessels (Fig. 3D). On the opposite, the factors secreted by B16 F10 cells (both in normoxic and hypoxic conditions) did not stimulate tube formation by MAGEC11.5, although in hypoxic-CM from B16 F10, the concentration of VEGF-A was similar to Renca normoxic-CM (Fig. 3C). This indicated that hypoxic RCC cells act by activating the secretion of proangiogenic factors that may recruit endothelial progenitors (Collet et al. 2016; Klimkiewicz et al. 2017).

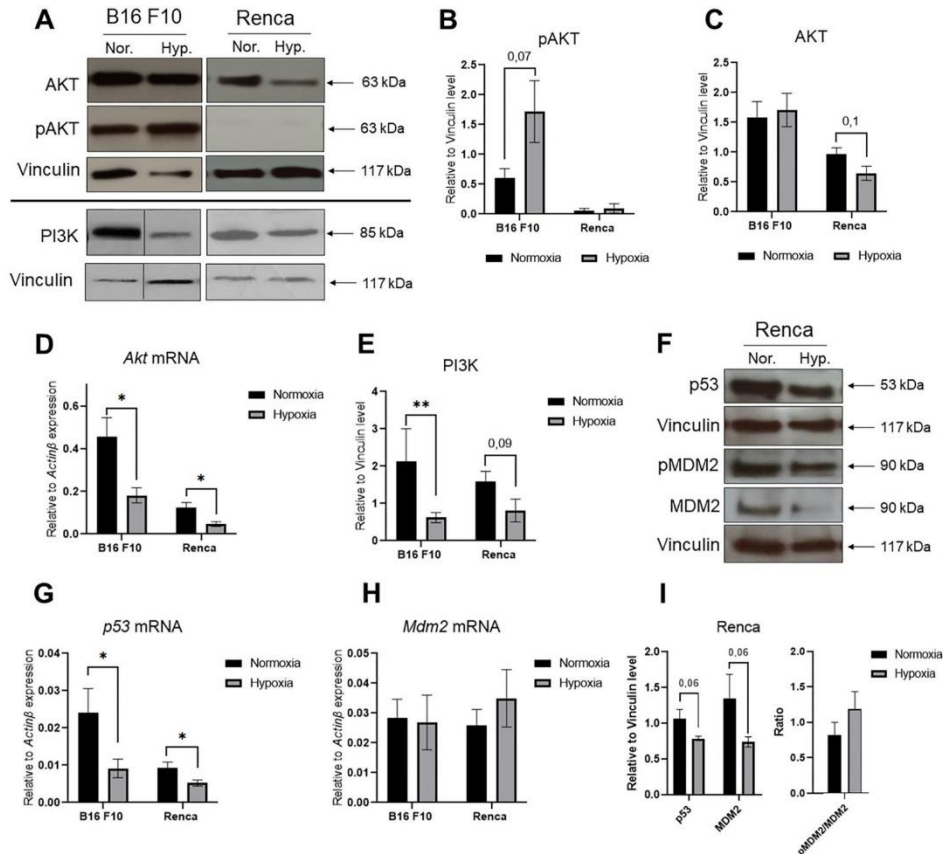
Additionally, the proangiogenic properties of the CM derived from Renca cells were also assessed using mature organospecific ECs derived from brain (MBr MEC FVB), as a model of metastatic niche for RCC. The strong potential of factors secreted by hypoxic Renca cells to form pseudo-vessels was confirmed in the tube formation assay (Figs. 4A–4C). The influence of factors contained in hypoxic-CM from Renca cells had also an impact on Claudin-1 level in MBr MEC FVB cultured with the presence of Renca CM (Figs. 4D, 4E). As Claudin-1 is responsible for tight junctions between cells, its decrease may explain the tendency to increase MBr MEC FVB monolayer permeability after addition of hypoxic-CM from Renca cells (Fig. 4F). Thus, factors secreted by RCC cells not only strongly stimulate angiogenesis, but may also be associated with the destabilization of EC barrier function and the formation of metastatic niches for tumor cells.

To identify the other secretory factors than VEGF-A, which could be responsible for the higher proangiogenic activity of Renca cells than B16 F10, the conditioned media were assayed for the presence of 111 cytokines and chemokines. RCC cells had a higher secretory potential and produced 16 factors at detectable level, while melanoma cells produced only 11 such factors, considering the threshold of detection. Low pO₂ increased the level of most factors in both cell lines (Figs. 5A and 5B). Proangiogenic factors present in RCC medium only, which production was increased by hypoxia, were CCL2, CXCL1, FGF21, and IGFBP-6 (Figs. 5A and 5B). Factors upregulated in response to low pO₂ common to both models were Osteopontin and VEGF-A, while the distinct modulation of FGF21 and IGFBP-6 indicates the involvement of other hypoxia-dependent-mechanisms than the HIFs/VEGF-related pathways.

Discussion

In RCC, low PTEN level was associated with an unfavorable outcome and a significant association of negative PTEN expression with poor progression-free survival was shown in patients with metastasis and treated by antiangiogenic therapy (Sunitinib and Sorafenib) (Sekino et al. 2020); however, its

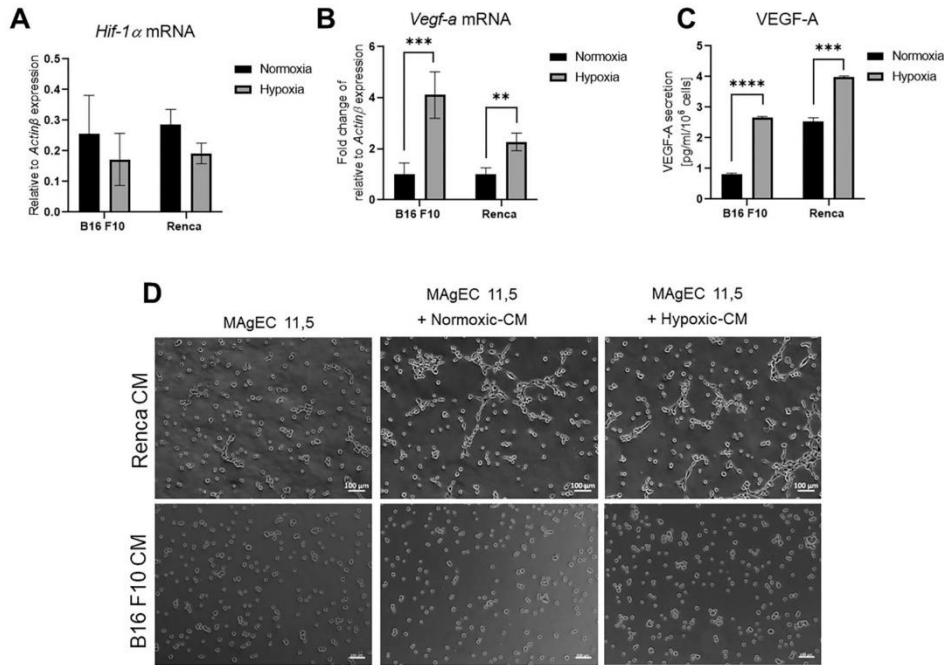
Fig. 2. Effect of hypoxia on PI3K/AKT and p53 signaling pathways in Renca and B16 F10 cells. (A) AKT, pAKT, and PI3K detection by Western blots with Vinculin as loading control in Renca and B16 F10 cells cultured in normoxia and hypoxia; the representative band for PI3K with loading control (Vinculin) in B16 F10 cells was cropped from different parts of the same membrane; the representative band for PI3K with loading control (Vinculin) in Renca cells was obtained in the same blot as PTEN and pPTEN presented in Fig. 1B Renca panel. (B) Quantification of the pAKT expression relative to Vinculin level ($n > 3$; t Student test for B16 F10; Mann-Whitney test for Renca). (C) Quantification of the AKT expression relative to Vinculin level ($n > 3$; Mann-Whitney test for B16 F10; t Student test for Renca). (D) Relative to Actin β expression of Akt gene $^*P < 0.05$ ($n = 3$; t Student test). (E) Quantification of the PI3K expression relative to Vinculin level $^{**}P < 0.01$ ($n > 3$; Mann-Whitney test for B16 F10; t Student test for Renca). (F) p53, MDM2, and pMDM2 detection by Western blots with Vinculin as loading control in Renca cells cultured in normoxia and hypoxia. (G) Relative to Actin β expression of p53 gene $^*P < 0.05$ ($n > 3$; Mann-Whitney test for B16 F10; t Student test for Renca). (H) Relative to Actin β expression of Mdm2 gene ($n > 3$; Mann-Whitney test). (I) Quantification of the p53, MDM2 levels, and ratio pMDM2/MDM2 relative to Vinculin ($n > 3$; Mann-Whitney test).



prognostic value remains controversial (Tang et al. 2017). In our study, long-term low pO_2 resulted in the downregulation of PTEN, mainly in terms of its cytoplasmic localization in Renca cells. The pPTEN/PTEN ratio increased in both RCC and melanoma cells, as also shown in lung cancer cells (Kohnoh et

al. 2016). The global amount of pPTEN remained unchanged in both oxygen conditions and simultaneously, no effect of hypoxia was observed at the level of transcript. It suggests that the PTEN decrease due to hypoxia could be mediated by protein degradation, especially as shown previously, PTEN

Fig. 3. Hypoxic response in melanoma and RCC models and impact on EPC's ability to form angiogenesis. (A) Relative to Actin β expression of Hif-1 α gene in B16 F10 and Renca cells culture in normoxia and hypoxia ($n > 3$, Mann-Whitney test). (B) Relative to Actin β expression of Vegf-a gene in B16 F10 and Renca cell culture in normoxia and hypoxia. $**P < 0.01$ $***P < 0.001$ ($n > 3$, Mann-Whitney test) shown as a fold change relative to normoxia. (C) Quantification of the VEGF-A secretion by B16 F10 and Renca cells cultured in normoxia and hypoxia measured by ELISA (normalized to 106 cells). $***P < 0.001$ $****P < 0.0001$ ($n = 3$; t Student test). (D) The images show tube-like structures formed by MAgEC 11.5 with or without the presence of normoxic- or hypoxic-CM from B16 F10 or Renca cells (scale bar: 100 μ m).



Biochem. Cell Biol. Downloaded from cdnsiencepub.com by Aleksandra Majewska on 09/08/23
For personal use only.

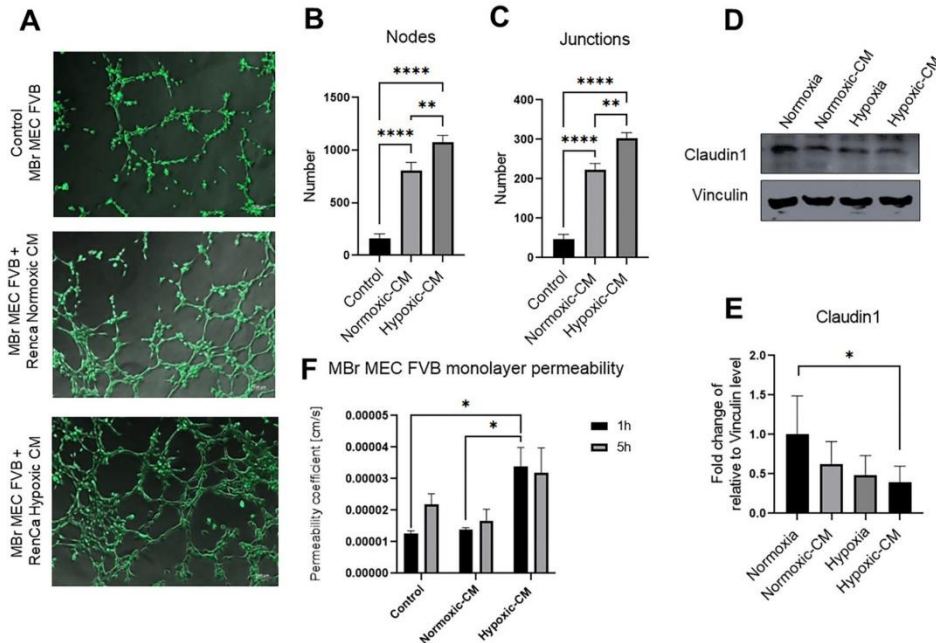
ubiquitinating enzymes (including Nedd4-1 and XIAP) are induced by low pO_2 (Yalcin et al. 2019), while PTEN deubiquitinating enzyme, ubiquitin C-terminal hydrolase 13 (USP13) is reduced (Geng et al. 2015). However, PTEN downregulation, induced by hypoxia, was not potent enough to induce concurrent PI3K activation and consequently led to pAKT accumulation in RCC cells, what is usually observed upon PTEN downregulation (Jung et al. 2013; Majewska et al. 2022). On the contrary, in both cell lines, level of total PI3K was significantly reduced; however, pAKT was increased in melanoma cells only. Considering the fact that hypoxia permitted us to evidence new mechanisms that are not discovered in commonly used normoxic conditions, the present hypoxia-mediated differences in both models related to the canonical roles of PTEN, prompting us to deepen the approach of other PTEN-related pathways.

PTEN directly regulates p53; it mediates p53 stabilization independently of PI3K/AKT/MDM2 and this interaction in-

creases p53 transcriptional activity (Freeman et al. 2003). Possibly the observed lower amount of PTEN resulted in an increased degradation of p53 mRNA in hypoxic cells. As AKT was shown to promote p53 degradation (Ogawara et al. 2002), it could mediate additional p53 down-regulation in melanoma cells. This mechanism was not activated in RCC cells but p53 expression was reduced by low pO_2 , suggesting a PTEN-independent regulation. In Renca cells, PTEN may act principally through the MDM2-dependant regulation of p53, while in B16 F10 cells regulation occurs predominantly through the pAKT activation. Hypoxia-induced changes in PTEN-related pathways differ in melanoma and RCC models that may cause differences in the expression therapeutic targets between both tested models and consequently their different responses to treatment of these cancer types.

To further understand the variances displayed by those two cell lines, in response to low pO_2 , their proangiogenic potential was studied comparatively. After exposure to hypoxia, a

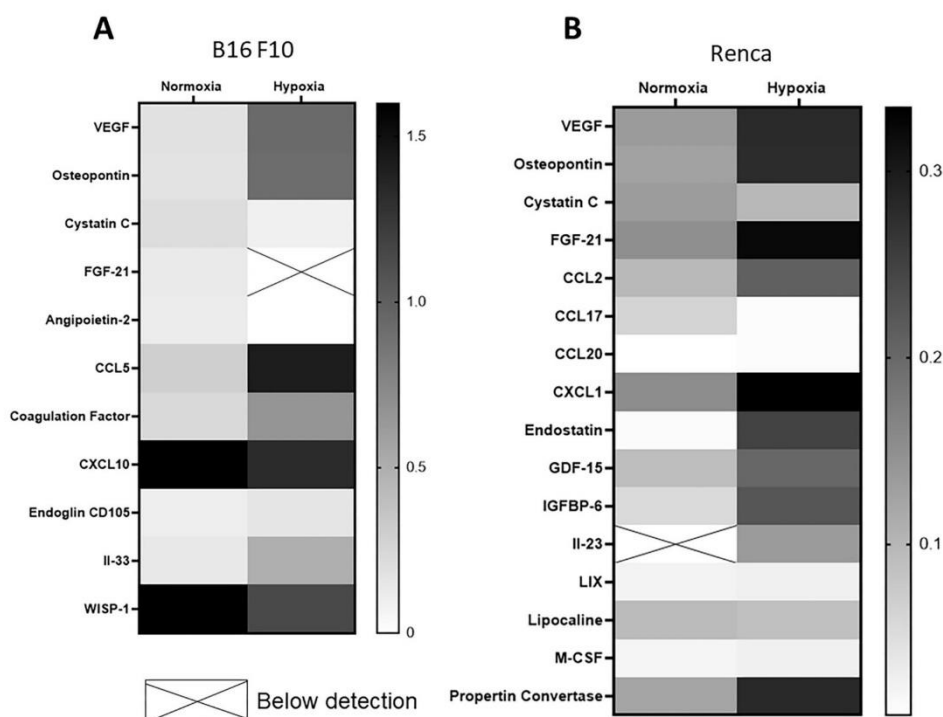
Fig. 4. Influence of hypoxia-induced factors secreted by Renca cells on MBr MEC FVB functions. (A) Tube-like structures formed by calcein-stained MBr MEC FVB with or without the presence of normoxic- or hypoxic-CM from Renca cells (scale bar: 100 μ m). (B and C) Quantification of the ability to form a pseudo-vessels by calcein-stained MBr MEC FVB with and without the presence of CM from Renca cells, measured by the number of nodes, $^{**}P < 0.01$, $^{****}P < 0.0001$ ($n = 3$; one-way Anova). (D) Claudin1 detection in MBr MEC FVB cells cultured in normoxia and hypoxia with or without CM from Renca cells by Western blots with Vinculin as a loading control. (E) Quantification of the Claudin1 expression in MBr MEC FVB cells cultured in normoxia and hypoxia with or without CM from Renca cells relative to Vinculin level $P < 0.05$ ($n >$; one-way Anova) shown as a fold change relative to normoxia. (F) Permeability coefficient measured in MBr MEC FVB monolayer in the presence of factors derived from Renca cells, measurement after 1 and 5 h.



strong increase in VEGF-A expression and secretion was observed in both tested models, which is characteristic of long-term hypoxia after stabilization of HIF1a (Calvani et al. 2012). We show that the factors secreted by RCC cells can mobilize EC progenitors to form pseudo-vessels rapidly (4 h), and this effect is stronger for factors secreted in hypoxia. Melanoma cells were not potent to induce this effect, even when pro-angiogenic of VEGF was produced. Nevertheless, it was shown that melanoma cells in 3D culture actively recruit preferentially early EPCs, as opposed to differentiated ECs (Collet et al. 2016; Klimkiewicz et al. 2017). Here, the strong pro-angiogenic effect of RCC was also demonstrated using mature organospecific ECs. Indeed, Renca cell-derived products were able to induce angiogenesis ability of MBr MEC FVB in vitro, which was further intensified by exposure to low pO_2 . Hypoxic RCC CM additionally affected ECs by downregulation of Claudin1. Repression of Claudin1, a tight junction protein

(Sladojevic et al. 2019), could mediate endothelium leakage as it increased ECs' monolayer permeability after exposure to hypoxic RCC CM. Oversecretion of pro-angiogenic factors by RCC cells in hypoxia deregulated EC activity and consequently led to pathological angiogenesis, which is a hallmark of cancer (Huang et al. 2019). Differences in pro-angiogenic properties of melanoma and RCC cells pointed to several factors produced by Renca cells and upregulated in low pO_2 as opposed to B16 F10 cells. Among them, CCL2 (MCP-1), CXCL1, FGF21, and IGFBP-6 are well described pro-angiogenic factors, mostly hypoxia-induced (Stamatovic et al. 2006; Mojsilovic-Petrovic et al. 2007; Huang et al. 2019; Ma et al. 2021). CXCL1, highly expressed in hypoxia in Renca cells, plays a key role in angiogenesis, by affecting EC proliferation and migration (Ma et al. 2021). The value of FGF21 in the mobilization and infiltration of EPCs into ischemic tissues has been demonstrated in diabetes model (Dai et al. 2021). CCL20, secreted only by

Fig. 5. Secretory potential of B16 F10 and Renca cells cultured in normoxia and hypoxia in relation to angiogenesis. Heat maps of results from Cytokine Membrane Array showing the secretory potential of (A) B16 F10 and (B) Renca cells cultured in normoxia and hypoxia.



Biochem. Cell Biol. Downloaded from cbsciencenpub.com by Aleksandra Majewska on 09/08/23 For personal use only.

Renca cells, but stable between oxygen conditions, is a direct proangiogenic factor for cells that possess the CCR6 receptors as ECs from the macro and microvasculature (Collet et al. 2016; Klimkiewicz et al. 2017; Benkheil et al. 2018). Noticeably, Osteopontin, which is an ECM (ECM) glycoprotein with many modulating functions, is here highly induced by hypoxia in both models indicating a common influence on the migration abilities of the cancer cells in low pO₂ microenvironment (Zhao et al. 2018). Osteopontin induces angiogenesis through activation of PI3K/AKT and ERK1/2 in ECs (Dai et al. 2009); however, the PI3K/AKT pathway was differentially regulated in both tested models. Thus, the pro-angiogenic potential and hypoxia-mediated EC-activating capacity differ between RCC and melanoma models.

Stable, long-lasting vessel normalization is a promising therapeutic approach with proven effects in the melanoma model (Kieda et al. 2013), but not in RCC. The application of the dose and schedule of ITTP treatment effective in melanoma did not achieve positive results in RCC. Differences in hypoxia-dependent PTEN dysregulation and proan-

giogenic response, observed in vitro in this study, may be crucial to the treatment outcome. The growth of Renca tumors and the need to discontinue the in vivo experiment (due to animal welfare related to the size of tumors), but also the potential inappropriate dose adjustment to the dynamic of the tumor, could have had a significant impact on the ITTP efficacy. Therefore, the differences on cellular and molecular level in various cancer cells need to be taken into account not only when choosing the therapy target, but also when designing the scheme of intervention to identify proper treatment window.

Conclusions

The similar response of PTEN activity (decrease PTEN and domination of pPTEN) in hypoxia observed in RCC and melanoma led to completely distinct molecular responses. Moreover, the pro-angiogenic potential of both cell types is different. These differences may be of key importance for the vessel normalization approaches to select proper treatment

attitude. It points to the necessity of controlled vascular normalization in such highly angiogenic tumor as RCC.

Acknowledgements

Authors are especially indebted to prof Józef Dulak from the Department of Medical Biotechnology, Faculty of Biochemistry, Biophysics and Biotechnology, Jagiellonian University, Cracow, Poland, for providing the B16 F10 cell line and Dr. Maria Paprocka from Hirsfeld Institute of Immunology and Experimental Therapy, Polish Academy of Sciences, who has been supportive of methodology of EC culture.

Article information

History dates

Received: 22 February 2023

Accepted: 22 June 2023

Accepted manuscript online: 17 July 2023

Version of record online: 29 August 2023

Copyright

© 2023 The Author(s). Permission for reuse (free in most cases) can be obtained from [creativecommons.org](https://creativecommons.org/licenses/by/4.0/).

Data availability

Data generated or analyzed during this study are provided in full within the published article and its supplementary materials.

Author information

Author ORCIDs

Aleksandra Majewska <https://orcid.org/0000-0003-1271-4679>

Author contributions

Conceptualization: CK

Data curation: AM, KB

Formal analysis: AM, KB

Funding acquisition: CK

Investigation: AM, KB, AF-D

Methodology: AM, KB, AF-D, CK

Supervision: CK

Writing – original draft: AM, KB, CK

Writing – review & editing: AM, KB, AF-D, CK

Competing interests

The authors declare no competing interest.

Funding information

The research was funded by National Science Centre grant no 2016/23/B/NZ1/03211 and subvention of the Ministry of Education and Science, project no. 1/8974 (519). AF-D was supported by European Social Fund: POWER “Next generation sequencing technologies in biomedicine and personalized medicine.”

Supplementary material

Supplementary data are available with the article at <https://doi.org/10.1139/bcb-2023-0047>.

References

- Baluk, P., Hashizume, H., and McDonald, D.M. 2005. Cellular abnormalities of blood vessels as targets in cancer. *Curr. Opin. Genet. Dev.* **15**(1): 102–111. doi:10.1016/j.gde.2004.12.005. PMID: 15661540.
- Benkheil, M., Van Haele, M., Roskams, T., Laporte, M., Noppen, S., Abbasi, K., et al. 2018. Ccl20, a direct-acting pro-angiogenic chemokine induced by hepatitis c virus (HCV): potential role in HCV-related liver cancer. *Exp. Cell. Res.* **372**(2): 168–177. doi:10.1016/j.yexcr.2018.09.023. PMID: 30287142.
- Bizouarne, N., Denis, V., Legrand, A., Monsigny, M., and Kieda, C. 1993. A SV-40 immortalized murine endothelial cell line from peripheral lymph node high endothelium expresses a new alpha-fucose binding protein. *Biol. Cell.* **79**(3): 209–218. doi:10.1016/0248-4900(93)90139-6. PMID: 7516229.
- Bratslavsky, G., Sudarshan, S., Neckers, L., and Linehan, W.M. 2007. Pseudohypoxic pathways in renal cell carcinoma. *Clin. Cancer Res.* **13**(16): 4667–4671. doi:10.1158/1078-0432.CCR-06-2510. PMID: 17699843.
- Calvani, M., Comito, G., Giannoni, E., and Chiarugi, P. 2012. Time-dependent stabilization of hypoxia inducible factor-1alpha by different intracellular sources of reactive oxygen species. *PLoS ONE*, **7**(10): e38388. doi:10.1371/journal.pone.0038388. PMID: 23144690.
- Collet, G., Szade, K., Nowak, W., Klimkiewicz, K., El Hafny-Rahbi, B., Szczepanek, K., et al. 2016. Endothelial precursor cell-based therapy to target the pathologic angiogenesis and compensate tumor hypoxia. *Cancer Lett.* **370**(2): 345–357. doi:10.1016/j.canlet.2015.11.008. PMID: 26577811.
- Dai, J., Peng, L., Fan, K., Wang, H., Wei, R., Ji, G., et al. 2009. Osteopontin induces angiogenesis through activation of pi3k/akt and erk1/2 in endothelial cells. *Oncogene*, **28**(38): 3412–3422. doi:10.1038/onc.2009.189. PMID: 19597469.
- Dai, Q., Fan, X., Meng, X., Sun, S., Su, Y., Ling, X., et al. 2021. FgF21 promotes ischaemic angiogenesis and endothelial progenitor cells function under diabetic conditions in an AMPK/NAD+ dependent manner. *J. Cell Mol. Med.* **25**(6): 3091–3102. doi:10.1111/jcmm.16369. PMID: 33599110.
- El Hafny-Rahbi, B., Brodaczewska, K., Collet, G., Majewska, A., Klimkiewicz, K., Delalande, A., et al. 2021. Tumour angiogenesis normalized by myo-inositol trispyrophosphate alleviates hypoxia in the microenvironment and promotes antitumor immune response. *J. Cell. Mol. Med.* **25**(7): 3284–3299. doi:10.1111/jcmm.16399. PMID: 33624446.
- Folkman, J. 1971. Tumor angiogenesis: therapeutic implications. *N. Engl. J. Med.* **285**(21): 1182–1186. PMID: 4938153.
- Folkman, J. 2002. Role of angiogenesis in tumor growth and metastasis. *Semin. Oncol.* **29**(6 Suppl 16): 15–18. doi:10.1053/sonc.2002.37263. PMID: 12516034.
- Freeman, D.J., Li, A.G., Wei, G., Li, H.H., Kertesz, N., Lesche, R., et al. 2003. PTEN tumor suppressor regulates p53 protein levels and activity through phosphatase-dependent and -independent mechanisms. *Cancer Cell.* **3**(2): 117–130. doi:10.1016/S1535-6108(03)00021-7. PMID: 12620407.
- Fusco, N., Sajjadi, E., Venetis, K., Gaudioso, G., Lopez, G., Corti, C., et al. 2020. PTEN alterations and their role in cancer management: Are we making headway on precision medicine? *Genes (Basel)*, **11**(7). doi:10.3390/genes11070719.
- Geng, J., Huang, X., Li, Y., Xu, X., Li, S., Jiang, D., et al. 2015. Down-regulation of USP13 mediates phenotype transformation of fibroblasts in idiopathic pulmonary fibrosis. *Respir. Res.* **16**: 124. doi:10.1186/s12931-015-0286-3. PMID: 26453058.
- Global Cancer Observatory. n.d. Available from <https://gco.iarc.fr/> [accessed 2023].
- Goel, S., Wong, A.H., and Jain, R.K. 2012. Vascular normalization as a therapeutic strategy for malignant and nonmalignant disease. *Cold Spring Harb. Perspect. Med.* **2**(3): a006486. doi:10.1101/eshperspect.a006486. PMID: 22393532.

- Grzymajlo, K., El Hafny-Rahbi, B., and Kieda, C. 2023. Tumour suppressor pten activity is differentially inducible by myo-inositol phosphates. *J. Cell. Mol. Med.* **27**(6): 879–890. doi:10.1111/jcmm.17699. PMID: 36852461.
- Hashizume, H., Baluk, P., Morikawa, S., McLean, J.W., Thurston, G., Roberge, S., et al. 2000. Openings between defective endothelial cells explain tumor vessel leakiness. *Am. J. Pathol.* **156**(4): 1363–1380. doi:10.1016/S0002-9440(10)65006-7. PMID: 10751361.
- Hayashi, Y., Yokota, A., Harada, H., and Huang, G. 2019. Hypoxia/pseudohypoxia-mediated activation of hypoxia-inducible factor-1alpha in cancer. *Cancer Sci.* **110**(5): 1510–1517. doi:10.1111/cas.13990. PMID: 30844107.
- Huang, J., and Kontos, C.D. 2002. Pten modulates vascular endothelial growth factor-mediated signaling and angiogenic effects. *J. Biol. Chem.* **277**(13): 10760–10766. doi:10.1074/jbc.M1110219200. PMID: 11784722.
- Huang, W., Shao, M., Liu, H., Chen, J., Hu, J., Zhu, L., et al. 2019. Fibroblast growth factor 21 enhances angiogenesis and wound healing of human brain microvascular endothelial cells by activating PPARgamma. *J. Pharmacol. Sci.* **140**(2): 120–127. doi:10.1016/j.jpshs.2019.03.010. PMID: 31255518.
- Jain, R.K. 2001. Normalizing tumor vasculature with anti-angiogenic therapy: a new paradigm for combination therapy. *Nat. Med.* **7**(9): 987–989. doi:10.1038/nm0901-987. PMID: 11533692.
- Jung, S., Li, C., Jeong, D., Lee, S., Ohk, J., Park, M., et al. 2013. Oncogenic function of p34SEI-1 via NEDD4-1-mediated PTEN ubiquitination/degredation and activation of the PI3K/AKT pathway. *Int. J. Oncol.* **43**(5): 1587–1595. doi:10.3892/ijo.2013.2064. PMID: 23970032.
- Kieda, C., El Hafny-Rahbi, B., Collet, G., Lamerant-Fayel, N., Grillon, C., Guichard, A., et al. 2013. Stable tumor vessel normalization with pO₂ increase and endothelial PTEN activation by inositol trispyrophosphate brings novel tumor treatment. *J. Mol. Med. (Berl.)* **91**(7): 883–899. doi:10.1007/s00109-013-0992-6. PMID: 23471434.
- Klimkiewicz, K., Weglarczyk, K., Collet, G., Paprocka, M., Guichard, A., Sarna, M., et al. 2017. A 3D model of tumour angiogenic microenvironment to monitor hypoxia effects on cell interactions and cancer stem cell selection. *Cancer Lett.* **396**: 10–20. doi:10.1016/j.canlet.2017.03.006. PMID: 28288873.
- Kohnoh, T., Hashimoto, N., Ando, A., Sakamoto, K., Miyazaki, S., Aoyama, D., et al. 2016. Hypoxia-induced modulation of PTEN activity and EMT phenotypes in lung cancers. *Cancer Cell. Int.* **16**: 33. doi:10.1186/s12935-016-0308-3. PMID: 27095949.
- Li, A.G., Piluso, L.G., Cai, X., Wei, G., Sellers, W.R., and Liu, X. 2006. Mechanistic insights into maintenance of high p53 acetylation by PTEN. *Mol. Cell.* **23**(4): 575–587. doi:10.1016/j.molcel.2006.06.028. PMID: 16916644.
- Liao, D., and Johnson, R.S. 2007. Hypoxia: a key regulator of angiogenesis in cancer. *Cancer Metastasis Rev.* **26**(2): 281–290. doi:10.1007/s10555-007-9066-y. PMID: 17603752.
- Lugano, R., Ramachandran, M., and Dimberg, A. 2020. Tumor angiogenesis: causes, consequences, challenges and opportunities. *Cell. Mol. Life Sci.* **77**(9): 1745–1770. doi:10.1007/s00018-019-03351-7. PMID: 31690961.
- Ma, C., Liu, G., Liu, W., Xu, W., Li, H., Piao, S., et al. 2021. Cxcl1 stimulates decidual angiogenesis via the VEGF-A pathway during the first trimester of pregnancy. *Mol. Cell. Biochem.* **476**(8): 2989–2998. doi:10.1007/s11010-021-04137-x. PMID: 33770315.
- Majewska, A., Brodaczewska, K., Filipiak-Duliban, A., Kajdasz, A., and Kieda, C. 2022. miRNA pattern in hypoxic microenvironment of kidney cancer-role of PTEN. *Biomolecules.* **12**(5). doi:10.3390/biom12050686. PMID: 35625614.
- Makhov, P., Joshi, S., Ghatalia, P., Kutikov, A., Uzzo, R.G., and Kolenko, V.M. 2018. Resistance to systemic therapies in clear cell renal cell carcinoma: mechanisms and management strategies. *Mol. Cancer Ther.* **17**(7): 1355–1364. doi:10.1158/1535-7163.MCT-17-1299. PMID: 29967214.
- Mayo, L.D., and Donner, D.B. 2001. A phosphatidylinositol 3-kinase/Akt pathway promotes translocation of Mdm2 from the cytoplasm to the nucleus. *Proc. Natl. Acad. Sci. U. S. A.* **98**(20): 11598–11603. doi:10.1073/pnas.181181198. PMID: 11504915.
- Mazzone, M., Dettori, D., de Oliveira, R.L., Loges, S., Schmidt, T., Jonckx, B., et al. 2009. Heterozygous deficiency of PHD2 restores tumor oxygenation and inhibits metastasis via endothelial normalization. *Cell.* **136**(5): 839–851. doi:10.1016/j.cell.2009.01.020. PMID: 19217150.
- McDonald, D.M., and Baluk, P. 2005. Imaging of angiogenesis in inflamed airways and tumors: newly formed blood vessels are not alike and may be wildly abnormal: Parker b. Francis lecture. *Chest.* **128**(6 Suppl): 602S–608S. doi:10.1378/chest.128.6_suppl.602S-a. PMID: 16373858.
- Milella, M., Falcone, I., Conciatori, F., Cesta Incani, U., Del Curatolo, A., and Inzerilli, N. 2015. PTEN: multiple functions in human malignant tumors. *Front. Oncol.* **5**: 24. doi:10.3389/fonc.2015.00024. PMID: 25763354.
- Mojsilovic-Petrovic, J., Callaghan, D., Cui, H., Dean, C., Stanimirovic, D.B., and Zhang, W. 2007. Hypoxia-inducible factor-1 (HIF-1) is involved in the regulation of hypoxia-stimulated expression of monocyte chemoattractant protein-1 (MCP-1/CCL2) and MCP-5 (Ccl12) in astrocytes. *J. Neuroinflammation.* **4**: 12. doi:10.1186/1742-2094-4-12. PMID: 17474992.
- Nascimento-Filho, C.H.V., Webber, L.P., Borgato, G.B., Goloni-Bertollo, E.M., Squarize, C.H., and Castilho, R.M. 2019. Hypoxic niches are endowed with a protumorigenic mechanism that supersedes the protective function of pten. *FASEB J.* **33**(12): 13435–13449. doi:10.1096/fj.201900722R. PMID: 31560860.
- Ogawara, Y., Kishishita, S., Obata, T., Isazawa, Y., Suzuki, T., Tanaka, K., et al. 2002. Akt enhances mdm2-mediated ubiquitination and degradation of p53. *J. Biol. Chem.* **277**(24): 21843–21850. doi:10.1074/jbc.M109745200. PMID: 11923280.
- Paez-Ribes, M., Allen, E., Hudock, J., Takeda, T., Okuyama, H., Vinals, F., et al. 2009. Antiangiogenic therapy elicits malignant progression of tumors to increased local invasion and distant metastasis. *Cancer Cell.* **15**(3): 220–231. doi:10.1016/j.ccr.2009.01.027. PMID: 19249680.
- Rini, B.I., and Small, E.J. 2005. Biology and clinical development of vascular endothelial growth factor-targeted therapy in renal cell carcinoma. *J. Clin. Oncol.* **23**(5): 1028–1043. doi:10.1200/JCO.2005.01.186. PMID: 15534359.
- Rong, Y., Post, D.E., Pieper, R.O., Durden, D.L., Van Meir, E.G., and Brat, D.J. 2005. PTEN and hypoxia regulate tissue factor expression and plasma coagulation for glioblastoma. *Cancer Res.* **65**(4): 1406–1413. doi:10.1158/0008-5472.CAN-04-3376. PMID: 15735028.
- Sato, Y. 2011. Persistent vascular normalization as an alternative goal of anti-angiogenic cancer therapy. *Cancer Sci.* **102**(7): 1253–1256. doi:10.1111/j.1349-7006.2011.01929.x. PMID: 21401807.
- Sekino, Y., Hagura, T., Han, X., Babasaki, T., Goto, K., Inoue, S., et al. 2020. PTEN is involved in Sunitinib and Sorafenib resistance in renal cell carcinoma. *Anticancer Res.* **40**(4): 1943–1951. doi:10.21873/anticancer.14149. PMID: 32234883.
- Serra, H., Chivite, I., Angulo-Urarte, A., Soler, A., Sutherland, J.D., Arruabarrena-Aristorena, A., et al. 2015. PTEN mediates notch-dependent stalk cell arrest in angiogenesis. *Nat. Commun.* **6**: 7935. doi:10.1038/ncomms8935. PMID: 26228240.
- Siegel, R.L., Miller, K.D., Wagle, N.S., and Jemal, A. 2023. Cancer statistics, 2023. *CA Cancer J. Clin.* **73**(1): 17–48. doi:10.3322/caac.21763. PMID: 36633525.
- Sladojevich, N., Stamatovic, S.M., Johnson, A.M., Choi, J., Hu, A., Dithmer, S., et al. 2019. Claudin-1-dependent destabilization of the blood-brain barrier in chronic stroke. *J. Neurosci.* **39**(4): 743–757. doi:10.1523/JNEUROSCI.1432-18.2018. PMID: 30504279.
- Stahl, J.M., Cheung, M., Sharma, A., Trivedi, N.R., Shanmugam, S., and Robertson, G.P. 2003. Loss of PTEN promotes tumor development in malignant melanoma. *Cancer Res.* **63**(11): 2881–2890. PMID: 12782594.
- Stamatovic, S.M., Keep, R.F., Mostarica-Stojkovic, M., and Andjelkovic, A.V. 2006. CCL2 regulates angiogenesis via activation of Ets-1 transcription factor. *J. Immunol.* **177**(4): 2651–2661. doi:10.4049/jimmunol.177.4.2651. PMID: 16888027.
- Tang, L., Li, X., Gao, Y., Chen, L., Gu, L., Chen, J., et al. 2017. Phosphatase and tensin homolog (PTEN) expression on oncologic outcome in renal cell carcinoma: a systematic review and meta-analysis. *PLoS ONE.* **12**(7): e0179437. doi:10.1371/journal.pone.0179437. PMID: 28672019.
- Tian, T., Nan, K.J., Wang, S.H., Liang, X., Lu, C.X., Guo, H., et al. 2010. PTEN regulates angiogenesis and VEGF expression through phosphatase-dependent and independent mechanisms in HepG2 cells. *Carcinogenesis.* **31**(7): 1211–1219. doi:10.1093/carcin/bgq085. PMID: 20430845.

Wilhelm, I., Fazakas, C., and Krizbai, I.A. 2011. In vitro models of the blood-brain barrier. *Acta. Neurobiol. Exp. (Wars)*, **71**(1): 113–128. PMID: 21499332.

Yalcin, E., Beker, M.C., Turkseven, S., Caglayan, B., Gurel, B., Kilic, U., et al. 2019. Evidence that melatonin downregulates Nedd4-1 E3 ligase and

its role in cellular survival. *Toxicol. Appl. Pharmacol.* **379**: 114686. doi:10.1016/j.taap.2019.114686. PMID: 31325559.

Zhao, H., Chen, Q., Alam, A., Cui, J., Suen, K.C., Soo, A.P., et al. 2018. The role of osteopontin in the progression of solid organ tumour. *Cell. Death Dis.* **9**(3): 356. doi:10.1038/s41419-018-0391-6. PMID: 29500465.

Biochem. Cell Biol. Downloaded from cdnsiencepub.com by Aleksandra Majewska on 09/08/23
For personal use only.

Title: Comparative analysis of the effect of hypoxia in two different tumor cell models

shows the differential involvement of PTEN control of proangiogenic pathways

Aleksandra Majewska, Klaudia Brodaczevska, Aleksandra Filipiak-Duliban and Claudine Kieda

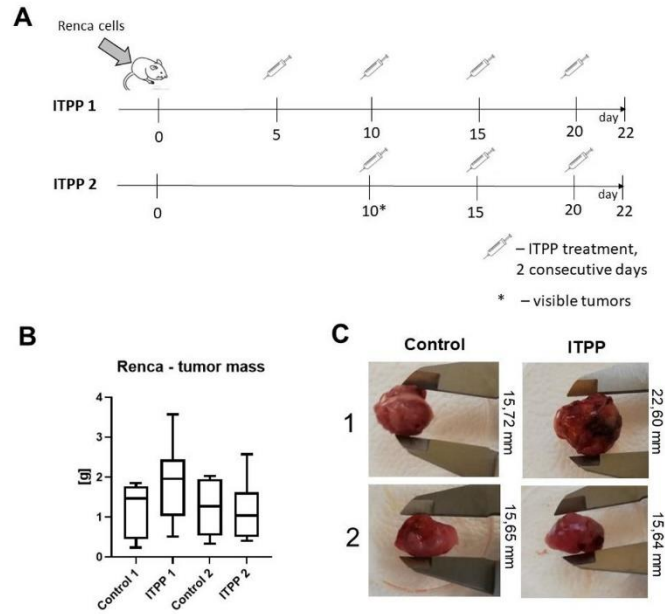


Figure 1 ITPP treatment of RCC tumors A) Scheme of the protocol of ITPP treatment in vivo B) Tumor mass [g] of Renca tumors after ITPP treatment (ITPP 1 Control 1 – ITPP/saline treatment started 5 days after cancer cells injection, ITPP 2 Control 2 – ITPP/saline treatment started 10 days after cancer cells injection C) Representative photos of tumors in each group.

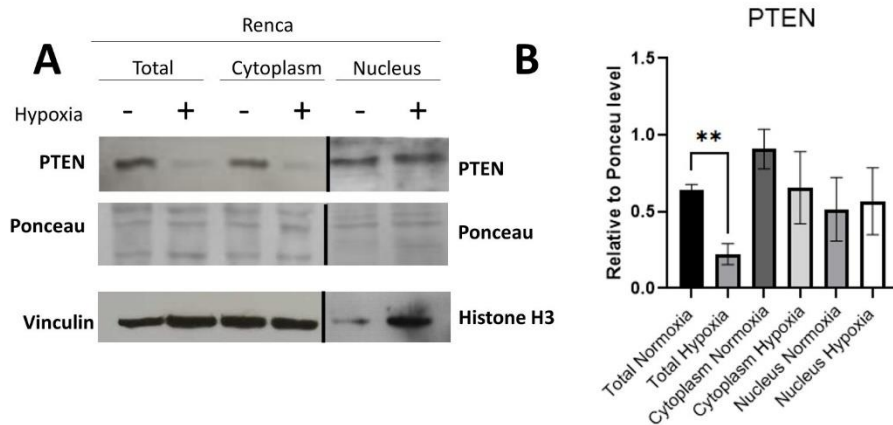


Figure 2 PTEN localization in RenCa cells cultured in normoxia and hypoxia **A)** PTEN detection by Western blotting in Renca cells in total, cytoplasmic and nuclear fractions of the cells, along with the loading controls: Ponceau staining and controls specific for the fractions (Vinculin for total and cytoplasmic and Histone H3 for nuclear **B)** Quantification of the PTEN expression in total cells and fractions (cytoplasmic and nuclear) relative to Ponceau level ******P < 0.01 (n > 3; t-Student test)

3.2 PUBLIKACJA 2

Pharmacological Reports
https://doi.org/10.1007/s43440-023-00523-y

ARTICLE



Pten knockout affects drug resistance differently in melanoma and kidney cancer

Klaudia Brodaczevska¹ · Aleksandra Majewska^{1,2} · Aleksandra Filipiak-Duliban^{1,2} · Claudine Kleda^{1,3}

Received: 2 June 2023 / Revised: 12 August 2023 / Accepted: 22 August 2023
© The Author(s) 2023

Abstract

Background PTEN is a tumor suppressor that is often mutated and nonfunctional in many types of cancer. The high heterogeneity of PTEN function between tumor types makes new *Pten* knockout models necessary to assess its impact on cancer progression and/or treatment outcomes.

Methods We aimed to show the effect of CRISPR/Cas9-mediated *Pten* knockout on murine melanoma (B16 F10) and kidney cancer (Renca) cells. We evaluated the effect of PTEN deregulation on tumor progression in vivo and in vitro, as well as on the effectiveness of drug treatment in vitro. In addition, we studied the molecular changes induced by *Pten* knockout.

Results In both models, *Pten* mutation did not cause significant changes in cell proliferation in vitro or in vivo. Cells with *Pten* knockout differed in sensitivity to cisplatin treatment: in B16 F10 cells, the lack of PTEN induced sensitivity and, in Renca cells, resistance to drug treatment. Accumulation of pAKT was observed in both cell lines, but only Renca cells showed upregulation of the p53 level after *Pten* knockout. PTEN deregulation also varied in the way that it altered PAI-1 secretion in the tested models, showing a decrease in PAI-1 in B16 F10 *PtenKO* and an increase in Renca *PtenKO* cells. In kidney cancer cells, *Pten* knockout caused changes in epithelial to mesenchymal transition marker expression, with downregulation of E-cadherin and upregulation of Snail, *Mmp9*, and *Acta2* (α -SMA).

Conclusions The results confirmed heterogeneous cell responses to PTEN loss, which may lead to a better understanding of the role of PTEN in particular types of tumors and points to PTEN as a therapeutic target for personalized medicine.

Keywords Cisplatin · Melanoma · PAI-1 · PTEN · RCC

Abbreviations

CSC	Cancer stem cell	Mmp9	Matrix metalloprotease 9
ECM	Extracellular Matrix	PAI-1	Plasminogen activator inhibitor 1
EMT	Epithelial to mesenchymal transition	PD-1	Programmed Death-1
IC50	Half-maximal inhibitory concentration	PTEN	Phosphatase and tensin homolog deleted from chromosome 10
KO	Knockout	RCC	Renal cell carcinoma
NSCLC	Non-small cell lung cancer	TME	Tumor microenvironment
		TKI	Tyrosine kinase inhibitor
		VEGF-A	Vascular endothelial growth factor A
		VEGFR2	Vascular endothelial growth factor receptor 2
		WT	Wild type
		α -SMA	Smooth muscle alpha-actin

Klaudia Brodaczevska and Aleksandra Majewska contributed equally to this work.

Klaudia Brodaczevska
kbrodaczewska@wim.mil.pl

¹ Laboratory of Molecular Oncology and Innovative Therapies, Military Institute of Medicine – National Research Institute, Szaserów 128, 01-141 Warsaw, Poland

² Postgraduate School of Molecular Medicine (Medical University of Warsaw), Żwirki I Wigury 61, 02-091 Warsaw, Poland

³ Center for Molecular Biophysics UPR 4301, CNRS, 45071 Orleans, France

Introduction

PTEN (phosphatase and tensin homolog deleted from chromosome 10) is an important factor that regulates many of the processes related to tumor development and progression. It is estimated that approximately 13.5% of human cancers

Published online: 06 September 2023

Springer

have PTEN-altered function or mutation [1]. The dysregulation of PTEN activity can be associated with many factors, including genetic alteration, post-transcriptional and post-translational modifications, or interactions with other proteins [2]. The main role of PTEN is associated with its lipid phosphatase activity, which acts as a negative regulator of PI3K/AKT signaling, affecting many basic processes of survival, growth, proliferation, angiogenesis, metabolism, and migration [3–5]. PTEN can also act in a lipid-phosphatase-independent manner, which is related to its localization in the cell [6]; nuclear PTEN affects DNA repair, cell cycle regulation, and chromosome stability [7, 8]. PTEN is known to interact with the other main tumor suppressor, p53. PTEN–p53 mutual regulation may occur at the transcriptional and protein levels, affecting major processes in cancer progression [8, 9]. Multifunctional PTEN activity is also crucial in modulating the tumor microenvironment (TME), affecting not only cancer cells but also additional features of the TME—immune response and angiogenesis [10, 11].

The diversity of PTEN cellular locations, corresponding to distinct functions with consequences for tumor progression, together with the possibility of various modifications of its expression and activity, makes the prognostic value of PTEN largely unknown [12]. Substantial evidence indicates that low PTEN levels correlate with poorer patient survival rates. In melanoma patients, the loss of PTEN expression correlates significantly with decreased overall survival and a shorter time to brain metastasis formation [13]. Similar results have been documented in other types of cancer, where PTEN loss was associated with increased aggressiveness, metastasis, and poorer prognosis (breast cancer [14], ovarian cancer [15] and hepatocellular carcinoma [16]). In glioblastoma, PTEN levels affected tumor differentiation and prognosis, but the impact of *PTEN* mutations was restricted to highly malignant tumors only [17]. Inconsistencies have also been found in kidney cancer—two independent meta-analyses showed different results: a significant effect of PTEN levels on tumor progression [18] and a low predictive value [19] in renal cell carcinoma (RCC) patients.

In addition to the effects of PTEN on cancer progression, it is also known to modulate sensitivity to different types of treatment. *PTEN* mutations caused resistance to radiotherapy and chemotherapy of prostate cancer cells by hyperactivating the AKT pathway [20]. In non-small cell lung carcinoma (NSCLC) models, PTEN loss contributed to radio-resistance, affecting the signaling pathways of DNA damage [21]. Resistance to cisplatin, a chemotherapeutic that causes DNA damage-mediated apoptotic signals, was observed in ovarian cancer cells after *PTEN* knockout (KO) [22]. A *PTEN* mutation in endometrial cancer cells resulted in drug resistance to docetaxel, a cell division inhibitor [23]. The loss of PTEN caused resistance to apoptosis by activating the anti-apoptotic mechanisms mediated by MDM2 in

acute lymphoblastic leukemia models [24]. In kidney cancer, PTEN alteration affected resistance to the tyrosine kinase inhibitors (TKIs) sunitinib and sorafenib, drugs primarily targeting tumor angiogenesis [25]. In melanoma, it was reported that PTEN loss promoted immune resistance and caused inferior outcomes of PD-1 (programmed death-1) inhibitor therapy [26]. PTEN's miscellaneous roles in the response to various treatments are strictly related to its multifunctionality in targeting distinct signaling pathways and cellular processes.

Thus, the high heterogeneity of tumor responses to PTEN dysregulation and its importance in key tumor progression processes make new *PTEN* knockout models necessary. Here, we aimed to establish stable murine melanoma B16 F10 and kidney cancer Renca cells with a loss of PTEN function to investigate the significance of this manipulation in tumor progression, molecular changes, and responses to treatment.

Materials and methods

Cell lines

Murine kidney cancer cells (Renca) were purchased from ATCC (Cat# CRL-2947, LOT# 63,226,315 ATCC, USA). Murine melanoma cells (B16 F10) were kindly gifted by Prof. Józef Dulak from the Department of Medical Biotechnology, Faculty of Biochemistry, Biophysics, and Biotechnology, Jagiellonian University, Cracow, Poland (authenticated by the ATCC Cell Authentication Service in 2021). The profiles of the B16 F10 samples were the same in 97% of cases as the reference profile ATCC MUSA0830. Both cell lines were cultured in RPMI-1640 GlutaMax™ medium (Thermo Fisher Scientific, Waltham, MA, USA), with 10% fetal bovine serum (FBS) (Thermo Fisher Scientific, Waltham, MA, USA) and regularly checked for the presence of mycoplasma using PCR assay (Biomedica, Poland).

The CRISPR/Cas9 system was used to knock out *Pten* expression in melanoma cells using the same protocol as that used in the Renca cell line that was described previously [27]. The same pSpCas9(BB)-2A-Puro(PX459)V2.0 (Gene Script, Piscataway, NJ, USA) plasmids, containing gRNAs targeting *Pten* (gRNA1: CCAATTCAGGACCCACGC GGCGG, gRNA2: GAACTGTCCTCCCGCGG-CGTGG), were used to transfect the B16 F10 cells. Cas9 nuclease only was used as a control (WT-wild type); the cells were transfected with empty plasmid and treated with the same protocol as the *Pten*-modified cells.

The cells were seeded in 24-well plates 24 h prior to transfection (1.25×10^4 per well), allowing them to adhere to the surface of the well. Five hours before transfection, the cells were starved with a medium without FBS.

Transfections were performed using Lipofectamine 2000 transfection reagent (Thermo Fisher Scientific, Waltham, MA, USA) according to the manufacturer's protocol. The selection of plasmid-containing cells was performed using puromycin (5 µg/mL; Thermo Fisher Scientific, Waltham, MA, USA; concentration established in preliminary experiments as effective for elimination of both cell lines) starting 5 h after transfection and continued for another 48 h. Cells treated with Lipofectamine 2000 only served as a control for selection with puromycin. Surviving cells transfected with *Pten* or control plasmids were used to limit dilution cloning. A single clone where *Pten* knockout was confirmed by no detection of protein using western blotting and the sequencing of the exon 7 fragment was selected. A WT control clone was selected randomly and sequenced to confirm no effect on the *Pten* gene. Detailed sequencing data of the obtained clones were prepared using the Mutation Surveyor® software and are presented in Supplementary Fig. 1. The sequences of both types of cells were compared to the original cells before transfection (termed Renca and B16 F10). Cells with *Pten* knockout are henceforth referred to as *Pten*/KO cells, while negative controls (transfected with empty plasmids) are referred to as *Pten*/WT.

In vivo experiments

To verify the effect of *Pten* knockout on tumor growth in vivo, Renca or B16 F10 cells in the *Pten*/WT and *Pten*/KO variants were implanted subcutaneously into the legs of mice—Renca into BALB/c and B16 F10 into C57BL6, respectively. The mice were obtained from the Medical University of Białystok, Poland. The animal care and experimental procedures were approved by the Second Warsaw Local Ethics Committee for Animal Experimentation (approval no. WAW2/76/2017) and performed following Directive 2010/63/EU regulations. The mice were housed in a controlled environment (12 h light / 12 h dark cycle) with ad libitum access to tap water and a fully-fledged diet.

Details about the Renca cells implanted into BALB/c mice have been shown previously [27]. Melanoma cells—B16 F10 (2×10^5 cells) with Matige1™ (Corning, NY, USA) diluted 1:3 in PBS—were implanted into the legs of six- to eight-week-old female C57BL6 mice as subcutaneous tumors. After 22 days of tumor growth, the mice were euthanized, and the tumors were weighed and measured. Fragments of tumor tissue were used for RNA isolation. The experiment was performed using two separate sets of animals, each containing four mice.

Assessment of susceptibility to treatment

The *Pten*/WT and *Pten*/KO cells of both tested models were cultured in standard conditions: 37 °C; 21% pO₂; 5%

CO₂. To assess the resistance to cisplatin (Sigma-Aldrich, Darmstadt, Germany) and sunitinib (Sigma-Aldrich, Darmstadt, Germany) treatments, experiments were performed in 96-well plates. Cells were seeded (5 000 cells per well Renca; 1 500 cells per well B16 F10) and cultured for 24 h, and the medium was exchanged to remove unadhered cells. After an additional 24 h, drugs were added at their final concentrations—cisplatin: 2.50, 3.75, 5.0, 7.5, 10.0, 15.0, 20.0, and 24.0 µM; sunitinib: 1.875, 2.5, 3.75, 5.0, 7.5, 10.0, and 15.0 µM. Cell viability was checked after 48 h of culture with the drug using Alamar Blue assay (Thermo Fisher Scientific, Waltham, MA, USA) according to the manufacturer's protocol. Fluorescence was measured using a VarioScan Lux (Thermo Fisher Scientific, Waltham, MA, USA), and the results are presented as a percentage of the untreated control. The IC₅₀ dose (half-maximal inhibitory concentration) was calculated using GraphPad Prism 9.0.

Colony formation assay

The soft agar colony formation test was performed on 24-well plates coated with 1.5% agar. Renca cells (*Pten*/WT and *Pten*/KO) were seeded on the 1.5% agar layer at a very low density (900 cells per well resuspended in 0.6% agar in RPMI 1640 10% FBS). A full medium was applied above the cell-agar layer to avoid drying. The cells were cultured for another three weeks under standard oxygen conditions: 37 °C; 21% pO₂; 5% CO₂. The formed colonies were fixed and stained with crystal violet. The number and average size (diameter [cm]) of the colonies were estimated using ImageJ software.

Protein detection using western blot

Proteins for western blot were collected from cells cultured in T75 flasks, detached with Accutase solution (Biolegend, USA), washed twice with PBS, and lysed with RIPA buffer containing Cocktail inhibitors (both from Thermo Fisher Scientific, Waltham, MA, USA). Total protein concentration was assessed by BCA assay. Twelve micrograms (12 µg) of protein were solubilized in a Laemmli sample buffer (AlfaAesar, Haverhill, MA, USA), separated on 12% polyacrylamide gel, and transferred onto nitrocellulose membranes (BioRad, Hercules, CA, USA). Proteins were detected on the membranes using Ponceau S staining. Nonspecific binding was diminished by a blocking step in 5% skimmed milk (2 h; room temperature). Membranes were incubated overnight at 4 °C in the solution of primary antibodies (Table 1) and then incubated for a further 2 h at room temperature, with the relevant secondary antibody conjugated with horseradish peroxidase (HRP) (Table 1). Bands were detected using Luminol as an HRP substrate (Santa-Cruz, CA, USA) with X-ray films. Quantification of the integrated

Table 1 List of antibodies used in Western Blot

Antibody	#Cat Number	Dilution
anti-AKT	#sc-5298, Santa Cruz Biotechnology	1:700
anti-PTEN	#9549, Cell Signalling Technology	1:750
anti-pAKT	#MAB 887, R&D System, USA	1:1000
anti-Snail	#3879 Cell Signalling Technology	1:1000
anti-p53	#2524, Cell Signalling Technology	1:1000
anti-E-cadherin	#3195, Cell Signalling Technology	1:1000
anti-Vinculin (loading control)	#sc-59803, Santa Cruz Biotechnology	1:1000
anti-Rabbit IgG Antibody (secondary antibody)	#PI-1000 Vector Laboratories, USA	1:10 000
anti-Mouse IgG Antibody (secondary antibody)	#PI-2000 Vector Laboratories, USA	1:10 000

optical density (IOD) of the bands was calculated using ImageJ software and normalized to the IOD of the loading control protein Vinculin.

2(-Delta C[T]) method, with normalization to the expression of β -Actin as a housekeeping gene.

Gene expression assessment by qRT-PCR

RNA was isolated from fragments of tumor tissue or cells cultured in T75 flasks using the column method (RNeasy Mini Kit; Qiagen, Germany). The samples were freed from DNA using the TURBO DNA-free kit (Thermo Fisher Scientific, USA), and reverse transcription was performed using 2 μ g of total RNA for the tumor samples and 1.5 μ g for the cell culture samples (High-Capacity cDNA Reverse Transcription Kit; Thermo Fisher Scientific, USA). Real-time PCR was performed using TaqMan™ Gene Expression Master Mix with TaqMan probes (all from Thermo Fisher Scientific, USA; listed in Table 2), or using PowerUp SYBR Master Mix (Thermo Fisher Scientific, USA) with the primers listed in Table 2. Reactions were run on a Bio-Rad CFX384 qPCR system (BioRad, Hercules, CA, USA). The relative mRNA levels were calculated using the

Detection of VEGF-A and PAI-1 secretion

The levels of VEGF-A (vascular endothelial growth factor A) and PAI-1 (plasminogen activator inhibitor 1) were measured in conditioned media from *Pten*/WT and *Pten*/KO B16 F10 and Renca cells using commercially available enzyme-linked immunosorbent assays Mouse VEGF DuoSet ELISA and Mouse PAI-1 DuoSet ELISA (both R&D Systems, USA), according to the manufacturer's protocol. Concentrations were calculated against the standard curve using recombinant proteins provided in the kits. Absorbance (450 nm) was measured using a VarioScan Lux (Thermo Fisher Scientific, Waltham, MA, USA).

In vitro experiments in hypoxic conditions

To assess *Pten*/WT and *Pten*/KO cells' susceptibility to cisplatin treatment in hypoxia (1% pO₂), cells were seeded in 96-well plates under standard oxygen conditions and allowed

Table 2 List of TaqMan probes and primers sequences used in real-time PCR

	TaqMan probes (Assay ID)	
<i>Vegfa</i>	Mm00437306	
<i>Pten</i>	Mm00477208	
<i>Akt1</i>	Mm00437306	
<i>p53</i>	Mm01731287	
β -Actin	Mm02619580	
	Primers sequences	
	Forward	Reverse
<i>Serpine1</i> (PAI-1)	CCTCCACAGCCTTTGTCTCT	TTCGTCCCAAATGAAGGCGT
<i>Mmp9</i>	CAGCCGACTTTTGGTCTTC	CGGTACAAGTATGCCTCTGCCA
<i>Acta2</i> (α -SMA)	CTTCGTGACTACTGCCGGAGC	AGGTGGTTTCGTGGAATGCC
β -Actin	CCTAGGCACCAGGGTGTGA	GTTGGCCTTAGGGTTCAGGG
<i>Vegf2</i>	AAACAAAAGTAAAGTACGCTGGTC	GCAGCAGGTTGCACAGTAATTT

to adhere to the culture surface. After 24 h, the medium was changed to a pre-equilibrated hypoxic medium, and the cells were cultured in an XVivo X3 workstation (Biospherix, USA) in 1% pO₂ and 5% CO₂ at 37 °C for a further 24 h. Next, cisplatin was added at the final testing concentrations, as previously used in normoxic conditions, and Alamar Blue was used, as described above. The conditioned media were collected from cells cultured in hypoxia for 72 h without drugs, and PAI-1 secretion was detected using a Mouse PAI-1 DuoSet ELISA (R&D Systems, USA), as described above.

Statistical analysis

All statistical analyses were performed using GraphPad Prism 9.0 software. The normality of the data distribution was checked using the Shapiro–Wilk’s test. Student’s t-test or the Mann–Whitney U test were used where applicable. The data are expressed as the mean ± standard error of the mean (SEM) for parametric data or as box plots with medians for non-parametric data. Detailed information is provided in the figure captions.

Results

Pten knockout does not affect melanoma or kidney cancer progression

To determine the effect of PTEN on melanoma and kidney cancer progression, CRISPR/Cas9-mediated *Pten* knockout models were developed. The morphology and PTEN protein levels of the B16 F10 cells are presented in Fig. 1A, while data concerning kidney cancer (Renca) cells were shown previously [27]. In both models, the *Pten* mutation did not cause significant changes in cell proliferation in vitro (Fig. 1B), measured as the changes in fluorescence in the Alamar Blue assay. A lack of *Pten*/KO impact on cell proliferation and survival in kidney cancer cells was also demonstrated in the colony formation assay (Fig. 1C–E); no changes were observed in the size or number of colonies formed in the soft agar.

As the TME is a complex system, and interactions between tumor cells and other components of the TME are important for cancer progression, the effect of *Pten* knockout was also checked in the in vivo models. Subcutaneous B16 F10 or Renca tumors, induced using *Pten*/WT or *Pten*/KO cells, were assessed (Fig. 1F). Despite the presence of other components of the TME, the reduced *Pten* expression was maintained in the tumor mass both at the transcript (Fig. 1G) and protein (Supplementary Figure S2A, B) levels. Although significant changes in PTEN levels were maintained, there

was no difference in tumor weight in both tested tumor types (Fig. 1H).

Pten knockout causes differential changes in cisplatin sensitivity in Renca and B16 F10 cells

Since no significant changes in the progression of *Pten*/KO tumors were observed, the sensitivity of cells to anticancer treatment was assessed in vitro. We performed initial experiments for drug sensitivity using cisplatin and sunitinib, which represent different models of action. Only cisplatin sensitivity was affected by *Pten* knockout. In the melanoma model, *Pten*/KO cells showed lower resistance to cisplatin treatment than *Pten*/WT cells in the whole range of tested concentrations (Fig. 2A). Based on this, the calculated IC₅₀ dose was almost two times lower for B16 F10 *Pten*/KO (Fig. 2B). An inverse relationship was observed in the kidney cancer model—the IC₅₀ dose was higher for *Pten*-mutated cells compared to wild-type cells (Fig. 2B). No significant changes in viability were observed for sunitinib (Supplementary Figure S3A, B), which suggests that the effect of *Pten* knockout on cell sensitivity to drugs is closely related to the mechanism of drug action. However, the differences between the two tested cancer types may be related to the distinct modulation of signaling pathways after *Pten* knockout.

Pten knockout induces distinct molecular changes in renal cell carcinoma and melanoma

To identify molecular changes in *Pten*/KO cells, the levels of proteins involved in PTEN-related signaling pathways were assessed. In both types of cancer, pAKT accumulated in *Pten*/KO cells (Fig. 3A, B). The inverse effect of *Pten* mutation in melanoma and RCC was demonstrated in p53 and AKT expression. *Pten*/KO Renca cells had higher levels of p53 than WT cells, while in B16 F10 cells, p53 tended to be downregulated after *Pten* knockout (Fig. 3A, C). AKT expression was reduced in *Pten*/KO cells in the kidney cancer model but not in the melanoma model (Fig. 3A, D). Such modifications of p53, AKT, and pAKT expression as a result of *Pten* knockout observed in both types of cancer were also confirmed in vivo in the tumors (Supplementary Figure S2A, D, E).

In addition to intracellular changes, secretory potential, which modulates TME, may also influence distinct drug sensitivity. In the tested models, *Pten* knockout did not cause changes in the secretion of the main proangiogenic factor VEGF-A in vitro (Fig. 3E)—which may correspond to the lack of changes in susceptibility to sunitinib (Supplementary Figure S3A, B). Also, in vivo, the expressions of *Vegfa* and *Vegfr2* (vascular endothelial growth factor receptor 2) were similar in *Pten*/WT and *Pten*/KO tumors in both melanoma

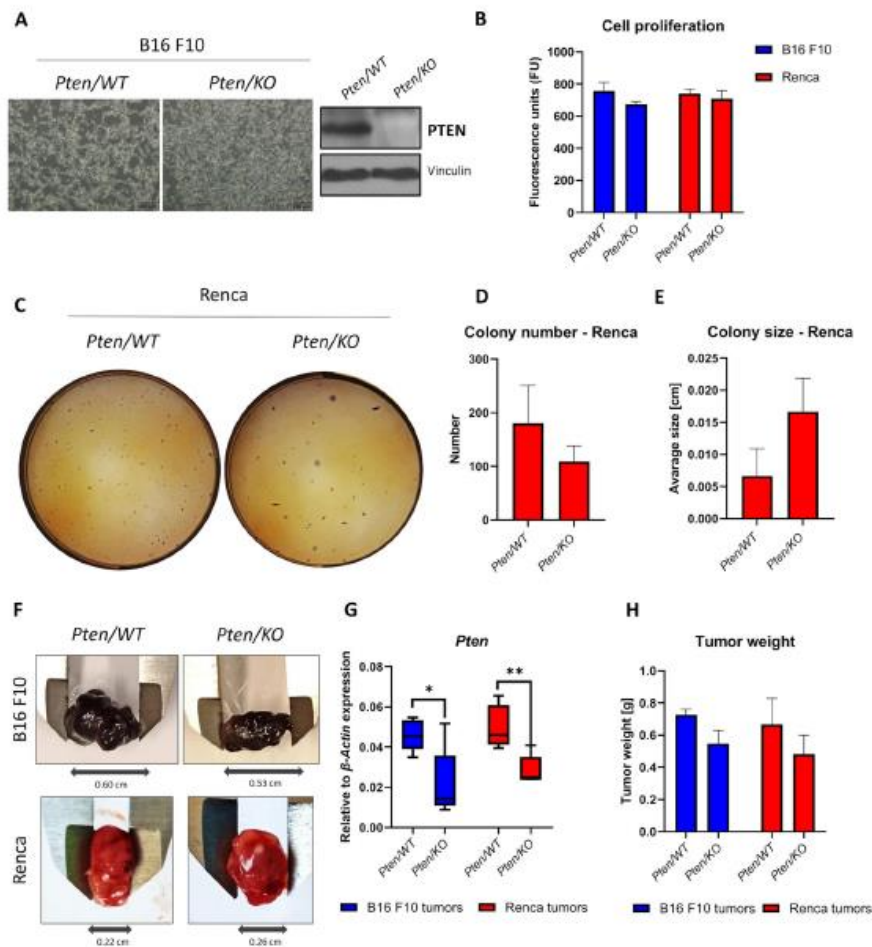


Fig. 1 Effect of *Pten* knockout on melanoma and kidney cancer growth. **A** Cell morphology (scale bar: 200 μ m) and PTEN protein levels assessed by western blot in B16 F10 *Pten*/WT and *Pten*/KO cells. **B** Cell proliferation measured as mitochondrial activity, after 72 h culture, of B16 F10 and Renca cells with different PTEN statuses, shown as fluorescence units (FU); values are shown as the mean \pm SEM; Student's *t*-test (B16 F10, not significant; Renca, not significant). **C** Representative photos of colony formation by Renca *Pten*/WT and *Pten*/KO cells. **D** Quantification of colony numbers formed by Renca cells with different PTEN statuses; values are shown as the mean \pm SEM; Student's *t*-test (not significant). **E** Quan-

tification of colony size, measured as diameter, formed by Renca cells with different PTEN statuses; values are shown as the mean \pm SEM; Student's *t*-test (not significant). **F** Representative photos of B16 F10 and Renca tumors formed by cells with different PTEN statuses. **G** Box plot represents relative to β -Actin *Pten* expression in *Pten*/WT and *Pten*/KO tumor masses; middle line in box represents the median; Mann-Whitney U test (B16 F10: $U = 4$, $n_1 = n_2 = 6$, p -value = 0.0260, two-tailed; Renca: $U = 1$, $n_1 = n_2 = 6$, p -value = 0.0043, two-tailed). **H** Weight of tumors formed by B16 F10 and Renca cells with different PTEN statuses; values are shown as the mean \pm SEM; Student's *t*-test ($n = 3$, not significant)

and renal cell carcinoma (Supplementary Fig. 4A, B). PAI-1 was also assessed due to its TME-modulating functions, which promote tumor progression [28]. PAI-1 secretion, high in B16 F10 *Pten*/WT cells, was downregulated

by *Pten*/KO (Fig. 3F), which corresponds to a lower cisplatin IC₅₀ dose in *Pten* mutations (Fig. 2B). Decreased *Serpine1* (gene encoding PAI-1) expression was also observed in B16 F10 *Pten*/KO tumors compared to the wild-type

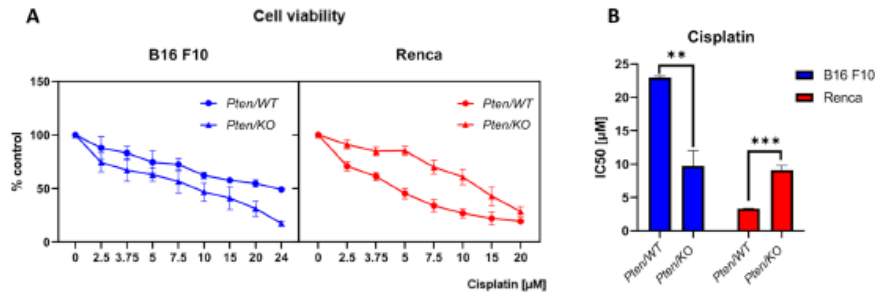


Fig. 2 Effect of *Pten* knockout on cisplatin sensitivity in B16 F10 and Renca cells. **A** Viability of B16 F10 and Renca cells with different *PTEN* statuses after various doses of cisplatin treatment, measured by Alamar Blue, shown as a percentage of untreated control for

each *PTEN* variant normalized to 100%. **B** IC50 dose (half-maximal inhibitory concentration) of cisplatin for different *PTEN* variant cells; values are shown as the mean \pm SEM; Student's *t*-test (B16 F10: ** *p*-value=0.0011, $t_6=5.846$, Renca: *** *p*-value=0.0001, $t_6=8.579$)

control (Supplementary Fig. 4C). This was not observed in the Renca model due to low, close to the limit of detection, PAI-1 secretion. However, the induction of PAI-1 secretion by low oxygen tension (Fig. 3G) showed that *Pten*/KO cells secreted more PAI-1 than *Pten*/WT cells, which corresponds to the changes in IC50 doses for cisplatin—higher in Renca *Pten*/KO cells in hypoxic conditions (Fig. 3G–I).

Pten knockout induces epithelial-to-mesenchymal transition in Renca cells

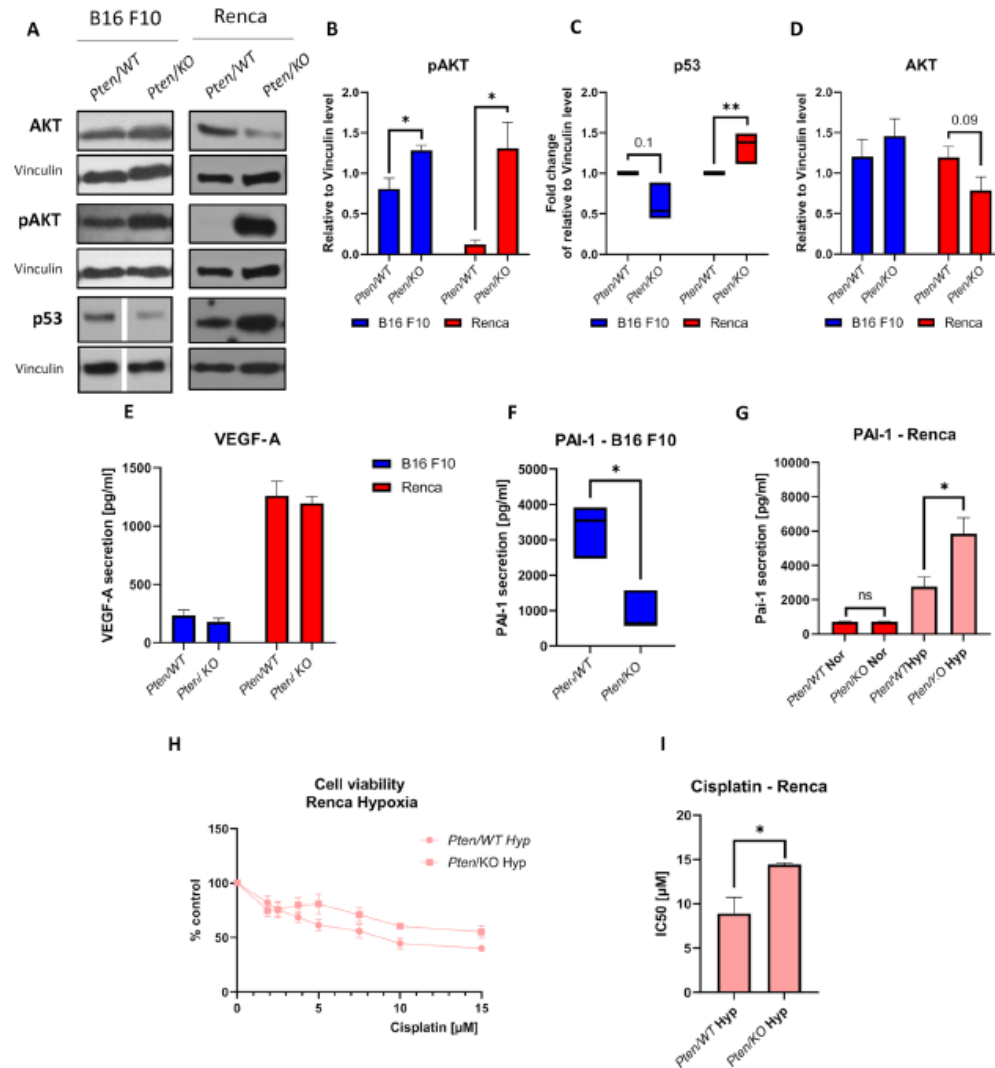
In the kidney cancer model, *Pten* knockout caused changes in cell growth and morphology—cells became more dispersed without forming tight groups (Fig. 4A). This prompted us to investigate the effect of *PTEN* downregulation on the induction of epithelial-to-mesenchymal transition (EMT). *Pten*/KO Renca cells were characterized by a lower level of E-cadherin with a simultaneous increase in Snail level (Fig. 4B, E). Compared to *Pten*/WT cells, the expression of *Acta2* (gene encoding α -SMA; smooth muscle alpha-actin) and *Mmp9* (matrix metalloprotease 9) was upregulated in *Pten*/KO cells (Fig. 4C, D). Changed gene expression was also confirmed in vivo; however, E-cadherin and Snail protein levels did not reach a statistically significant level of change in the tumor mass (Supplementary Figure S5A–D).

Discussion

PTEN is a tumor suppressor [29, 30] that is among the most often mutated genes in cancers [2]; however, its prognostic value in most cancers remains debatable [31]. Here, we characterized the effect of *Pten* knockout in two different cancer cell models that were shown previously to differ in *PTEN*-related regulation [32]. *PTEN* is a master

regulator of several cellular processes; it controls proliferation, migration, and apoptosis [6]. However, in our models, despite pAKT accumulation, *PTEN*-lacking cells were not significantly different functionally from WT cells. We observed that the lack of *PTEN* does not influence cell proliferation, clonogenicity in vitro, or, importantly, tumor growth in vivo. In many models, such as breast cancer, glioma, and colon cancer, it has been observed that *PTEN*-mutated cells proliferate faster [33–36]; however, in other models, it has been reported that *PTEN* status does not always alter proliferation [37]. It is worth noting that in some models, *PTEN* loss causes growth arrest [38], related to senescence; therefore, the functional effect of *PTEN* knockout is strongly dependent on the cell type. In our model, no effect on cell growth was observed in anchorage-independent growth in the clonogenic assay. In mammary carcinoma and prostate cancer, the depletion of *PTEN* leads to the increased formation of colonies in terms of their size and/or number [39–41]. In our case, there was a tendency (*p*-value=0.2) for *Pten*/KO cells to form larger colonies; however, no change was observed in their number. Therefore, our study confirms that heterogenous cell responses to *PTEN* loss are dependent upon the type of cancer.

Because *PTEN* downregulation did not alter cancer progression in the tested models, we examined other mechanisms that could be affected. *PTEN* is a prognostic factor of treatment response in cancer patients, and it has been observed that *PTEN* status affects tumor sensitivity to drugs [42]. Indeed, we observed that *Pten* mutated cells responded differently to some chemotherapeutics; however, again, the response was not uniform. Out of both tested drugs, only resistance to cisplatin was significantly affected by *PTEN* status, but, importantly, the effect was inverse in RCC and melanoma cells. In Renca cells, *PTEN* loss increased cell



resistance to the drug, with IC₅₀ values being over twice those of WT cells.

This is in accordance with observations carried out in ovarian cancer, where cells with high PTEN levels were sensitive to cisplatin treatment [43]. However, melanoma cells were more sensitive to the drug after PTEN depletion. To explain the differential effect of PTEN inactivation on the cells, we checked the level of p53, since it was shown that p53 is required for cisplatin toxicity in

PTEN-overexpressing cells [43]. The effect of *Pten* knock-out on p53 expression was inverse in RCC and melanoma, similar to cisplatin resistance. However, sensitized melanoma cells tended to downregulate p53, while desensitized RCC cells increased this protein. Although both cell lines carry functional p53 [44, 45], the mechanism of PTEN and p53-mediated response to cisplatin was different from that previously reported in ovarian cells. It may be that the different reactions of cells to PTEN loss can be related

Fig. 3 Effect of *Pten* knockout on molecular changes and secretory factors in melanoma and kidney cancer models. **A** AKT, pAKT, and p53 detection by western blot, with Vinculin as loading control, in B16 F10 and Renca with different PTEN statuses. The gap between *Pten*/WT and *Pten*/KO shows that samples on the gel were in a different order and were rearranged for the figure. **B** pAKT level relative to Vinculin in B16 F10 and Renca cells with different PTEN statuses; values are shown as the mean \pm SEM; Student's *t*-test (B16 F10: * *p*-value=0.0167, $t_6=8.579$; Renca: * *p*-value=0.021, $t_4=3.285$). **C** Box plot represents fold change of p53 level relative to Vinculin in *Pten*/KO cells compared to *Pten*/WT cells normalized to 1; middle line in box represents the median; Mann-Whitney U test (B16 F10: U=0, $n_1=n_2=3$, *p*-value=0.100, two-tailed; Renca: U=0, $n_1=n_2=5$, * *p*-value=0.0079, two-tailed). **D** AKT level relative to Vinculin in B16 F10 and Renca cells with different PTEN statuses; values are shown as the mean \pm SEM; Student's *t*-test (B16 F10: not significant; Renca: *p*-value=0.0911, $t_3=1.920$). **E** VEGF-A secretion by B16 F10 and Renca cells with different PTEN statuses, measured by ELISA; values are shown as the mean \pm SEM; Student's *t*-test (B16 F10, not significant; Renca, not significant). **F** Box plot of PAI-1 secretion by B16 F10 cells with different PTEN statuses, measured by ELISA; middle line in box represents the median; Mann-Whitney U test (U=0, $n_1=n_2=4$, * *p*-value=0.0286, two-tailed). **G** PAI-1 secretion by Renca cells with different PTEN statuses cultured in normoxia and hypoxia, measured by ELISA; values are shown as the mean \pm SEM; Student's *t*-test (normoxia: *n*=4, not significant; hypoxia: * *p*-value=0.03, $t_6=2.830$). **H** Viability of Renca *Pten*/WT and *Pten*/KO cells after various doses of cisplatin in hypoxic conditions, measured by Alamar Blue, shown as a percentage of the untreated control for each PTEN variant. **I** IC50 dose (half-maximal inhibitory concentration) of cisplatin treatment in *Pten*/WT and *Pten*/KO Renca cells in hypoxia; values are shown as the mean \pm SEM; Student's *t*-test (* *p*-value=0.026, $t_6=3.014$)

to their starting sensitivity to cisplatin. The IC50 value of the WT melanoma cells was over 20 μ M and 10 times smaller for the RCC cells; therefore, we could treat B16 F10 cells as intrinsically resistant, while Renca was sensitive to cisplatin.

As p53 expression could not explain cisplatin sensitivity, other mechanisms of drug resistance were examined for their possible modulation by *Pten* knockout. The complex tumor microenvironment and, thus, cancer development can be diversely shaped by factors secreted by cells of different origins that compose the tumor tissue. We evaluated the levels of VEGF, as the major angiogenic factor, and PAI-1, an extracellular matrix (ECM)-regulating protein affecting, among others, cell survival, migration, and invasion [46]. The production of VEGF-A was not altered by PTEN dysregulation, either in highly proangiogenic RCC cells or VEGF-low-secreting melanoma cells. It has been established in other models that PTEN regulates VEGF expression through the control of the AKT/HIF-1 α pathway [47]. Lack of regulation of the VEGF pathway could partly explain no observed effect of PTEN loss on resistance to antiangiogenic therapy in our model. Other studies have shown that *Pten* knockout promotes RCC cell resistance to sunitinib and sorafenib in vitro [25], while in our study, in murine RCC, there was no effect on TKI sensitivity.

However, in our study, PTEN dysregulation caused a very strong decrease in PAI-1 secretion in melanoma cells. This effect could not be observed in RCC cells, which are poor PAI-1 secretors. Nonetheless, when exposed to hypoxia, the production of PAI-1 was induced in RCC cells and was potentiated by *Pten* knockout. Therefore, an inverse reaction of melanoma and RCC cells was evidenced again, similar to cisplatin resistance. These phenomena could be related; indeed, it has been observed that both overexpression and addition of recombinant PAI-1 protect cancer cells from cisplatin-induced apoptosis [48, 49]. A product of the *Serpine1* gene, PAI-1 is a member of the serine protease inhibitor family and a key modulator of the plasminogen/plasminase system [50]. It has also been reported to play a role in cancer; it induces tumor migration, invasion, and angiogenesis, and thereby promotes the progression and metastasis of tumors. However, the specific molecular mechanisms underlying the role of PAI-1 in cancer remain insufficiently documented. In our study, melanoma cells, characterized by high IC50 cisplatin values, displayed high basic PAI-1 secretion. Upon PTEN loss, *Serpine1* production was halted, which could mediate reduced cisplatin resistance, as observed for paclitaxel [51].

Renca cells, which are sensitive to cisplatin, have low background PAI-1 expression, and PTEN dysregulation did not alter it. However, it has been shown that cisplatin and carboplatin treatment can induce the secretion of this protein, both by cancer and stromal cells [49, 52]. Here, we observed that hypoxia increased the production of PAI-1, which was accompanied by increased cisplatin IC50 values. The effects of hypoxia and *Pten* knockout were additive both in the case of cisplatin resistance and in PAI-1 production. Therefore, our results suggest that the differential effects of *Pten* knockout on drug resistance might be related to distinct *Serpine1* regulation, although we could not explain the background of this phenomenon. It has previously been reported that *Serpine1* modulates the AKT/PI3K/PTEN pathway and that PAI-1 loss causes the activation of AKT and the inactivation of PTEN [31]. Consequently, our results suggest that the status of PTEN and, thus, AKT may reciprocally affect PAI-1 regulation.

EMT is a fundamental mechanism of cancer resistance that can be induced by PTEN modification and the regulation of drug response. In breast cancer, it has been reported that *Pten* knockout induces more epithelial phenotypes in vitro, although the cells migrated more actively than WT cells [39]. In the case of our model, *Pten* knockout RCC cells acquired more mesenchymal phenotypes—there was a reduced expression of E-cadherin with a concomitant increase in EMT markers (Snail, *Mmp9*, and *Acta2*), which was also partly maintained in tumors in vivo. Our data are in concordance with observations showing that PTEN down-regulation leads to EMT [53]. Additionally, it was observed

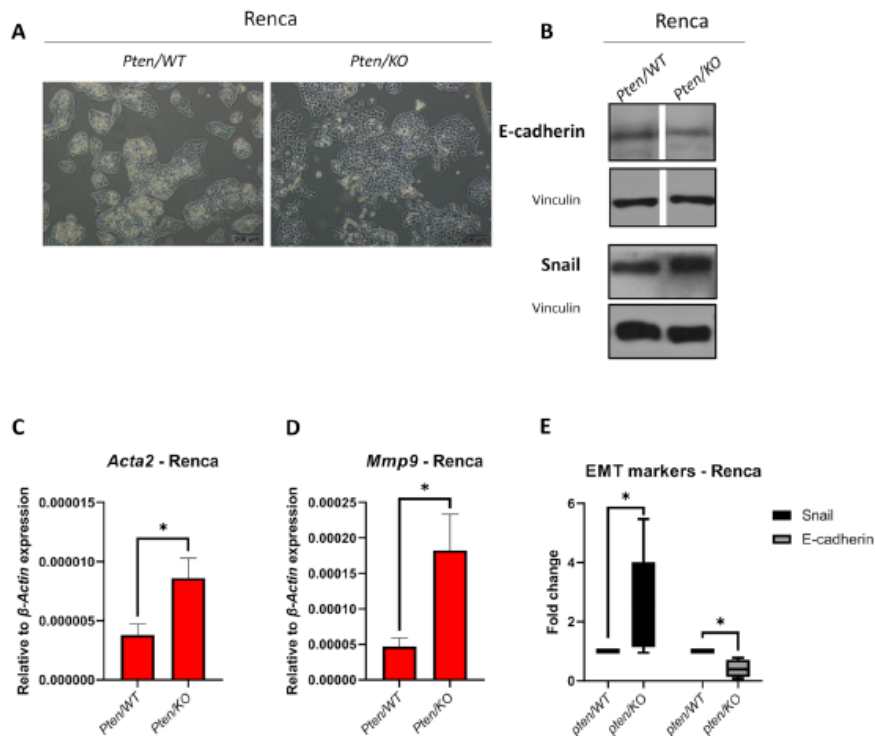


Fig. 4 Effect of *Pten* knockout on EMT markers in kidney cancer model. **A** Representative photos showing Renca *Pten*/WT and *Pten*/KO morphology; scale bar: 200 μ m. **B** EMT (epithelial to mesenchymal transition) markers: E-cadherin and Snail detection by western blots with Vinculin as loading control in Renca *Pten*/WT and *Pten*/KO cells. The gap between *Pten*/WT and *Pten*/KO shows that samples on the gel were in a different order and were rearranged for the figure. **C** Expression of *Acta2* (encoding α -SMA) relative to β -Actin in Renca *Pten*/WT and *Pten*/KO cells; values are shown as

the mean \pm SEM; Student's *t*-test (p -value = 0.0483, $t_6 = 2.472$). **D** Expression of *Mmp9* relative to β -Actin in Renca *Pten*/WT and *Pten*/KO cells; values are shown as the mean \pm SEM; Student's *t*-test (p -value = 0.0273, $t_{10} = 2.583$). **E** Box plot represents fold change of Snail and E-cadherin levels relative to Vinculin in *Pten*/KO cell compared to *Pten*/WT cells normalized to 1; middle line in box represents the median; Mann-Whitney U test (Snail: $U = 6$, $n_1 = n_2 = 6$, * p -value = 0.0476, two-tailed; E-cadherin: $U = 0$, $n_1 = n_2 = 4$, * p -value = 0.0286, two-tailed)

that PTEN-loss-mediated EMT causes upregulation of cancer stem cell (CSC) populations within tumor cells [54], which could mediate the reduced sensitivity to cisplatin, as CSCs are largely responsible for drug resistance in cancers [55]. Therefore, it may be that *Pten* knockout induced cisplatin resistance in Renca cells by EMT induction and the protective secretion of PAI-1.

Conclusions

Our data show the diversity of cell responses to PTEN loss. Although tumor growth was unaffected in both cell models, drug sensitivity was modulated differently by

Pten mutations in RCC and melanoma cells. We showed that *Pten* knockout can alter the cell microenvironment by regulating secreted factors, including PAI-1, which could explain the differential cell reactions to drug treatment. Additionally, PTEN loss causes EMT features in RCC cells that could contribute to cisplatin resistance.

Supplementary Information The online version contains supplementary material available at <https://doi.org/10.1007/s43440-023-00523-y>.

Author's contribution KB: conceptualization, methodology, investigation, analysis, writing, review; AM: conceptualization, methodology, investigation, analysis, writing, review; AF-D: investigation, review; CK: conceptualization, review.

Funding This research was funded by a subvention from the Ministry of Education and Science, Military Institute of Medicine (intramural grant no 1/8974 [519]). Experiments related to PAI-1 were funded by the National Science Centre (grant no 2020/37/N/NZ5/04024). AF-D was supported by the European Social Fund: POWER, "Next generation sequencing technologies in biomedicine and personalized medicine."

Data availability All data presented in this manuscript (raw and analyzed results) are available upon request from the corresponding author.

Declarations

Conflict of interest The authors declare no conflict of interest.

Open Access This article is licensed under a Creative Commons Attribution 4.0 International License, which permits use, sharing, adaptation, distribution and reproduction in any medium or format, as long as you give appropriate credit to the original author(s) and the source, provide a link to the Creative Commons licence, and indicate if changes were made. The images or other third party material in this article are included in the article's Creative Commons licence, unless indicated otherwise in a credit line to the material. If material is not included in the article's Creative Commons licence and your intended use is not permitted by statutory regulation or exceeds the permitted use, you will need to obtain permission directly from the copyright holder. To view a copy of this licence, visit <http://creativecommons.org/licenses/by/4.0/>.

References

1. Masson GR, Williams RL. Structural Mechanisms of PTEN Regulation. *Cold Spring Harb Perspect Med*. 2020. <https://doi.org/10.1101/cshperspect.a036152>.
2. Fusco N, Sajjadi E, Venetis K, Gaudio G, Lopez G, Corti C, et al. PTEN alterations and their role in cancer management: are we making headway on precision medicine? *Genes (Basel)*. 2020. <https://doi.org/10.3390/genes11070719>.
3. Stiles B, Groszer M, Wang S, Jiao J, Wu H. PTENless means more. *Dev Biol*. 2004;273(2):175–84. <https://doi.org/10.1016/j.ydbio.2004.06.008>.
4. Simpson L, Parsons R. PTEN: life as a tumor suppressor. *Exp Cell Res*. 2001;264(1):29–41. <https://doi.org/10.1006/excr.2000.5130>.
5. Manning BD, Cantley LC. AKT/PKB signaling: navigating downstream. *Cell*. 2007;129(7):1261–74. <https://doi.org/10.1016/j.cell.2007.06.009>.
6. Chen CY, Chen J, He L, Stiles BL. PTEN: tumor suppressor and metabolic regulator. *Front Endocrinol (Lausanne)*. 2018;9:338. <https://doi.org/10.3389/fendo.2018.00338>.
7. Song MS, Salmela L, Pandolfi PP. The functions and regulation of the PTEN tumour suppressor. *Nat Rev Mol Cell Biol*. 2012;13(5):283–96. doi: <https://doi.org/10.1038/nrm3330>
8. Freeman DJ, Li AG, Wei G, Li HH, Kertesz N, Lesche R, et al. PTEN tumor suppressor regulates p53 protein levels and activity through phosphatase-dependent and -independent mechanisms. *Cancer Cell*. 2003;3(2):117–30. [https://doi.org/10.1016/s1535-6108\(03\)00021-7](https://doi.org/10.1016/s1535-6108(03)00021-7).
9. Nakanishi A, Kitagishi Y, Ogura Y, Matsuda S. The tumor suppressor PTEN interacts with p53 in hereditary cancer (Review). *Int J Oncol*. 2014;44(6):1813–9. <https://doi.org/10.3892/ijo.2014.2377>.
10. Ma J, Sawai H, Ochi N, Matsuo Y, Xu D, Yasuda A, et al. PTEN regulates angiogenesis through PI3K/Akt/VEGF signaling pathway in human pancreatic cancer cells. *Mol Cell Biochem*. 2009;331(1–2):161–71. <https://doi.org/10.1007/s11010-009-0154-x>.

11. Vidotto T, Melo CM, Castelli E, Koti M, Dos Reis RB, Squire JA. Emerging role of PTEN loss in evasion of the immune response to tumours. *Br J Cancer*. 2020;122(12):1732–43. <https://doi.org/10.1038/s41416-020-0834-6>.
12. Bazzichetto C, Conciatori F, Pallocca M, Falcone I, Fanciulli M, Cognetti F, et al. PTEN as a prognostic/predictive biomarker in cancer: an unfulfilled promise? *Cancers (Basel)*. 2019. <https://doi.org/10.3390/cancers11040435>.
13. Bucheit AD, Chen G, Siroy A, Tetzlaff M, Broadus R, Milton D, et al. Complete loss of PTEN protein expression correlates with shorter time to brain metastasis and survival in stage IIIB/C melanoma patients with BRAFV600 mutations. *Clin Cancer Res*. 2014;20(21):5527–36. <https://doi.org/10.1158/1078-0432.CCR-14-1027>.
14. Li S, Shen Y, Wang M, Yang J, Lv M, Li P, et al. Loss of PTEN expression in breast cancer: association with clinicopathological characteristics and prognosis. *Oncotarget*. 2017;8(19):32043–54. <https://doi.org/10.18632/oncotarget.16761>.
15. Martins FC, Couturier DL, Paterson A, Karnezis AN, Chow C, Nazeran TM, et al. Clinical and pathological associations of PTEN expression in ovarian cancer: a multicentre study from the Ovarian Tumour Tissue Analysis Consortium. *Br J Cancer*. 2020;123(5):793–802. <https://doi.org/10.1038/s41416-020-0900-0>.
16. Hu TH, Huang CC, Lin PR, Chang HW, Ger LP, Lin YW, et al. Expression and prognostic role of tumor suppressor gene PTEN/MMAC1/TEP1 in hepatocellular carcinoma. *Cancer*. 2003;97(8):1929–40. <https://doi.org/10.1002/ncr.11266>.
17. Rasheed BK, Stenzel TT, McLendon RE, Parsons R, Friedman AH, Friedman HS, et al. PTEN gene mutations are seen in high-grade but not in low-grade gliomas. *Cancer Res*. 1997;57(19):4187–90.
18. Que WC, Qiu HQ, Cheng Y, Liu MB, Wu CY. PTEN in kidney cancer: A review and meta-analysis. *Clin Chim Acta*. 2018;480:92–8. <https://doi.org/10.1016/j.cca.2018.01.031>.
19. Tang L, Li X, Gao Y, Chen L, Gu L, Chen J et al. Phosphatase and tensin homolog (PTEN) expression on oncologic outcome in renal cell carcinoma: A systematic review and meta-analysis. *PLoS One*. 2017;12(7):e0179437. doi: <https://doi.org/10.1371/journal.pone.0179437>.
20. Chang L, Graham PH, Hao J, Ni J, Bucci J, Cozzi PJ, et al. PI3K/Akt/mTOR pathway inhibitors enhance radiosensitivity in radioresistant prostate cancer cells through inducing apoptosis, reducing autophagy, suppressing NHEJ and HR repair pathways. *Cell Death Dis*. 2014;5(10):e1437. doi: <https://doi.org/10.1038/cddis.2014.415>.
21. Fischer T, Hartmann O, Reissland M, Prieto-Garcia C, Klann K, Pahor N, et al. PTEN mutant non-small cell lung cancer require ATM to suppress pro-apoptotic signalling and evade radiotherapy. *Cell Biosci*. 2022;12(1):50. <https://doi.org/10.1186/s13578-022-00778-7>.
22. Wu H, Cao Y, Weng D, Xing H, Song X, Zhou J, et al. Effect of tumor suppressor gene PTEN on the resistance to cisplatin in human ovarian cancer cell lines and related mechanisms. *Cancer Lett*. 2008;271(2):260–71. <https://doi.org/10.1016/j.canlet.2008.06.012>.
23. Zhang H, Wang S, Cacalano N, Zhu H, Liu Q, Xie M, et al. Oncogenic Y68 frame shift mutation of PTEN represents a mechanism of docetaxel resistance in endometrial cancer cell lines. *Sci Rep*. 2019;9(1):2111. <https://doi.org/10.1038/s41598-019-38585-9>.
24. Zhou M, Gu L, Findley HW, Jiang R, Woods WG. PTEN reverses MDM2-mediated chemotherapy resistance by interacting

- with p53 in acute lymphoblastic leukemia cells. *Cancer Res.* 2003;63(19):6357–62.
25. Sekino Y, Hagura T, Han X, Babasaki T, Goto K, Inoue S, et al. PTEN is involved in sunitinib and sorafenib resistance in renal cell carcinoma. *Anticancer Res.* 2020;40(4):1943–51. <https://doi.org/10.21873/anticancer.14149>.
 26. Peng W, Chen JQ, Liu C, Malu S, Creasy C, Tetzlaff MT, et al. Loss of PTEN promotes resistance to T cell-mediated immunotherapy. *Cancer Discov.* 2016;6(2):202–16. <https://doi.org/10.1158/2159-8290.CD-15-0283>.
 27. Majewska A, Brodaczevska K, Filipiak-Duliban A, Kajdasz A, Kieda C. miRNA pattern in hypoxic microenvironment of kidney cancer-role of PTEN. *Biomolecules.* 2022. <https://doi.org/10.3390/biom12050686>.
 28. Kubala MH, DeClerck YA. The plasminogen activator inhibitor-1 paradox in cancer: a mechanistic understanding. *Cancer Metastasis Rev.* 2019;38(3):483–92. <https://doi.org/10.1007/s10555-019-09806-4>.
 29. Suzuki A, de la Pompa JL, Stambolic V, Elia AJ, Sasaki T, del Barco BI, et al. High cancer susceptibility and embryonic lethality associated with mutation of the PTEN tumor suppressor gene in mice. *Curr Biol.* 1998;8(21):1169–78. [https://doi.org/10.1016/S0960-9822\(07\)00488-5](https://doi.org/10.1016/S0960-9822(07)00488-5).
 30. Di Cristofano A, Pesce B, Cordon-Cardo C, Pandolfi PP. Pten is essential for embryonic development and tumour suppression. *Nat Genet.* 1998;19(4):348–55. <https://doi.org/10.1038/1235>.
 31. Balsara RD, Castellino FJ, Ploplis VA. A novel function of plasminogen activator inhibitor-1 in modulation of the AKT pathway in wild-type and plasminogen activator inhibitor-1-deficient endothelial cells. *J Biol Chem.* 2006;281(32):22527–36. <https://doi.org/10.1074/jbc.M512819200>.
 32. Majewska A, Brodaczevska K, Filipiak-Duliban A, Kieda C. Comparative analysis of the effect of hypoxia in two different tumor cell models shows the differential involvement of PTEN control of proangiogenic pathways. *Biochem Cell Biol.* 2023. <https://doi.org/10.1139/bccb-2023-0047>.
 33. Bowen KA, Doan HQ, Zhou BP, Wang Q, Zhou Y, Rychahou PG, et al. PTEN loss induces epithelial–mesenchymal transition in human colon cancer cells. *Anticancer Res.* 2009;29(11):4439–49.
 34. Wu J, Gao H, Ge W, He J. Over expression of PTEN induces apoptosis and prevents cell proliferation in breast cancer cells. *Acta Biochim Pol.* 2020;67(4):515–9. https://doi.org/10.18388/abp.2020_5371.
 35. Chen Z, Trotman LC, Shaffer D, Lin HK, Dotan ZA, Niki M, et al. Crucial role of p53-dependent cellular senescence in suppression of Pten-deficient tumorigenesis. *Nature.* 2005;436(7051):725–30. <https://doi.org/10.1038/nature03918>.
 36. Banerjee S, Crouse NR, Emmett RJ, Gianino SM, Gutmann DH. Neurofibromatosis-1 regulates mTOR-mediated astrocyte growth and glioma formation in a TSC/Rheb-independent manner. *Proc Natl Acad Sci U S A.* 2011;108(38):15996–6001. <https://doi.org/10.1073/pnas.1019012108>.
 37. Nowak DG, Cho H, Herzka T, Watrud K, DeMarco DV, Wang VM, et al. MYC Drives Pten/Trp53-Deficient Proliferation and Metastasis due to IL6 Secretion and AKT Suppression via PHLPP2. *Cancer Discov.* 2015;5(6):636–51. <https://doi.org/10.1158/2159-8290.CD-14-1113>.
 38. Kim JS, Lee C, Bonifant CL, Ransom H, Waldman T. Activation of p53-dependent growth suppression in human cells by mutations in PTEN or PIK3C. *Mol Cell Biol.* 2007;27(2):662–77. <https://doi.org/10.1128/MCB.00537-06>.
 39. Dayoub A, Fokin AI, Lomakina ME, James J, Plays M, Jacquin T, et al. Inactivation of PTEN and ZFH3 in Mammary Epithelial Cells Alters Patterns of Collective Cell Migration. *Int J Mol Sci.* 2022;24(1). doi: <https://doi.org/10.3390/ijms24010313>.
 40. Chiang KC, Chen HY, Hsu SY, Pang JH, Wang SY, Hsu JT, et al. PTEN insufficiency modulates ER+ breast cancer cell cycle progression and increases cell growth in vitro and in vivo. *Drug Des Devel Ther.* 2015;9:4631–8. <https://doi.org/10.2147/DDDT.S86184>.
 41. Takao A, Yoshikawa K, Karnan S, Ota A, Uemura H, De Velasco MA, et al. Generation of PTEN-knockout (–/–) murine prostate cancer cells using the CRISPR/Cas9 system and comprehensive gene expression profiling. *Oncol Rep.* 2018;40(5):2455–66. <https://doi.org/10.3892/or.2018.6683>.
 42. Nagata Y, Lan KH, Zhou X, Tan M, Esteve FJ, Sahin AA, et al. PTEN activation contributes to tumor inhibition by trastuzumab, and loss of PTEN predicts trastuzumab resistance in patients. *Cancer Cell.* 2004;6(2):117–27. <https://doi.org/10.1016/j.ccr.2004.06.022>.
 43. Yan X, Fraser M, Qiu Q, Tsang BK. Over-expression of PTEN sensitizes human ovarian cancer cells to cisplatin-induced apoptosis in a p53-dependent manner. *Gynecol Oncol.* 2006;102(2):348–55. <https://doi.org/10.1016/j.ygyno.2005.12.033>.
 44. Kiweler N, Wunsch D, Wirth M, Mahendrarajah N, Schneider G, Stauber RH, et al. Histone deacetylase inhibitors dysregulate DNA repair proteins and antagonize metastasis-associated processes. *J Cancer Res Clin Oncol.* 2020;146(2):343–56. <https://doi.org/10.1007/s00432-019-03118-4>.
 45. Ingelsheid K, Spiegelberg D, Kannan P, Pavenius L, Hacheney J, Jiang L, et al. The MDM2 inhibitor navtemadlin arrests mouse melanoma growth in vivo and potentiates radiotherapy. *Cancer Res Commun.* 2022;2(9):1075–88. <https://doi.org/10.1158/2767-9764.CRC-22-0053>.
 46. Yang JD, Ma L, Zhu Z. SERPINE1 as a cancer-promoting gene in gastric adenocarcinoma: facilitates tumour cell proliferation, migration, and invasion by regulating EMT. *J Chemother.* 2019;31(7–8):408–18. <https://doi.org/10.1080/1120009X.2019.1687996>.
 47. Tian T, Nan K-J, Wang S-H, Liang X, Lu C-X, Guo H, et al. PTEN regulates angiogenesis and VEGF expression through phosphatase-dependent and -independent mechanisms in HepG2 cells. *Carcinogenesis.* 2010;31(7):1211–9. <https://doi.org/10.1093/carcin/bgq085>.
 48. Pavon MA, Arroyo-Solera I, Tellez-Gabriel M, Leon X, Viros D, Lopez M, et al. Enhanced cell migration and apoptosis resistance may underlie the association between high SERPINE1 expression and poor outcome in head and neck carcinoma patients. *Oncotarget.* 2015;6(30):29016–33. <https://doi.org/10.18632/oncotarget.5032>.
 49. Che Y, Wang J, Li Y, Lu Z, Huang J, Sun S, et al. Cisplatin-activated PAI-1 secretion in the cancer-associated fibroblasts with paracrine effects promoting esophageal squamous cell carcinoma progression and causing chemoresistance. *Cell Death Dis.* 2018;9(7):759. <https://doi.org/10.1038/s41419-018-0808-2>.
 50. Wang S, Pang L, Liu Z, Meng X. SERPINE1 associated with remodeling of the tumor microenvironment in colon cancer progression: a novel therapeutic target. *BMC Cancer.* 2021;21(1):767. <https://doi.org/10.1186/s12885-021-08536-7>.
 51. Zhang Q, Lei L, Jing D. Knockdown of SERPINE1 reverses resistance of triple-negative breast cancer to paclitaxel via suppression of VEGFA. *Oncol Rep.* 2020;44(5):1875–84. <https://doi.org/10.3892/or.2020.7770>.
 52. Pan JX, Qu F, Wang FF, Xu J, Mu LS, Ye LY, et al. Aberrant SERPINE1 DNA methylation is involved in carboplatin induced epithelial-mesenchymal transition in epithelial ovarian cancer. *Arch Gynecol Obstet.* 2017;296(6):1145–52. <https://doi.org/10.1007/s00404-017-4547-x>.
 53. Kohnoh T, Hashimoto N, Ando A, Sakamoto K, Miyazaki S, Aoyama D, et al. Hypoxia-induced modulation of PTEN activity and

- EMT phenotypes in lung cancers. *Cancer Cell Int.* 2016;16:33. <https://doi.org/10.1186/s12935-016-0308-3>.
54. Qi Y, Liu J, Chao J, Scheuerman MP, Rahimi SA, Lee LY, et al. PTEN suppresses epithelial-mesenchymal transition and cancer stem cell activity by downregulating Abi1. *Sci Rep.* 2020;10(1):12685. <https://doi.org/10.1038/s41598-020-69698-1>.
55. Li Y, Wang Z, Ajani JA, Song S. Drug resistance and Cancer stem cells. *Cell Commun Signal.* 2021;19(1):19. <https://doi.org/10.1186/s12964-020-00627-5>.

Pten knockout affects drug resistance differently in melanoma and kidney cancer

Klaudia Brodaczevska^{1,*}, Aleksandra Majewska^{1,2,*}, Aleksandra Filipiak-Duliban^{1,2}, Claudine Kieda^{1,3}

¹ Military Institute of Medicine – National Research Institute, Laboratory of Molecular Oncology and Innovative Therapies, Szaserów 128, 01-141 Warsaw, Poland

² Postgraduate School of Molecular Medicine (Medical University of Warsaw), Żwirki i Wigury 61, 02-091 Warsaw, Poland

³ Center for Molecular Biophysics UPR 4301 CNRS, 45071 Orleans, France

* These authors contributed equally to this work

Corresponding author: Klaudia Brodaczevska; kbrodaczewska@wim.mil.pl; Szaserów 128, 01-141 Warsaw, Poland

SUPPLEMENTARY MATERIALS

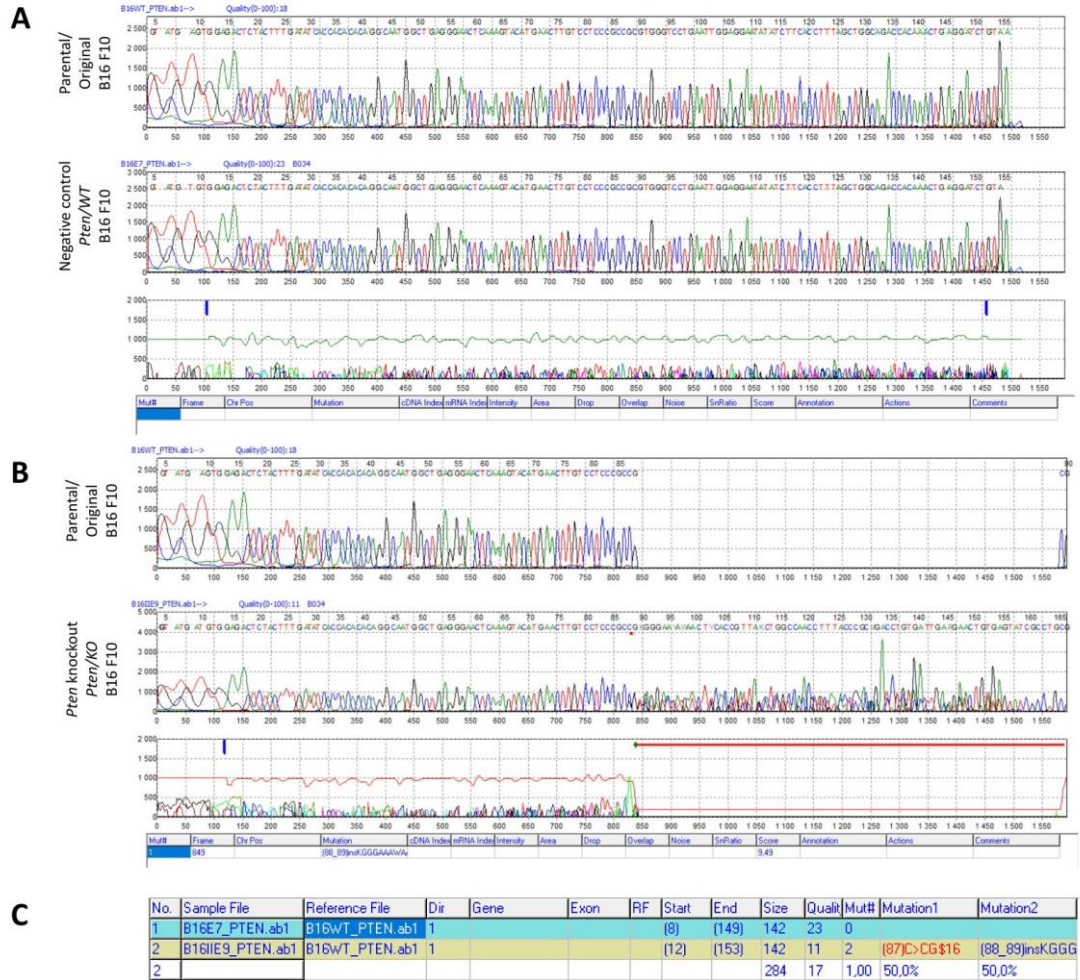


Figure S1. Sequencing results.

(A) Comparison of parental/original B16 F10 cell line to *Pten*/WT B16 F10 cells – negative control. (B) Comparison of parental/original B16 F10 cell line to *Pten*/KO B16 F10 cells – model of *Pten* knockout. (C) Summary of mutation analysis.

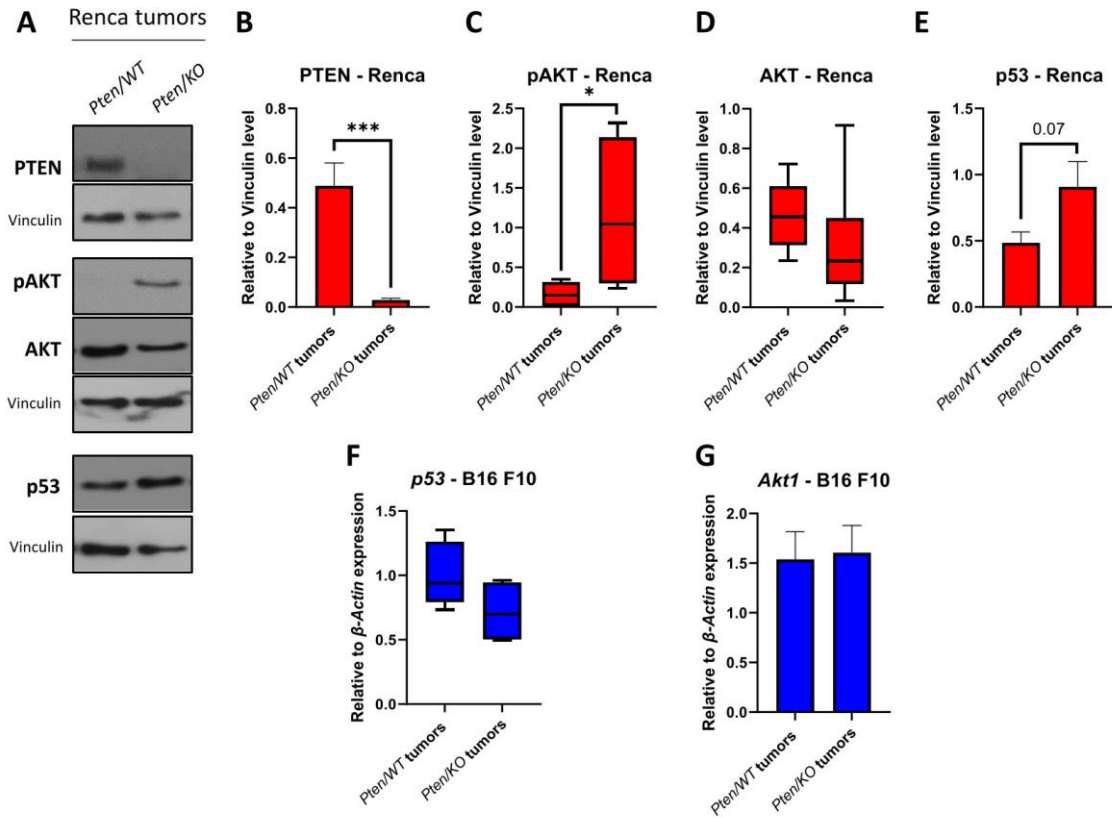


Figure S2. Molecular changes in B16 F10 and Renca tumors with different PTEN status.

(A) PTEN, p-AKT, AKT and p53 detection by western blots with Vinculin as loading control in Renca tumors with different PTEN statuses. (B) PTEN level relative to Vinculin in Renca *Pten/WT* and *Pten/KO* tumors mass; values are shown as the mean \pm SEM; Student's *t*-test (***) p-value = 0.0006, $t_{10} = 4.928$). (C) Box-plot of relative to Vinculin pAKT level in Renca *Pten/WT* and *Pten/KO* tumors mass; middle line in box represents the median; Mann-Whitney U test ($U = 4$, $n_1 = n_2 = 6$, * p-value = 0.0260, two-tailed). (D) Box-plot of relative to Vinculin AKT level in Renca *Pten/WT* and *Pten/KO* tumors mass; middle line in box represents the median; Mann-Whitney U test ($U = 8$, $n_1 = n_2 = 6$, p-value = 0.1320, two-tailed). (E) p53 level relative to Vinculin in Renca *Pten/WT* and *Pten/KO* tumors mass; values are shown as the mean \pm SEM; Student's *t*-test (p-value = 0.0707, $t_{10} = 2.023$). (F) Box-plot of relative to β -Actin expression of p53 in B16 F10 *Pten/WT* and *Pten/KO* tumors mass; middle line in box represents the median; Mann-Whitney U test ($U = 9$, $n_1 = n_2 = 6$, p-value = 0.1797, two-tailed). (G) Relative to β -Actin expression of *Akt1* in B16 F10 *Pten/WT* and *Pten/KO* tumors mass; values are shown as the mean \pm SEM; Student's *t*-test (p-value = 0.8641, $t_{10} = 0.1756$).

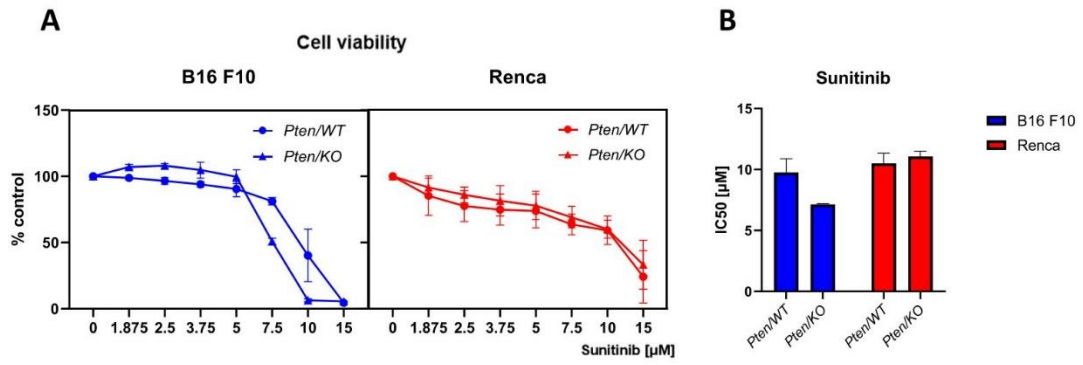


Figure S3. Effect of *Pten* knockout on sunitinib sensitivity in B16 F10 and Renca cells.

(A) Viability of B16 F10 and Renca cells with different PTEN statuses after various doses of sunitinib (Sigmaaldrich, Darmstadt, Germany) treatment, measured by Alamar Blue, shown as a percentage of untreated control for each PTEN variant normalized to 100 %; B16 F10 n = 4, Renca n = 3. (B) IC50 dose (half-maximal inhibitory concentration) of sunitinib treatment for different PTEN variant cells; values are shown as the mean \pm SEM; Student's *t*-test (B16 F10: p-value = 0.0627, $t_6 = 2.281$; Renca p-value = 0.5745, $t_4 = 0.6105$).

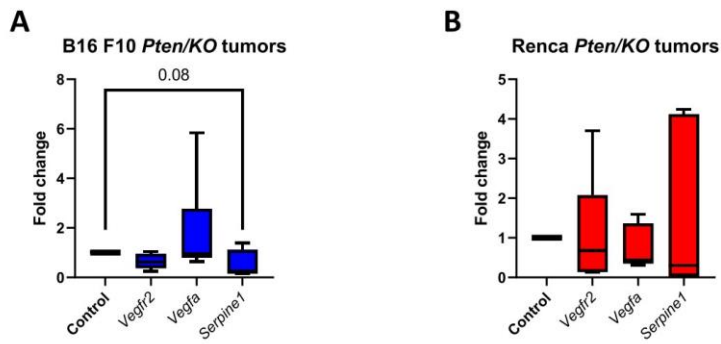


Figure S4. Molecular changes in B16 F10 and Renca tumors with different PTEN status.

(A) Box plot represents fold change of relative to β -Actin *Vegfr2*, *Vegfa*, and *Serpine1* expression in B16 F10 *Pten*/KO tumors, compared to Control - *Pten*/WT tumors normalized to 1; middle line in box represents the median; Mann-Whitney U test (*Vegfr2*: U = 5, n = 5, * p-value = 0.1270, two-tailed; *Vegfa*: U = 12, n = 6, * p-value = 0.3636; *Serpine1*: U = 6, n = 5, * p-value = 0.0801). (B) Box plot represents fold change of relative to β -Actin *Vegfr2*, *Vegfa*, and *Serpine1* expression in Renca *Pten*/KO tumors, compared to Renca *Pten*/WT tumors normalized to 1; middle line in box represents the median; Mann-Whitney U test (not significant).

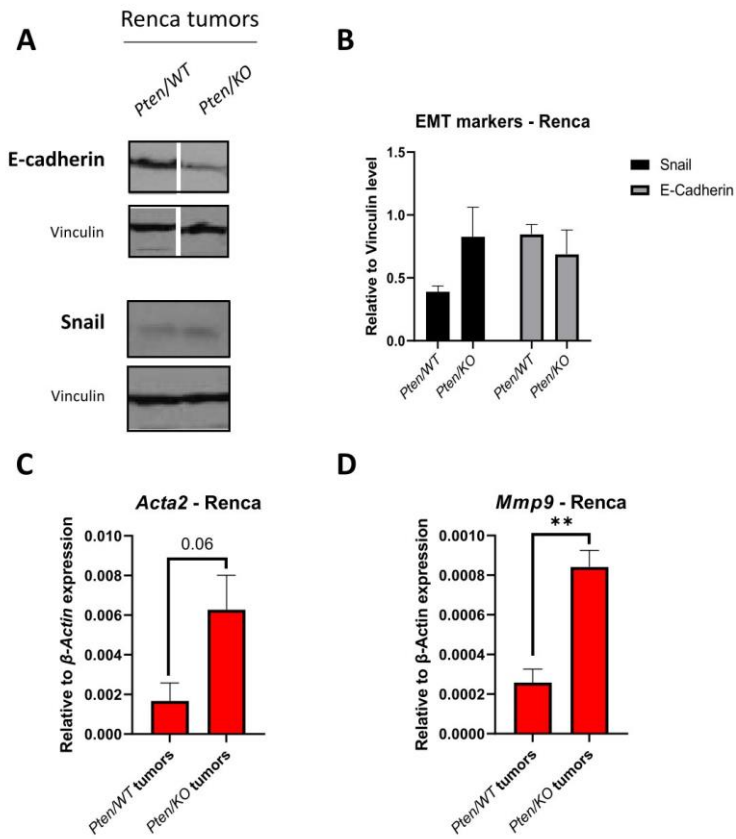


Figure S5. Expression of EMT markers in Renca tumors with different PTEN status.

(A) Epithelial to mesenchymal transition (EMT) markers: E-cadherin and Snail detection by western blots with Vinculin as loading control in Renca tumors with different PTEN status. The gap between *Pten/WT* and *Pten/KO* shows that samples on the gel were in a different order and were rearranged for the figure. (B) E-cadherin and Snail levels relative to Vinculin in Renca *Pten/WT* and *Pten/KO* tumor masses; values are shown as the mean \pm SEM; Student's *t*-test (not significant). (C) Relative to β -Actin expression of *Acta2* (encoding α -SMA) in Renca *Pten/WT* and *Pten/KO* tumor masses; values are shown as the mean \pm SEM; Student's *t*-test (*p*-value = 0.0594, $t_6 = 2.321$). (D) Relative to β -Actin expression of *Mmp9* in Renca *Pten/WT* and *Pten/KO* tumor masses; values are shown as the mean \pm SEM; Student's *t*-test (** *p*-value = 0.0016, $t_6 = 5.457$).

Article

miRNA Pattern in Hypoxic Microenvironment of Kidney Cancer—Role of PTEN

Aleksandra Majewska ^{1,2,*} , Klaudia Brodaczevska ¹ , Aleksandra Filipiak-Duliban ^{1,2} , Arkadiusz Kajdasz ^{3,4} and Claudine Kieda ^{1,5} 

- ¹ Laboratory of Molecular Oncology and Innovative Therapies, Military Institute of Medicine, 128 Szaserow Street, 04-141 Warsaw, Poland; kbrodaczewska@wim.mil.pl (K.B.); afilipiak1@wim.mil.pl (A.F.-D.); ckieda@wim.mil.pl (C.K.)
 - ² Postgraduate School of Molecular Medicine (SMM), Warsaw Medical University, 61 Zwirki and Wigury Street, 02-091 Warsaw, Poland
 - ³ Department of RNA Metabolism, Institute of Bioorganic Chemistry, Polish Academy of Sciences, Noskowskiego 12/14, 61-704 Poznan, Poland; akajdasz@ibch.poznan.pl
 - ⁴ Laboratory of Human Molecular Genetics, Faculty of Biology, Institute of Molecular Biology and Biotechnology, Adam Mickiewicz University Poznan, 61-614 Poznan, Poland
 - ⁵ Centre for Molecular Biophysics, UPR 4301 French National Centre for Scientific Research CNRS, 45071 Orleans, France
- * Correspondence: amajewska1@wim.mil.pl

Abstract: MicroRNAs are post-transcriptional regulators of gene expression, and disturbances of their expression are the basis of many pathological states, including cancers. The miRNA pattern in the context of tumor microenvironment explains mechanisms related to cancer progression and provides a potential target of modern therapies. Here we show the miRNA pattern in renal cancer focusing on hypoxia as a characteristic feature of the tumor microenvironment and dysregulation of PTEN, being a major tumor suppressor. Methods comprised the CRISPR/Cas9 mediated PTEN knockout in the Renca kidney cancer cell line and global miRNA expression analysis in both in vivo and in vitro (in normoxic and hypoxic conditions). The results were validated on human cancer models with distinct PTEN status. The increase in miR-210-3p in hypoxia was universal; however, the hypoxia-induced decrease in PTEN was associated with an increase in miR-221-3p, the loss of PTEN affected the response to hypoxia differently by decreasing miR-10b-5p and increasing miR-206-3p. In turn, the complete loss of PTEN induces miR-155-5p, miR-100-5p. Upregulation of miR-342-3p in knockout PTEN occurred in the context of the whole tumor microenvironment. Thus, effective identification of miRNA patterns in cancers must consider the specificity of the tumor microenvironment together with the mutations of key suppressors.

Keywords: microRNA; RCC; tumor hypoxia; PTEN



Citation: Majewska, A.; Brodaczevska, K.; Filipiak-Duliban, A.; Kajdasz, A.; Kieda, C. miRNA Pattern in Hypoxic Microenvironment of Kidney Cancer—Role of PTEN. *Biomolecules* **2022**, *12*, 686. <https://doi.org/10.3390/biom12050686>

Academic Editors: Klaudia Skrzypek and Agnieszka Loboda

Received: 27 February 2022

Accepted: 9 May 2022

Published: 11 May 2022

Publisher's Note: MDPI stays neutral with regard to jurisdictional claims in published maps and institutional affiliations.



Copyright: © 2022 by the authors. Licensee MDPI, Basel, Switzerland. This article is an open access article distributed under the terms and conditions of the Creative Commons Attribution (CC BY) license (<https://creativecommons.org/licenses/by/4.0/>).

1. Introduction

MicroRNAs (miRNAs, miRs) are small (20–24 nucleotides), non-coding, single-stranded RNA molecules that regulate gene expression at the post-transcriptional level. Their main action consists of suppressing gene expression by recognizing the complementary 3' untranslated region (UTR) of the target mRNA, which allows its cleavage with subsequent degradation or translation inhibition [1]. It is estimated that about 30% of human genes are regulated by miRNAs [2], making them significant in many basic biological processes including development, cell differentiation, proliferation and apoptosis. Dysregulation of miRNA expression plays a role in the pathogenesis of many diseases including tumors; the impact of altered miRNA expression has been well documented in many types of cancer. Among others, it has been shown to promote aggressiveness [3], metastases [4], vascularization [5] or resistance to treatment [6]. miRNAs have also been proposed as being useful in diagnostics as biomarkers for cancers [7]. Altogether, miRNAs are important

potential therapeutic targets in the treatment of cancer, contributing to the need to expand knowledge in this area.

Hypoxia, low, non-physiological oxygen tension is a characteristic feature of the microenvironment of solid tumors. It is well established that low pO_2 causes pathological vascularization, promotes aggressive phenotypes and increases metastasis [8]. The cellular response to hypoxia leads to changes mainly regulated by hypoxia-inducible factors (HIFs) [9]. Apart from low oxygen tension, the HIF pathway is modulated in a hypoxia-independent manner—HIF-1 α (Hypoxia inducible factor 1 alpha), stabilization may result from VHL mutations. Renal cell carcinoma (RCC) are characterized by frequent VHL (Von Hippel-Lindau) mutations—which, by activating the pathways related to HIF-1 α and further VEGF (Vascular Endothelial Growth Factor) [10], makes them highly angiogenic tumors [11]. Despite advances in the treatment of kidney cancer using anti-angiogenesis molecular-based therapies as anti-VEGF antibodies or tyrosine kinase inhibitors (TKI) [12], treatment resistance or relapse are a current problem [13]. The development of new, effective therapies and diagnostic markers may focus on miRNAs deregulated in hypoxic RCC, but new research is required to better understand their role in cancer progression and make their regulation a tool to counteract the pathologic microenvironment.

Many of the mechanisms involved in cancer response to hypoxia are related to changes in miRNA expression induced by low oxygen tension [14]. Hypoxia may regulate miRNA biogenesis at the transcriptional level, epigenetic modification, or the activity of enzymes associated with miRNA maturation [15]. It has been proven that hypoxia affects the reduction of Drosha and Dicer levels in cancer cells through the ETS1/ELK1 transcription factors, which leads to dysregulation of miRNA biogenesis and increased tumor progression [16]. A key regulator of hypoxic response—HIF-1 α regulates expression of proangiogenic factors, together with miRNAs expression including miR-210, miR-382, miR-224 and others, as reviewed by Peng et al. [17].

In a meta-analysis of a potential miRNA signature panel comparing RCC to normal renal cells, miR-21 and miR-210 were identified as significantly upregulated and miR-141, miR-200c and miR-429 as downregulated [18]. MiR-210, due to its regulation by HIF-1 α , is of particular importance in kidney cancer for the disruption the HIF-1 α /VHL complex formation impaired by frequent VHL mutations in RCC. It had been shown that VHL silencing, causing pseudo-hypoxia, also caused higher expression of miR-210 than hypoxia in human RCC cell lines and was elevated in samples from patients with VHL mutation compared to non-mutated tumors [19]. As VHL-dependent regulation of miRNAs is well known in RCC [20], it is important to find the means to overcome such a mutation-related deleterious imbalance by taking advantage of the potential regulation by activation of other tumor suppressors able to control the tumor growth. To this aim we focused on the PTEN (phosphatase and tensin homolog deleted from chromosome 10) tumor suppressor and its miRNA pattern dependence.

PTEN, a tumor suppressor gene, is frequently mutated in many types of tumors [21]. The loss of PTEN in RCC patients is well documented [22]; however, its prognostic value is still debatable [23]. It is a dual specificity phosphatase that dephosphorylates phosphatidylinositol 3,4,5-trisphosphate (PIP3) to phosphatidylinositol 4,5-diphosphate (PIP2), reversing Phosphoinositide 3-kinase (PI3K) action and resulting in the inhibition of the AKT/mTOR pathway, which controls basic cellular processes such as cell growth, metabolism and apoptosis [24]. The activity of PTEN may be of particular importance in hypoxia, as the role of PTEN in the stabilization of HIF-1 α has been demonstrated [25].

PTEN expression may be regulated by miRNA, by directly targeting PTEN mRNA (among others: miR-21, miR-221/22, miR-301a), or inducing the hypomethylation of the PTEN promoter (miR-29, miR-101, miR-185) [26]. However, the loss of PTEN may also have other, miRNA-independent backgrounds such as germline and somatic PTEN mutations, genomic deletion or protein-protein interactions [27], but there is a lack of research showing how the loss of PTEN modulates miRNA expression in RCC. In a mouse model of prostate cancer, PTEN loss resulted in a significant increased expression of

sixteen miRNAs including miR-155 and miR-132, and a decreased expression of five miRNAs expression (among others: miR-133a and miR-181) [28]. In *Pten*-deficient T-ALL (T-cell acute lymphoblastic leukemia), miR-26b was identified as deregulated in mice [29]. PTEN's implication in regulation of the tumor growth is strategic for its upstream position controlling the PI3K/AKT/mTOR pathway activation cascade on the one hand, and for its ability to also control the p53 activity on the other hand, making it the decisive supervisor of the biochemical balance in tumor cell development [30]. The status of PTEN is thus a decisive factor in diseases and is becoming highly significant in hypoxia-dependent pathologies. Indeed, it was demonstrated that PTEN is downregulated by hypoxia, the microenvironment hallmark of solid tumors [31], or cardiac pathologies [32,33]. Along the establishment of hypoxic conditions the produced miRNAs are crucial molecular regulators whose composition and action reflect the effect of such selection pressure. Thus, the evaluation cannot be interpreted independently of the hypoxic microenvironmental context that modulates the expression of the cell regulators as factors as well as miRNAs. Here we aimed to determine the miRNA pattern characteristic for RCC in relation to PTEN status, especially taking into account the tumor hypoxic microenvironment.

2. Materials and Methods

2.1. Cell Lines

Kidney cancer cell lines with different PTEN status were purchased from ATCC (Manassas, VA, USA). PTEN wild-type: murine Renca (Cat# CRL-2947, ATCC, USA), human Caki-1 (Cat# HTB-48, ATCC, Manassas, VA, USA) and PTEN mutant 786-O cell line (Cat# CRL-1932, ATCC, Manassas, VA, USA). All cancer cells were cultured in RPMI-1640 GlutaMax™ medium (Thermo Fisher Scientific, Waltham, MA, USA), with 10% Fetal Bovine Serum (FBS) (Thermo Fisher Scientific, Waltham, MA, USA). Murine brain derived mature endothelial cells (ECs) (MBr MEC FVB) [34], were cultured in OPTI MEM medium (Thermo Fisher Scientific, USA), with 2% FBS (Thermo Fisher Scientific, Waltham, MA, USA). All cell lines and were passaged at 80% confluence by detaching with Accutase solution (Biological, San Diego, CA, USA). Cells used in the experiments were Mycoplasma free as assayed with PCR Mycoplasma Test (Biomedica, Piaseczno, Poland) and did not exceed the 15th passage.

2.2. CRISPR/Cas9 Mediated PTEN Knockout in Renca Cells

The CRISPR/Cas9 System was used to knock out the *Pten* expression in Renca cells [35]. Using the Benchling platform (<https://www.benchling.com/>, accessed on 10 June 2019), two guide RNA (gRNA) sequences targeting the sequence of the *Pten* gene on chromosome 6 were designed: gRNA1: CCAATTCAGGACCCACGCGGCGG, gRNA2: GAACTGTCTCCCGCCG-CGTGG.

A commercially available plasmid pSpCas9(BB)-2A-Puro(PX459)V2.0 (Gene Script, Piscataway, NJ, USA) was used in the procedure. Briefly, a single gRNA targeting *Pten* was introduced into the plasmid by ligating oligonucleotides into the GAAGAC site of BpII. Plasmids for a single gRNA sequence were amplified with competent bacteria, isolated using ZymoPURE™ II Plasmid MidiprepKit (Zymo Research, Irvine, CA, USA), and used to transfect Renca cells.

Renca cells were seeded in a 24-well plate (10^4 cells per well) 24 h prior to transfection, allowing them to stick to the surface of the well. Five hours before transfection, cells were starved with medium without enrichment of fetal bovine serum. A mixture of gRNA1 and gRNA2 containing plasmids in a 1:1 ratio was used for transfection. Transfections were performed with Lipofectamine 2000 Transfection Reagent (Thermo Fisher Scientific, Waltham, MA, USA) according to the manufacturer's protocol. Selections of plasmid containing cells were started 5 h after transfection and continued for another 48 h with puromycin at a concentration of 5 µg/mL. A single clone was selected, expanded, and then used for biological assays. PTEN knockout was confirmed by no detection of protein on a western blot and the sequencing of exon 7 fragment, where gRNA was targeting (single

nucleotide duplication was detected). Cells transfected with a plasmid lacking gRNA were used as a negative control. Detailed sequencing data of the obtained clones were prepared using Mutation Surveyor[®] software and are presented in Supplementary Figure S1.

2.3. Healthy and Tumor Kidney Cancer Tissue

Commercially available RNA isolates of the human healthy kidney and kidney tumor (TaKaRa, San Jose, CA, USA) were used to verify the potential clinical significance of tested miRNAs. Details about patient samples are described in Supplementary Materials. Total RNA was used for reverse transcription reactions as described below.

2.4. Cell Culture Methods in Normoxic and Hypoxic Conditions

Cancer cells were seeded on standard tissue culture treated flasks (VWR International, Radnor, PA, USA) in the right density (7000 cells/cm² Renca pten/WT pten/KO, 12,000 cells/cm² Caki-1 and 1000 cells/cm² 786-O) and allowed to adhere to the culture surface for 24 h. Media were exchanged with pre-equilibrated normoxic or hypoxic medium and cultured in a standard cell culture incubator (21% pO₂; 5% CO₂) or XVivo X3 workstation (Biospherix, Parish, NY, USA) in 1% pO₂; 5% CO₂, respectively. After 72 h, cells were harvested using Accutase (Biolegend, San Diego, CA, USA), cell counts and viability were assessed by a Trypan blue exclusion test using a Burker chamber. Collected cells were used for further analysis—protein and RNA isolation. The scheme of the in vitro experiments is presented in Figure 1A.

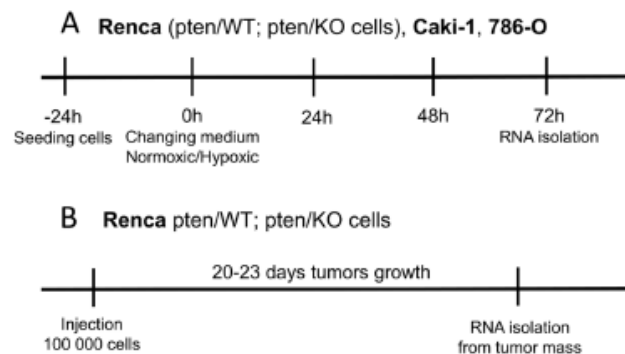


Figure 1. Experimental protocols: (A) culture cancer cells in hypoxic and normoxic conditions (B) in vivo experiment obtaining tumors composed of Renca pten/WT or pten/KO cells.

2.5. In Vivo Renca pten/WT and pten/KO Tumor Implantation and Development

BALB/c, six-to-eight-week-old female mice were obtained from the Medical University of Bialystok. Animal care and experimental procedures were approved by the Second Warsaw Local Ethics Committee for Animal Experimentation (no. WAW2/76/2017) and performed following Directive 2010/63/EU regulations. Mice were housed in a controlled environment with a 12 h light/12 h dark cycle with ad libitum access to tap water and full-fledged diet.

Renca cells were implanted in BALB/c mice leg as subcutaneous tumors by injection of a plug constituted by 10⁵ cells in 100 µL Matrigel[™] (Corning, NY, USA) diluted in 1:3 in PBS. After 22 days of tumor growth, the mice were sacrificed and fragments of tumor tissue were used to isolate RNA (Figure 1B). The groups consisted of 4 mice and the experiment was performed using two separate sets of animals.

2.6. Total RNA Isolation

Total RNA was extracted from 4 × 10⁶ cancer cells cultured in normoxia and hypoxia or 40 mg of tumor tissues using an RNeasy Mini Kit (Qiagen, Hilden, Germany). The samples

were freed from DNA using TURBO DNA-free kit (Thermo Fisher Scientific, Waltham, MA, USA) and RNA quality and concentrations were evaluated using the fluorometer Qubit (Qubit RNA BR Assay Kit, RNA with Qubit RNA IQ Assay Kit, Thermo Fisher Scientific, Waltham, MA, USA) according to the manufacturer's instructions.

2.7. Next Generation Sequencing

Total RNA from Renca cells and tumors (pten/WT, pten/KO) was used to prepare libraries and perform high-throughput sequencing by an external service (Lexogen GmbH, Vienna, Austria) with a NextSeq 500 system (Illumina, San Diego, CA, USA). Briefly, RNA concentration was measured by UV-Vis spectrophotometry (Nanodrop 2000c, Thermo Fisher), and RNA integrity was assessed on a Fragment Analyzer System using the DNF-471 RNA Kit (15 nt) (Agilent, Santa Clara, CA, USA). Sequencing-ready libraries were produced using a Small RNA-SeqLibrary Prep Kit by Lexogen (052UG128V0110) per manufacturer instructions. Indexed library preparation was performed to allow for multiplexed sequencing. For library preparation, 100 ng of each provided RNA sample was used. All libraries were analyzed for adapter dimers, size distribution and concentration on a Fragment Analyzer System using the DNF-474 HS NGS Fragment kit (1–6000 bp) (Agilent, Santa Clara, CA, USA). Libraries were pooled in an equimolar ratio. After pooling, 1.3× magnetic bead purification and agarose gel size selection was performed to target miRNA fraction. The concentration and the size distribution of the final lane mix was analyzed by Qubit ds-DNA HS assay (Thermo Fisher Scientific, Waltham, MA, USA) and by a Fragment Analyzer system using the DNF-474 HS NGS Fragment Kit (1–6000 bp) (Agilent, Santa Clara, CA, USA). Dilution of the lane mix (2 nm) was denatured and diluted to loading concentration for sequencing on a NextSeq 500 instrument with a SR75 High Output Kit (Illumina). Differentially expressed miRNA (DEmiRNAs) were classified according to $-1 < \log_{2}FC > 1$, adjusted *p*-value—FDR (False Discovery Rate) < 0.05 . NGS data have been deposited in NCBI's Gene Expression Omnibus [36] and are accessible through GEO Series accession number GSE197301 (<https://www.ncbi.nlm.nih.gov/geo/query/acc.cgi?acc=GSE197301>, published on 10 May 2022).

2.8. Validation of DEmiRNAs Expression by qRT-PCR

The expression of potential DEmiRNAs were analyzed by qRT-PCR both in Renca cells and tumors (pten/WT, pten/KO), as well as human cells with functional and mutant PTEN (Caki-1 and 786-O). Total RNA (10 ng) was used to obtain cDNA using TaqMan™ Advanced miRNA cDNA Synthesis Kit (Thermo Fisher Scientific, CA, USA, USA) according to the manufacturer's protocol. Briefly, PolyA tailing, adapter ligation and reverse transcription reaction with universal primers were performed. The product of reverse transcription was amplified, then diluted 1:10 and used for the qRT-PCR reaction with TaqMan™ Fast Advanced Master Mix and TaqMan™ Advanced miRNA Assays (listed in Table 1, Thermo Fisher Scientific, Waltham, MA, USA). Reactions were run on Bio-Rad CFX384 qPCR System (BioRad, Hercules, CA, USA), according to the protocol described in Table 2. The relative miRNAs levels were calculated with 2^{(-Delta C(T))} method, with normalization to the expression of reference miRNAs: miR-16-5p and miR-25-3p. For tissue samples from healthy and kidney cancer, only miR-25-3p was used as reference miRNA.

Table 1. List of TaqMan probes used to detect miRNA expression.

miRNA	Assay Number
miR-210-3p	mmu481343_mir
miR-206-3p	mmu481645_mir
miR-100-5p	mmu478224_mir
miR-155-5p	mmu480953_mir
miR-100-5p	478224_mir
miR-155-5p	483064_mir

Table 1. Cont.

miRNA	Assay Number
miR-342-3p	mmu481074_mir
miR-221-3p	mmu481005_mir
miR-10b-5p	mmu478494_mir
miR-21a-5p	mmu482709_mir
miR-25-3p	mmu483226_mir
miR-16-5p	mmu482960_mir

Table 2. qRT-PCR conditions—TaqMan™ Fast Advanced Master Mix (miRNA detection).

Step	Temperature	Time	Cycle
Enzyme activation	95 °C	20 s	1
Denature	95 °C	1 s	40
Anneal/Extend	60 °C	20 s	

2.9. Prediction of Potential Targets for DE miRNAs

The target genes for validated DE miRNAs were assessed using an miRNet (<http://www.mimnet.ca/>, accessed on 1 December 2021), bioinformatics tool for target prediction based on 11 different databases. The same software was used to assess potential pathways regulated by target genes of DE miRNAs based on the Function Explorer and KEGG database.

2.10. Evaluation of the Expression of Target Genes for DE miRNAs by qRT-PCR

For cDNA synthesis, 2 µg of total RNA was used for reverse transcription reaction (High-Capacity cDNA Reverse Transcription Kit; Thermo Fisher Scientific, Waltham, MA, USA) and the product was diluted 3×. Real-time PCR was performed using TaqMan™ Gene Expression Master Mix with TaqMan probes or using PowerUp™ SYBR™ Green Master Mix (all from Thermo Fisher Scientific, Waltham, MA, USA, listed in Tables 3 and 4). Reactions were run on Bio-Rad CFX384 qPCR System or CFX Connect qPCR System (BioRad, Hercules, CA, USA), according to the protocol described in Tables 5 and 6. The relative mRNA level was calculated with the 2^{(-Delta C(T))} method, with normalization to the expression of *Actinβ* as a house-keeping gene for mouse models and *GusB* for human models.

Table 3. List of TaqMan probes used to detect gene expression.

Gene	Taq Man Probes
<i>Hif-1α</i>	Mm00468869; Hs00153153
<i>Vegfa</i>	Mm00437306; Hs00900055
<i>Alk1</i>	Mm00437306
<i>Tp53</i>	Mm01731287
<i>mTOR</i>	Mm01731287
<i>Pten</i>	Hs02621230
<i>Actinβ</i>	Mm02619580
<i>GusB</i>	Hs00939627

Table 4. List of primers sequences used to detect gene expression.

Gene	Primers Sequences
<i>Bcl2</i>	F: GACTGAGTACCTGAACCGGC
	R: AGTTCACAAAGGCATCCCAG
<i>Tgfbβ3</i>	F: AGTGCTCTGAGTGTCCCTA
	R: TACTCCACACAGGGGAGAC
<i>Actinβ</i>	F: CCTAGGCACCAAGGTGTGA
	R: GTTGGCCTTAGGGTTCAGGG

Table 5. qRT-PCR conditions TaqMan™ Gene Expression Master Mix.

Step	Temperature	Duration	Cycle
UNG incubation	50 °C	2 min	Hold
Polymerase Activation	95 °C	10 min	Hold
Denature	95 °C	15 s	40
Anneal/extend	60 °C	15 s	

Table 6. qRT-PCR conditions PowerUp™ SYBR™ Green Master Mix.

Step	Temperature	Duration	Cycle
UDG activation	50 °C	2 min	Hold
Dual-Lock™ DNA polymerase	95 °C	2 min	Hold
Denature	95 °C	15 s	40
Anneal	60 °C	45 s	
Extend	60 °C	1 min	

2.11. Western Blot

Samples were lysed with an RIPA buffer containing Cocktail inhibitors (both Thermo Fisher Scientific, Waltham, MA, USA). 12 µg of total protein, assessed by BCA assay, were solubilized in a Laemmli sample buffer (AlfaAesar, Haverhill, MA, USA), separated on 12% polyacrylamide gel and transferred onto nitrocellulose membranes (BioRad, Hercules, CA, USA). PonceauS staining was performed to detect proteins on the membrane. Non-specific binding was reduced by a blocking step for 2 h in 5% skimmed milk at room temperature. Membranes were incubated overnight at 4 °C in the presence of a solution containing primary antibodies: anti-PTEN (#9549, dilution 1:700, Cell Signaling Technology, Danvers, MA, USA), anti-Vinculin (#SC-59803, dilution 1:1000, Santa Cruz Biotechnology, Dallas, TX, USA), anti-GAPDH (#SC-32233, dilution 1:1000, Santa Cruz Biotechnology, Dallas, TX, USA), anti-pAKT (#MAB887, dilution 1:1000, R&D System, Minneapolis, MN, USA), and then incubated for 2 h in the relevant secondary antibody (Goat Anti-Rabbit IgG Antibody or Horse Anti-Mouse IgG Antibody conjugated with horseradish peroxidase (HRP) (#PI-1000, #PI-2000, both used at 1:10,000, from Vector Laboratories, Burlingame, CA, USA). Reactive bands were revealed by reaction with enhanced chemiluminescence substrate (Santa Cruz Biotechnology, Dallas, TX, USA) and visualized using X-ray films (Carestream Health, Rochester, NY, USA). Quantification of the integrated optical density (IOD) of the bands was performed using ImageJ analysis software. In quantitative analysis, the relative IOD of target proteins were normalized to the IOD of Vinculin.

2.12. Exosomes Isolation

Exosome isolation from Renca pten/WT cells cultured 72 h in normoxic and hypoxic conditions was performed using ExoQuick-TC (System Bioscience, Palo Alto, CA, USA) according to the manufacturer's instructions. In brief, conditioned medium was collected and centrifuged at 2000 × g for 30 min to remove cell residues. ExoQuick-TC exosome precipitation solution was added to the supernatant (in ratio 1:5) and incubated overnight at 4 °C. The suspension was then centrifuged at 1500 × g for 30 min and a pellet was used to isolate RNA or proteins. The presence of the exosomal TSG101 marker was confirmed on the protein isolate by the western blot method (anti-TSG101 antibody #NBP1-80659, dilution 1:500, Novus Biologicals, Littleton, CO, USA; secondary antibody Goat Anti-Rabbit IgG Antibody, conjugated with horseradish peroxidase (HRP), dilution 1:10,000, Vector Laboratories, Burlingame, CA, USA), the size of the isolated nanoparticles was estimated using the Zeta Viewer Nanoparticle Analyzer (Supplementary Figure S2).

2.13. Culture MBr MEC FVB with Conditioned Medium from Renca Cells

MBr MEC FVB immortalized brain endothelial cells as described were seeded on tissue culture flasks (Falcon-Corning, NY, USA) at 3000 cells/cm² and allowed to adhere to the culture surface for 24 h (protocol of the experiment is represented as scheme on Figure 1B). Media were exchanged with pre-equilibrated normoxic or hypoxic medium or mixed (1:1) with conditioned medium from Renca cells from appropriate aerobic conditions and cultured in normoxia and hypoxia for the following 48 h and used for protein isolation.

2.14. Statistical Analysis

Each in vitro experiment was performed at least three times in independent biological replicates. The results are shown as a mean \pm SEM, where appropriate results are presented as fold change as compared to normoxia. All statistical analyses were performed using GraphPad Prism 9 version 9.1.2 for Windows (GraphPad Software, San Diego, CA, USA, www.graphpad.com, accessed on 26 February 2022).

3. Results

3.1. PTEN Status in Tested Models

To determine the miRNA patterns characteristic for RCC in relation to hypoxia and PTEN status, both in vitro (in normoxic and hypoxic conditions) and in vivo samples from murine kidney cancer model Renca (pten/WT, pten/KO) were analyzed using next generation sequencing. Then, to expand and validate the obtained results by comparison with human species, renal cancer cell lines with functional and mutated PTEN (Caki1 and 786-O respectively) were examined in normoxic and hypoxic conditions. The level of PTEN in all tested cell lines was confirmed by western blot (Figure 2A). Dysregulation of the PTEN activity in 786-O and Renca pten/KO cells is demonstrated by a high level of pAKT (Figure 2A). In a murine PTEN knockout model, p-AKT expression was approximately 14-fold higher than in pten/WT cells, respectively in the human models, the increase was 7-fold. Potential clinical significance of tested miRNAs was marked using commercially available RNA isolates from healthy kidney and kidney tumor, characterized by reduced PTEN levels in cancer tissue as compared to a healthy one (Figure 2B). In all models tested, the expression of miRNA and target genes was assessed in hypoxic conditions and depending on PTEN status in the order described in the graphical workflow (Figure 2C).

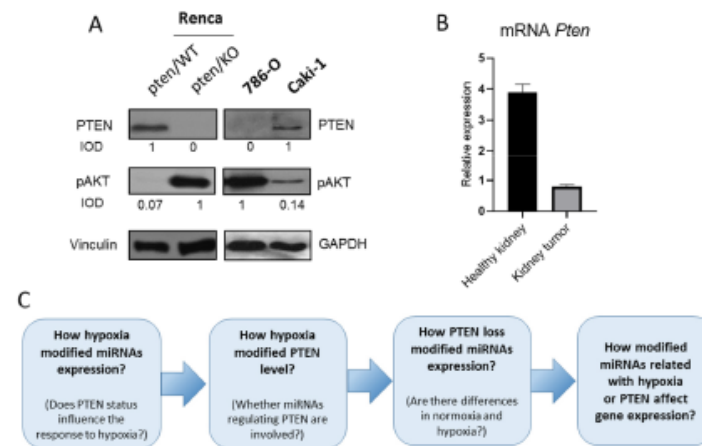


Figure 2. PTEN status in tested models (A) PTEN and pAKT levels in kidney cancer cell lines, IOD calculated relative to Vinculin (B) Relative to *Gusb* expression of *Pten* in RNA isolates from kidney cancer and healthy kidney tissues (C) graphical workflow.

3.2. Hypoxia-Induced miRNA Signature in Murine Kidney Cancer Models with Different PTEN Status

A global miRNA analysis showed only a few changed miRNAs in response to low oxygen tension in both PTEN variants, as presented by volcano plots (Figure 3A,F). In hypoxic Renca pten/WT, nine deregulated miRNAs reached statistical significance (six up-regulated, three down-regulated) compared to normoxic cells (Figure 3A). However, even fewer changes were noted in pten/KO cells in response to low pO₂—5 DE miRNAs of which only one was downregulated (Figure 3F). To verify the standard hypoxic response, miR-210-3p and miR-206-3p expression, which was up-regulated in both PTEN variants, was further studied using additional models. qRT-PCR analysis confirmed that miR-210-3p is upregulated in hypoxia regardless of the status of PTEN, however in PTEN mutants (Renca pten/KO and 786-O) this increase was considerably lower than in PTEN wild-type cells (Renca pten/WT, Caki-1) (Figure 3B,C). No difference was noticed between miR-210-3p levels in the tissues from pten/WT and pten/KO tumors, which suggests that the regulation of miR-210-3p occurs in a PTEN independent manner (Figure 3D). As expected, miR-210-3p expression was at an undetectable level in tissue isolated from a healthy kidney and was strongly expressed in kidney tumor tissue (Figure 3E). In turn, miR-206-3p expression measured by qPCR was upregulated by hypoxia only in pten/KO cells, not in pten/WT (Figure 3G). These results are consistent with NGS analysis; the changes in miR-206-3p expression in Renca pten/WT was characterized by lower logFC (1.9) (Figure 3A), while in Renca pten/KO logFC = 2.46 (Figure 3F). Increasing miR-206-3p after exposure to low pO₂ in pten/KO cells resulted in a strong tendency to change the expression of this miRNA between pten/WT and pten/KO cells in hypoxia (p-value = 0.08) (Figure 3G). This tendency was also observed in in vivo samples, which reflect the hypoxic conditions (Figure 3H).

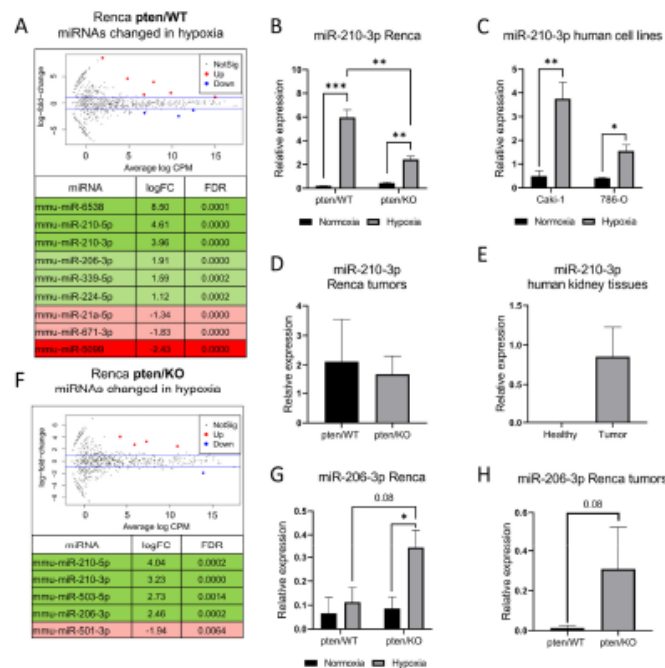


Figure 3. Hypoxia-induced miRNA signature in murine kidney cancer models with different PTEN status (A) Volcano plots and list of significantly differentially expressed miRNAs after exposure to

hypoxia in Renca pten/WT cells; shades of green represent miRNA upregulated in hypoxia; shades of red downregulated in hypoxia (B) Relative to miR-25-3p and miR-16-5p expression of miR-210-3p in cells cultured in normoxic and hypoxic condition: Renca pten/WT and pten/KO (C), Caki-1 and 786-O (D) Relative to miR-25-3p and miR-16-5p expression of miR-210-3p in tumors derived from Renca pten/WT and pten/KO cells (E) Relative to miR-25-3p expression of miR-210-3p in human tissues from healthy kidney and kidney cancer (F) Volcano plots and list of significantly differentially expressed miRNA after exposure to hypoxia in Renca pten/KO cells (G) Relative to miR-25-3p and miR-16-5p expression of miR-206-3p: in Renca pten/WT and pten/KO cultured in normoxia and hypoxia (H) in the tissues from Renca pten/WT and pten/KO tumors, Student's *t*-test *** *p*-value < 0.001; ** *p*-value < 0.01; * *p*-value < 0.05.

3.3. Identification of PTEN-Related miRNA in Hypoxic Conditions

NGS analysis showed miR-21a-5b to be downregulated in response to hypoxia in pten/WT cells. As miR-21a is a well-known regulator of PTEN, and its expression was further validated in the context of the hypoxia-induced decreased PTEN level observed in Renca pten/WT cells (Figure 4A). We confirmed the strong tendency to downregulate miR-21a-5p in wild-type cells in response to hypoxia, but the same tendency was observed in pten/KO (Figure 4B). This may suggest that downregulation of miR-21a-5b is not involved in the modulation of PTEN levels in our model (the same pattern in pten/WT and pten/KO cells). Moreover, miR-21a is known to directly degrade *Pten* mRNA, so its decrease does not correlate with a decreased PTEN level.

Thus, we checked whether other miRNAs affecting PTEN described in the literature are changed by hypoxia. miR-221-3p was upregulated in low pO₂ only in pten/WT cells, while in the absence of PTEN, the level was stable between oxygen conditions (Figure 4C). A different response to hypoxia in pten/WT and pten/KO cells in the context of miR-221-3p expression may suggest its effect on hypoxia-dependent PTEN downregulation in pten/WT cells. Since such changes were not observed in the human PTEN wild-type kidney cancer model Caki-1, no increase in miR-221-3p (Figure 4E) in hypoxia resulted in a stable level of PTEN between oxygen conditions (Figure 4D). In a human PTEN mutant model, 786-O miR-221-3p was also stable between oxygen condition (Figure 4F).

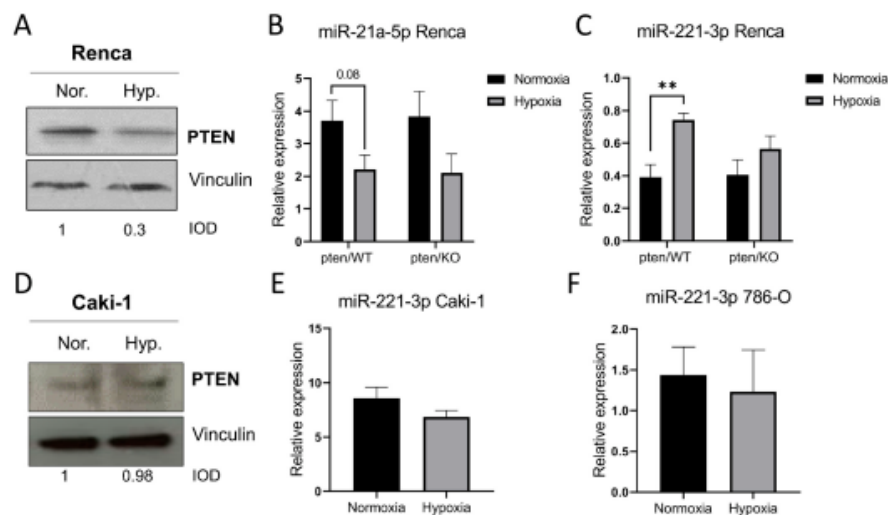


Figure 4. Cont.

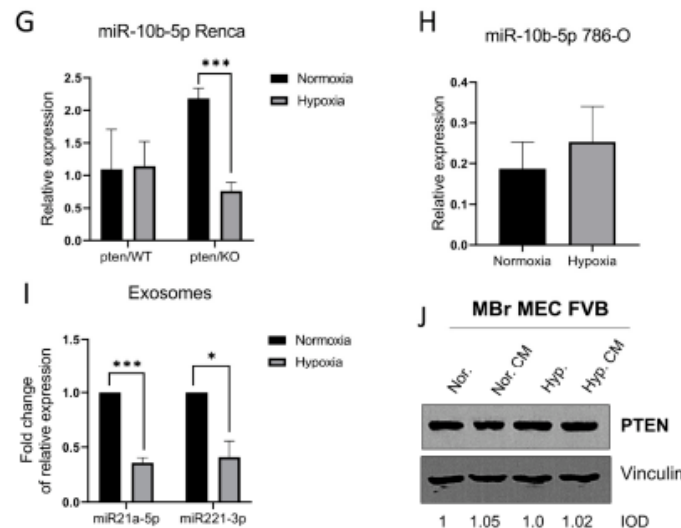


Figure 4. PTEN-related miRNAs in hypoxic conditions (A) PTEN detection by western blot in Renca pten/WT cells cultured in normoxic and hypoxic condition, IOD calculated relative to Vinculin (B) Relative to miR-25-3p and miR-16-5p expression of miR-21a-5p and (C) miR-221-3p in Renca pten/WT and pten/KO cells cultured in normoxia and hypoxia (D) PTEN detection by western blot in Caki-1 cells cultured in normoxic and hypoxic condition, IOD calculated relative to Vinculin (E) Relative to miR-25-3p and miR-16-5p expression of miR-221-3p in Caki-1 cells, and (F) in 786-O cells cultured in normoxia and hypoxia (G) Relative to miR-25-3p and miR-16-5p expression of miR-10b-5p in Renca pten/WT and pten/KO cells and (H) 786-O cells cultured in normoxia and hypoxia (I) Fold change of relative to miR-25-3p and miR-16-5p expression of miR-21a-5p and miR-221-3p in exosomes isolated from Renca pten/WT cells cultured in normoxia and hypoxia (J) PTEN detection by western blot in MBr MEC FVB cells cultured in normoxic and hypoxic condition with or without conditioned medium (CM) from Renca pten/WT cells, IOD calculated relative to Vinculin, Student's *t* test *** *p*-value < 0.001; ** *p*-value < 0.01; * *p*-value < 0.05.

Another tested PTEN-related miRNA was miR-10b-5p, which was stable between the oxygen condition in Renca pten/WT cells, but was significantly downregulated in hypoxia in pten/KO cells (Figure 4G), indicating that miR-10b-5p may be involved in the altered hypoxia response due to the complete loss of PTEN. However, this trend has not been confirmed in a human RCC model with non-functional PTEN (Figure 4H).

We also checked the expression of PTEN-related miRNAs in exosomes secreted by Renca pten/WT cells to determine the impact of these changes on other components of the tumor microenvironment (TME). Expression of miR-21a-5p was lower in hypoxic exosomes compared to normoxic ones, which corresponds to the level of this miRNA in cells (Figure 4I). At the same time, upregulation of miR-221-3p was not transferred to exosomes secreted by Renca cells in hypoxic conditions. (Figure 4I). Additionally, exosomes secreted by Renca cells, present in the conditioned medium, did not affect PTEN levels in brain-derived healthy endothelial cells (MBr MEC FVB) (Figure 4J). miR-10b-5p was below detection in samples from exosomes (data not shown).

3.4. PTEN-Dependent miRNA Pattern

We next verified how the total loss of PTEN affects the miRNA pattern in RCC in normoxic and hypoxic conditions, as well as in *in vivo* samples. Surprisingly, NGS analysis showed no significantly deregulated miRNAs in *in vitro* samples from pten/KO cells

compared to the wild-type in both normoxic and hypoxic conditions (Supplementary Figure S3A,B). However, despite the lack of altered expression in vitro, in vivo samples revealed some DE miRNAs. In tumors derived from KO cells compared to WT 7, deregulated miRNAs were identified (5 up, 2 down) (Figure 5A). In in vitro samples, these miRNAs did not achieve statistical significance (FDR > 0.05), as demonstrated in Supplementary Figure S3A,B. Next we validated the expression of miR-155-5p, miR-100-5p and miR-342-3p, since they were shown to be important in the PTEN mediated pathways, namely miR-155-5p and miR-100-5p, were the most efficiently changed in vivo together with miR-7115 that had no validated target, as yet.

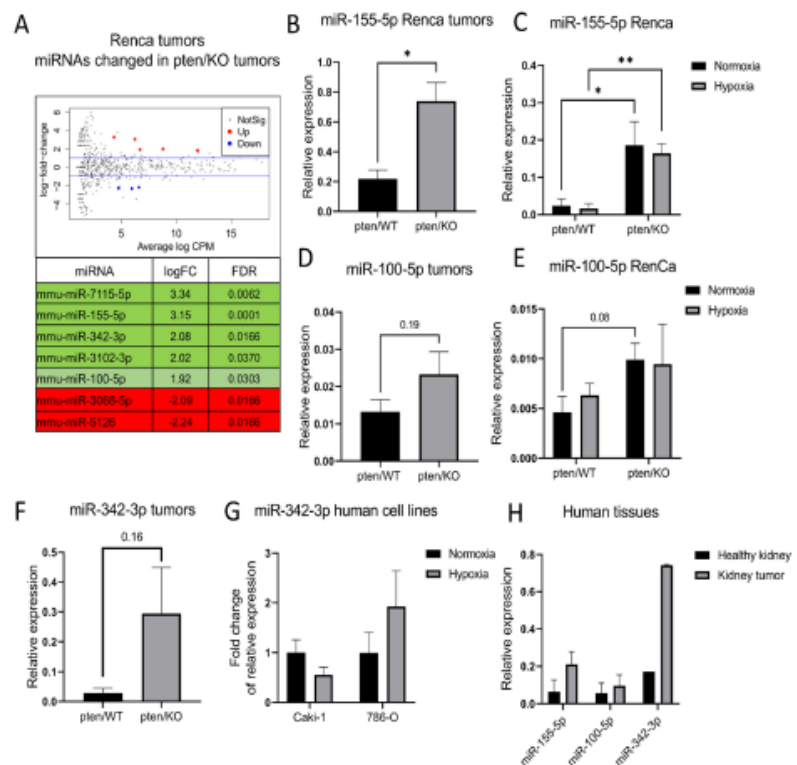


Figure 5. PTEN-dependent miRNA pattern in RCC models (A) Volcano plots and list of significantly differentially expressed miRNAs after in pten/KO tumors; shades of green represent miRNA upregulated in pten/KO cells; shades of red downregulated in pten/KO cells (B) Relative to miR-25-3p and miR-16-5p expression of miR-155-5p in tumors derived from Renca pten/WT and pten/KO cells (C) Relative to miR-25-3p and miR-16-5p expression of miR-155-5p in Renca pten/WT and pten/KO cells cultured in normoxic and hypoxic condition (D) Relative to miR-25-3p and miR-16-5p expression of miR-100-5p in tumors derived from Renca pten/WT and pten/KO cells (E) Relative to miR-25-3p and miR-16-5p expression of miR-100-5p in Renca pten/WT and pten/KO cells cultured in normoxic and hypoxic condition (F) Relative to miR-25-3p and miR-16-5p expression of miR-342-3p in tumors derived from Renca pten/WT and pten/KO cells and in tumors derived from Renca pten/WT and pten/KO cells (G) Fold change of relative to miR-25-3p and miR-16-5p expression of miR-342-3p in Caki-1 and 786-O cells cultured in normoxia and hypoxia (H) Relative to miR-25-3p expression of miR-155-5p, miR-100-5p and miR-342-3p in human tissues from healthy kidney and kidney tumor; Student's *t*-test ** *p*-value < 0.01; * *p*-value < 0.05.

MiR-155-5p was significantly upregulated in *pten*/KO tumors compared to the wild-type as confirmed by qPCR (Figure 5B). The same was observed in *in vitro* samples both in hypoxic and normoxic conditions (Figure 5C). Interestingly, the hypoxia-induced decrease in PTEN in Renca cells was insufficient to induce miR-155-5p expression. The increase in miR-100-5p expression observed by NGS was not validated by qRT-PCR from *in vivo* samples, however in *in vitro* experiments the tendency was strong (p -value = 0.08) (Figure 5D,E). The same as miR-155-5p, expression of miR-100-5p was independent of oxygen conditions. miR-342-3p was not detected in Renca *in vitro* samples (data not shown), however in Renca *pten*/KO tumors it tended to be upregulated compared to *pten*/WT (Figure 5F). Experiments on human models showed that miR-342-3p regulation occurs in a hypoxia-independent manner regardless of the PTEN status (Figure 5G). In kidney cancer tissue, characterized by the decreased expression of PTEN compared to healthy kidney, miR-155-5p and miR-342-3p were upregulated, and no difference in expression of miR-100-5p was observed (Figure 5H).

3.5. Identification of Potential Hypoxia- and PTEN-Dependent miRNAs Targets

Next, we identified the potential targets of miRNAs that were validated and significantly changed either by hypoxia or PTEN deregulation. Figure 6A presents networks of potential target genes, showing the number of targets for each miRNA (Figure 6B), as well as the signaling pathways related to the appointed target genes (Figure 6C). They are strongly involved in the PI3K/ AKT pathway regulated by PTEN or HIF-1 α signaling regulated by hypoxia, but also in apoptosis and the TGF- β signaling pathway. To establish whether deregulation of the tested miRNAs affects the expression of genes, we checked the levels of transcripts of some of the targets. We checked the expression of *Hif-1 α* as the main modulator of hypoxic response associated with miR-210-3p activity, but no changes were observed in all tested cell lines (Figure 7A,B). However, *Vexfa*, which is a downstream target of HIF-1 α , was upregulated in PTEN wild-type Renca and Caki-1 cell lines in response to hypoxia. In Renca *pten*/KO this increase was weaker than in Renca *pten*/WT, and we did not observe an increase in PTEN mutant 786-O cells (Figure 7C,D), which reflects the results of miR-210-3p expression. As the pathway associated with apoptosis was altered in the context of the DE miRNAs, we checked the expression of antiapoptotic *Bcl2*, which is also associated with HIF-1 α signaling, and regulated by miR-210-3p. *Bcl2* was downregulated in hypoxia in both PTEN variants (Figure 7E), and this was correlated with a decreased number of live cells in all tested cell lines (Figure 7F,G). PTEN knockout caused upregulation of miR-155-5p, and we assessed two potential targets of this miRNA: *Akt1* and *mTOR*. *Akt1* tended to be downregulated in Renca *pten*/KO compared to the wild-type (Figure 7H); however, hypoxia also caused downregulation of *Akt1*, what may suggest that expression is also regulated independently of miR-155-5p, which was stable in *pten*/WT cells in normoxic and hypoxic condition (Figure 5C). Moreover, no change was observed in *mTOR* expression between both PTEN variants an oxygen level (Figure 7I). Due to the altered expression of miR-21a-5p in response to hypoxia and significant changes in the TGF- β signaling pathway, we assessed the level of *Tgfb β 3*, which is modulated by miR-21a-5p. *Tgfb β 3* was upregulated in hypoxia in both PTEN variants (Figure 7J). *p53*, which may also be regulated by miR-21a-5p, miR-10b-5p and miR-221-3p, is downregulated by hypoxia and in *pten*/KO independently (Figure 7K).

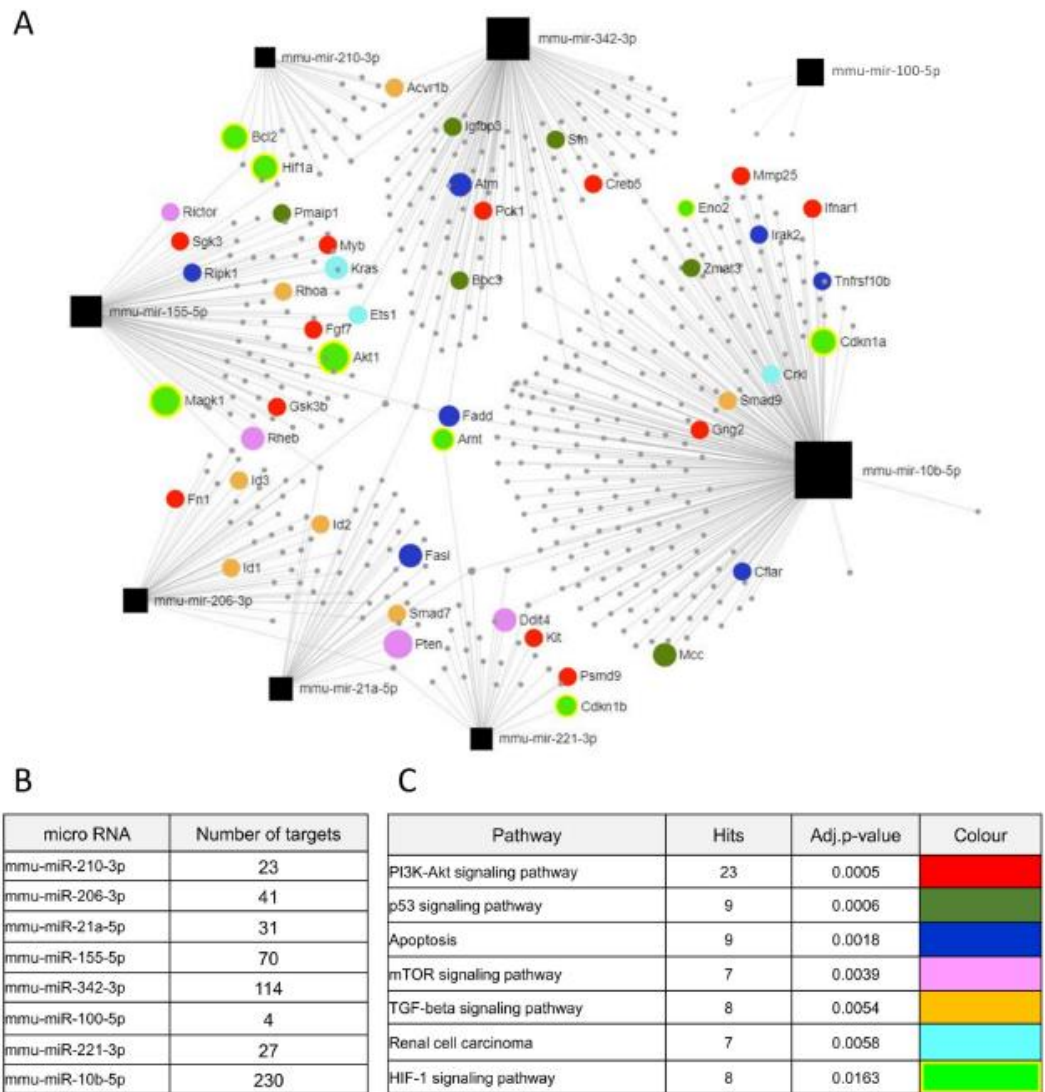


Figure 6. The predicted target genes of DEMiRNAs (A) Network of target gene, with marked genes involved in potentially dysregulated signaling pathways, predicted using the miRNET software (B) Number of target genes for each DEMiRNA (C) Potentially deregulated signalling pathways for predicted target genes analyzed through susceptibility genes enrichment.

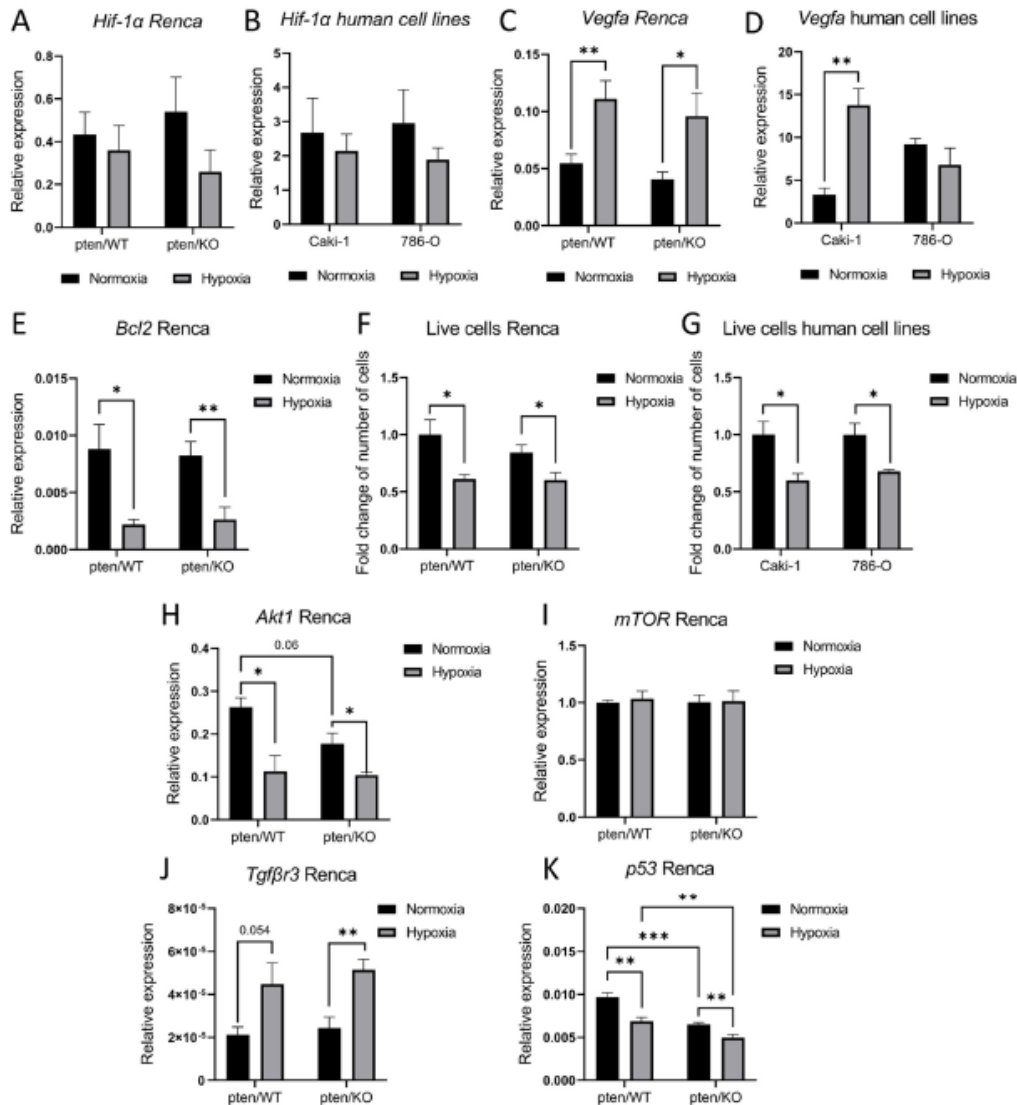


Figure 7. Expression of predicted target genes in RCC models (A) Relative to *Actinβ* expression of *Hif-1α* in Renca pten/WT ptenKO cells cultured in normoxia and hypoxia (B) Relative to *GusB* expression of *Hif-1α* in Caki-1 and 786-O cells cultured in normoxia and hypoxia (C) Relative to *Actinβ* expression of *Vegfa* in Renca pten/WT ptenKO cells cultured in normoxia and hypoxia (D) Relative to *GusB* expression of *Vegfa* in Caki-1 and 786-O cells cultured in normoxia and hypoxia (E) Relative to *Actinβ* expression of *Bcl2* in Renca pten/WT ptenKO cells cultured in normoxia and hypoxia (F) Fold change of number of live cells collected from normoxic and hypoxic culture: Renca pten/WT pten/ KO (G) and Caki-1, 786-O (H) Relative to *Actinβ* expression of *Akt1* (I) *mTOR* (J) *Tgfβ3* (K) *p53* in Renca pten/WT ptenKO cells cultured in normoxia and hypoxia, Student's *t*-test *** *p*-value < 0.001; ** *p*-value < 0.01; * *p*-value < 0.05.

4. Discussion

PTEN is a tumor suppressor that is frequently mutated in cancers. The frequency of PTEN alterations is around 8% for all cancers, but for some, like endometrial cancer or gliomas, it is almost as high as for p53 mutations [37,38]. Corroborating the limited mRNA hypoxic signatures in cancer cells [39,40] after exposure to hypoxia, we identified only nine differentially expressed miRNA in Renca PTEN wild-type cells as compared to the liver cancer response to hypoxia by 165 altered miRNAs [41]. PTEN knockout altered the expression of seven miRNAs in tumor samples. Similarly, few changes were observed in prostate cancer of a PTEN knockout mouse model [28].

Exposure to hypoxia increased miR-210-3p expression in both PTEN variants. MiR-210 expression increase in low pO₂ is a well-known and general effect [42]. In RCC patients, miR-210 was one of the five most changed miRNAs in tumors [43], as confirmed here. MiR-210 is induced by HIF-1 α , although we observed no difference in *Hif-1 α* expression, which might be due to a prolonged exposure to low pO₂ (72 h), since the downstream *Vegfa* gene expression was increased. This could be partly mediated by miR-210, reported to be proangiogenic [44,45]. However, in 786-O, hypoxia did not upregulate *Vegfa* expression, despite the miR-210-3p increase. As these cells are characterized by VHL mutation, it is clear that a pseudo hypoxic stress is installed and may prevent the miR-210-3p and *Vegfa* sensitivity to hypoxia itself. Apoptosis is also regulated by miR-210-3p. Indeed, fewer viable cells were collected upon hypoxia, coinciding with the downregulation of the Bcl2-antiapoptotic protein, shown to be regulated by this miRNA in neuroblastoma or in the spermatocyte cell line [46,47].

To our knowledge, this is the first study to show the effect of PTEN knockout on miR-210-3p demonstrated by the lower increase of miR-210-3p expression in low pO₂ in cells with mutant PTEN compared to WT cells. This confirms a role for PTEN in regulating cell responses to low pO₂ [48]. Together with weaker miR-210-3p upregulation, we observed the induction of miR-206-3p in pten/KO cells in response to hypoxia. VEGF is a target for miR-206, and a negative correlation between miR-206 levels and VEGF expression has been proven in human renal cancer lines [49]. VEGF is differentially regulated by miR-210 (up-regulation) and miR-206 (down-regulation); however, this did not presently result in a disturbed induction of gene expression; in response to hypoxia pten/KO VEGF upregulation was as efficient as in wild-type cells. miR-206 is suggested to be a tumor suppressor [50,51]; it inhibits cancer cell growth and metastasis. MiR-206 was downregulated in RCC compared to non-tumor tissues and in cell lines (Caki-1 and Caki-2) compared to normal human kidney cells [49]. Surprisingly, in PTEN mutated cells, miR-206-3p was elevated in response to hypoxia, suggesting lower aggressiveness. MiR-206 was reported to indirectly regulate the MAPK-PI3K/Akt pathway [50], therefore this miRNA can serve as a regulator of pAKT accumulation upon PTEN mutation. The direct link between miR-206-3p and PTEN could not be established since its activation was a response to hypoxia in pten/KO cells, while PTEN mutation only was not enough to activate miR-206-3p.

At the same time, hypoxia reduced the miR-10b-5p level that was strongly induced in normoxic pten/KO. MiR-10b-5p is an oncomiR, as it promotes cell proliferation, protects against apoptosis [52], and mediates cancer progression [53]. It targets PTEN mRNA [54] leading to the activation of the PI3K/AKT pathway. In our study, cells with dysfunctional PTEN had a higher expression of this miRNA than pten/WT cells, but its level in pten/KO cells was reduced by hypoxia as compared to normoxic controls. Whether a reciprocal regulation of miR-10b by PTEN exists needs to be evaluated, but it might be that in our model miR-10b induction by PTEN-KO could be partially mediated by p53 downregulation [55]. Indeed, PTEN/p53 interaction is described on a protein level [30]; however, they might also share miRNAs regulatory pathways.

Although miR-206-3p and miR-10b-5p were not affected by hypoxia in pten/WT cells, they were differently modulated by low pO₂ in PTEN mutated cells. This points to the oxygen-dependent role of PTEN as a tumor suppressor, as the observed PTEN inactivation is more frequent in hypoxic tumors [56]. Additionally, the modulation of miRNAs response

to hypoxia by PTEN inactivation is of interest for a potential therapeutical approach. miR-206-3p was shown to indirectly repress ABCB1, a multidrug resistance gene [57], and was shown to reduce Cisplatin resistance in gastric cancer [58]. Also, Wang et al. observed that this miRNA increases cancer response to radiotherapy [59]. miR-10b-5b was also shown to alter cancer response to therapy; it mediates resistance to 5-fluorouracil (5-FU) by promoting cancer cell survival [60] and decreases sensitivity to radiotherapy [61]. Therefore, the miRNA profile of hypoxic PTEN mutated cells identified in our study may suggest the promotion of a therapy-sensitive phenotype of tumor cells.

On the other hand, reduced miR-210 levels were observed in cells resistant to 5FU, which promoted their DNA repair and metabolic adaptation to drug treatment [62]. Therefore, the modulated response to hypoxia by PTEN dysregulation, as observed by levels of miR-206-3p, miR-10b-5p and miR-210-3p in this study, can alter the induction of drug resistance pathways. Knowing that reduction [63] or inactivation [64] of PTEN and also hypoxia can increase cancer cell resistance to chemo- and radiotherapy [65], information that PTEN dysregulation disturbs miRNA response to low pO₂ might serve as a cue for redefining treatment selection in hypoxic PTEN mutated tumors.

MiRNAs regulated by PTEN mutation independently of oxygen level included: miR-155-5p, miR-100-5p, and miR-342-3p. In our research, miR-155-5p was significantly upregulated in pten/KO cells and tumors and was not affected by the oxygen level. In a mouse prostate cancer model with PTEN mutation, the same miRNA was the most upregulated. PTEN is a target for miR-155 [66], so accumulation of miR-155-5p in pten/KO cells may be related with the lack of target. On the other hand, analysis based on miRNet software showed that *Akt1* could also be a target of miR-155-5p. *Akt1* was decreased after PTEN knockout, but hypoxia also caused a decrease in *Akt1* expression independently of PTEN which, together with a stable miR-155-5p level between normoxia and hypoxia in pten/WT and pten/KO cells, may indicate no influence of miR-155-5p on *Akt1* level or other hypoxia-dependent mechanisms regulating *Akt*, not related with miR-155-5p. Other miRNAs that tended to be deregulated in PTEN mutant cells were miR-100-5p and miR-342-3p. miR-100-5p overexpression is strongly associated with tumor progression and adverse clinical outcomes in RCC patients [67]. Although in ovarian cancer the key relationship between miR-100 and the mTOR pathway was confirmed [68], in our RCC model the tendency to increase miR-100-5p after PTEN knockout was not sufficient to change *mTOR* expression. More recently, miR-342-3p was identified as a significant immune-related miRNA, with elevated levels in RCC associated with poorer patient survival [69]. Here, miR-342-3p was not detected in in vitro samples but tended to be upregulated in pten/KO tumors as in kidney tumors. This may indicate the significance of miR-342-3p for immunological components of the tumor microenvironment and these aspects of cancer progression might be deregulated in PTEN mutated tumors.

Other miRNAs modulating PTEN expression in cancer have been identified. We proved that the upregulation in miR-221-3p expression may be involved in PTEN level modulation in low pO₂, as there was no increase in miR-221-3p in pten/KO hypoxic cells. Modulation of PTEN expression by miR-221 was also described in gastric carcinoma [70], however in the human RCC model Caki-1, no changes were observed in both PTEN level and miR-221-3p expression. This sheds light on the diversity of the miRNA pattern, even in the same tumor types, and points to the need to interpret miRNA expression in a personalized way [71]. Upregulation of miR-221-3p in a mouse kidney cancer model was not transferred through exosomes to cells of TME and we did not observe changes in PTEN expression in mature brain-derived endothelial cells, but in cervical cancer, cell-secreted exosomal miR-221 promoted angiogenesis through Thrombospondin-2 [72]. miR-21a, also targeting PTEN, is described as one of the most upregulated in RCC compared to healthy kidney, which was confirmed by our results performed on total RNA from RCC samples. Surprisingly, miR-21a-5p was downregulated in hypoxia in both PTEN variants in Renca cells, and does not seem to regulate the PTEN levels in a pten/WT model. However, others also showed miR-21a downregulation in response to hypoxia [73], therefore it seems that

the miR-21a response to low pO₂ depends on cancer type [74]. To establish what could be the role of miR-21a-5p inhibition, we looked for targets other than PTEN for this miRNA. Based on miRNet analysis, we demonstrated that *Tgfb3* may be a target for miR-21a-5p, as confirmed in a glioblastoma model [75]. In response to hypoxia and a simultaneous miR-21a-5p decrease, *Tgfb3* was upregulated in both PTEN models. The overexpression of *Tgfb3* in nasopharyngeal carcinoma cells has been demonstrated to increase apoptosis through the downregulation of Bcl2 [76]. This suggests that in some cancers the other effects of miR-21a-5p than its PTEN-regulatory role prevail in response to hypoxia.

5. Conclusions

We showed hypoxia-/PTEN-dependent miRNA patterns in RCC and their effects on target gene expression. We confirmed the upregulation of miR-210-3p and miR-221-3p but the downregulation of miR-21a-5p in response to low pO₂. Loss of PTEN caused limited miRNA expression modifications, mostly oncomiR-155 upregulation, miR-100-5p and miR-342-3p induction. However, PTEN mutation changed the response to hypoxia. The increase in miR-210-3p is weaker than in cells with functional PTEN; expression of miR-206-3p (suppressor) was upregulated with a simultaneous decrease in miR-10b-5p expression (oncogene), suggesting compensation to the lower aggressiveness of hypoxic pten/KO vs pten/WT cells. PTEN mutation annihilated miR-221-3p responsiveness to hypoxia by induced expression in PTEN-functional cells. Our study shows that miRNAs regulated by/responding to TME (hypoxia) and tumor mutation status (PTEN) might interact and mutually regulate cancer responses. Simultaneously, we demonstrated that low pO₂ can regulate PTEN levels and miRNA may be involved, showing the complexity of the relationship between the various features of TME. The identification of miRNAs that are modulated by distinct variables might allow for a better understanding of the mechanisms of the pathogenesis of kidney cancers and contribute to the development of effective therapies.

Supplementary Materials: The following supporting information can be downloaded at: <https://www.mdpi.com/article/10.3390/biom12050686/s1>, Figure S1: Results of sequencing—PTEN knockout clones; Figure S2: Size of nanoparticles isolated with the ExoQuick Buffer from Renca cells conditioned medium (A) normoxic (B) hypoxic, measured using Zeta Viewer Nanoparticle Analyzer (C) level of exosomal marker TSG101 in samples of isolated nanoparticles; Figure S3: Volcano plots of DE miRNA between Renca pten/WT and pten/KO cell in (A) normoxic (B) hypoxic conditions. Listed miRNAs significantly changed in pten/KO in vivo samples compared to pten/WT.

Author Contributions: Conceptualization, C.K.; Formal analysis, A.M., K.B. and A.K.; Funding acquisition, K.B. and C.K.; Investigation, A.M., K.B. and A.F.-D.; Methodology, A.M., K.B. and A.F.-D.; Supervision, C.K.; Writing—original draft, A.M., K.B. and C.K.; Writing—review & editing, C.K. All authors have read and agreed to the published version of the manuscript.

Funding: The research was funded by National Scientific Center grant no 2016/23/B/NZ1/03211. K.B. and A.M. were supported by Military Institute of Medicine intramural grant no 1/8974 (519); A.F.-D. was supported by European Social Fund: POWER “Next generation sequencing technologies in biomedicine and personalized medicine”.

Institutional Review Board Statement: The animal study protocol was approved by the Ethics Committee Second Warsaw Local Ethics Committee for Animal Experimentation (no. WAW2/76/2017 and date of approval 19 September 2017, valid until 30 May 2021).

Informed Consent Statement: Not applicable.

Data Availability Statement: All data generated or analyzed during this study are included either in this article or in the Supplementary Figures. The data that support the findings of this study are available from the corresponding author upon reasonable request.

Acknowledgments: The authors are especially indebted to Mirosław Szczepański from Department of Biochemistry, First Faculty of Medicine, Medical University of Warsaw for providing the Zeta Viewer Nanoparticle Analyzer. The authors are grateful to all of those with whom we have had the pleasure to work during this and other related projects.

Conflicts of Interest: The authors declare that they have no conflict of interest.

References

- O'Brien, J.; Hayder, H.; Zayed, Y.; Peng, C. Overview of MicroRNA Biogenesis, Mechanisms of Actions, and Circulation. *Front. Endocrinol.* **2018**, *9*, 402. [\[CrossRef\]](#) [\[PubMed\]](#)
- Garzon, R.; Fabbri, M.; Cimmino, A.; Calin, G.A.; Croce, C.M. MicroRNA expression and function in cancer. *Trends Mol. Med.* **2006**, *12*, 580–587. [\[CrossRef\]](#) [\[PubMed\]](#)
- Qu, H.; Zheng, L.; Pu, J.; Mei, H.; Xiang, X.; Zhao, X.; Li, D.; Li, S.; Mao, L.; Huang, K.; et al. miRNA-558 promotes tumorigenesis and aggressiveness of neuroblastoma cells through activating the transcription of heparanase. *Hum. Mol. Genet.* **2015**, *24*, 2539–2551. [\[CrossRef\]](#) [\[PubMed\]](#)
- Lou, W.; Liu, J.; Gao, Y.; Zhong, G.; Chen, D.; Shen, J.; Bao, C.; Xu, L.; Pan, J.; Cheng, J.; et al. MicroRNAs in cancer metastasis and angiogenesis. *Oncotarget* **2017**, *8*, 115787–115802. [\[CrossRef\]](#)
- Goradel, N.H.; Mohammadi, N.; Haghi-Aminjan, H.; Farhood, B.; Negahdari, B.; Sahebkar, A. Regulation of tumor angiogenesis by microRNAs: State of the art. *J. Cell. Physiol.* **2018**, *234*, 1099–1110. [\[CrossRef\]](#)
- Pratama, M.Y.; Pascut, D.; Massi, M.N.; Tiribelli, C. The role of microRNA in the resistance to treatment of hepatocellular carcinoma. *Ann. Transl. Med.* **2019**, *7*, 577. [\[CrossRef\]](#)
- Sohel, M.H. Circulating microRNAs as biomarkers in cancer diagnosis. *Life Sci.* **2020**, *248*, 117473. [\[CrossRef\]](#)
- Nejad, A.E.; Najafgholian, S.; Rostami, A.; Sistani, A.; Shojaeifar, S.; Esparvarinha, M.; Nedaeinia, R.; Javanmard, S.H.; Taherian, M.; Ahmadi, M.; et al. The role of hypoxia in the tumor microenvironment and development of cancer stem cell: A novel approach to developing treatment. *Cancer Cell Int.* **2021**, *21*, 1–26. [\[CrossRef\]](#)
- Majmundar, A.J.; Wong, W.J.; Simon, M.C. Hypoxia-Inducible Factors and the Response to Hypoxic Stress. *Mol. Cell* **2010**, *40*, 294–309. [\[CrossRef\]](#)
- Hayashi, Y.; Yokota, A.; Harada, H.; Huang, G. Hypoxia/pseudohypoxia-mediated activation of hypoxia-inducible factor-1 α in cancer. *Cancer Sci.* **2019**, *110*, 1510–1517. [\[CrossRef\]](#)
- Cowey, C.L.; Rathmell, W.K. VHL gene mutations in renal cell carcinoma: Role as a biomarker of disease outcome and drug efficacy. *Curr. Oncol. Rep.* **2009**, *11*, 94–101. [\[CrossRef\]](#) [\[PubMed\]](#)
- Escudier, B.; Worden, F.; Kudo, M. Sorafenib: Key lessons from over 10 years of experience. *Expert Rev. Anticancer Ther.* **2018**, *19*, 177–189. [\[CrossRef\]](#) [\[PubMed\]](#)
- Makhov, P.; Joshi, S.; Ghatalia, P.; Kutikov, A.; Uzzo, R.G.; Kolenko, V.M. Resistance to Systemic Therapies in Clear Cell Renal Cell Carcinoma: Mechanisms and Management Strategies. *Mol. Cancer Ther.* **2018**, *17*, 1355–1364. [\[CrossRef\]](#) [\[PubMed\]](#)
- Shen, G.; Li, X.; Jia, Y.-F.; Piazza, G.; Xi, Y. Hypoxia-regulated microRNAs in human cancer. *Acta Pharmacol. Sin.* **2013**, *34*, 336–341. [\[CrossRef\]](#) [\[PubMed\]](#)
- Nallamshetty, S.; Chan, S.Y.; Loscalzo, J. Hypoxia: A master regulator of microRNA biogenesis and activity. *Free Radic. Biol. Med.* **2013**, *64*, 20–30. [\[CrossRef\]](#)
- Rupaimoole, R.; Wu, S.Y.; Pradeep, S.; Ivan, C.; Pecot, C.V.; Gharipure, K.M.; Nagaraja, A.S.; Armaiz-Pena, G.N.; McGuire, M.; Zand, B.; et al. Hypoxia-mediated downregulation of miRNA biogenesis promotes tumour progression. *Nat. Commun.* **2014**, *5*, 5202. [\[CrossRef\]](#)
- Peng, X.; Gao, H.; Xu, R.; Wang, H.; Mei, J.; Liu, C. The interplay between HIF-1 α and noncoding RNAs in cancer. *J. Exp. Clin. Cancer Res.* **2020**, *39*, 27. [\[CrossRef\]](#)
- Tang, K.; Xu, H. Prognostic value of meta-signature miRNAs in renal cell carcinoma: An integrated miRNA expression profiling analysis. *Sci. Rep.* **2015**, *5*, 10272. [\[CrossRef\]](#)
- McCormick, R.; Blick, C.; Ragoussis, J.; Schoedel, J.; Mole, D.R.; Young, A.C.; Selby, P.J.; Banks, R.; Harris, A.L. miR-210 is a target of hypoxia-inducible factors 1 and 2 in renal cancer, regulates ISCU and correlates with good prognosis. *Br. J. Cancer* **2013**, *108*, 1133–1142. [\[CrossRef\]](#)
- Neal, C.S.; Michael, M.Z.; Rawlings, L.H.; Van Der Hoek, M.B.; Gleade, J.M. The VHL-dependent regulation of microRNAs in renal cancer. *BMC Med.* **2010**, *8*, 64. [\[CrossRef\]](#)
- Milella, M.; Falcone, I.; Conciatori, F.; Cesta Incari, U.; Del Curatolo, A.; Inzerilli, N.; Nuzzo, C.M.; Vaccaro, V.; Vari, S.; Cognetti, F.; et al. PTEN: Multiple Functions in Human Malignant Tumors. *Front. Oncol.* **2015**, *5*, 24. [\[CrossRef\]](#) [\[PubMed\]](#)
- Brenner, W.; Färber, G.; Herget, T.; Lehr, H.-A.; Hengstler, J.G.; Thüroff, J.W. Loss of tumor suppressor protein PTEN during renal carcinogenesis. *Int. J. Cancer* **2002**, *99*, 53–57. [\[CrossRef\]](#) [\[PubMed\]](#)
- Tang, L.; Li, X.; Gao, Y.; Chen, L.; Gu, L.; Chen, J.; Lyu, X.; Zhang, Y.; Zhang, X. Phosphatase and tensin homolog (PTEN) expression on oncologic outcome in renal cell carcinoma: A systematic review and meta-analysis. *PLoS ONE* **2017**, *12*, e0179437. [\[CrossRef\]](#) [\[PubMed\]](#)
- Simpson, L.; Parsons, R. PTEN: Life as a Tumor Suppressor. *Exp. Cell Res.* **2001**, *264*, 29–41. [\[CrossRef\]](#) [\[PubMed\]](#)

25. Emerling, B.M.; Weinberg, F.; Liu, J.-L.; Mak, T.W.; Chandel, N.S. PTEN regulates p300-dependent hypoxia-inducible factor 1 transcriptional activity through Forkhead transcription factor 3a (FOXO3a). *Proc. Natl. Acad. Sci. USA* **2008**, *105*, 2622–2627. [[CrossRef](#)] [[PubMed](#)]
26. Li, W.; Zhang, T.; Guo, L.; Huang, L. Regulation of PTEN expression by noncoding RNAs. *J. Exp. Clin. Cancer Res.* **2018**, *37*, 223. [[CrossRef](#)] [[PubMed](#)]
27. Dillon, L.M.; Miller, T.W. Therapeutic targeting of cancers with loss of PTEN function. *Curr. Drug Targets* **2014**, *15*, 65–79. [[CrossRef](#)]
28. Dart, D.A.; Uysal-Onganer, P.; Jiang, W.G. Prostate-specific PTEN deletion in mice activates inflammatory microRNA expression pathways in the epithelium early in hyperplasia development. *Oncogenesis* **2017**, *6*, 400. [[CrossRef](#)]
29. Yuan, T.; Yang, Y.; Chen, J.; Li, W.; Zhang, Q.; Mi, Y.; Goswami, R.; You, J.Q.; Lin, D.; Qian, M.D.; et al. Regulation of PI3K signaling in T-cell acute lymphoblastic leukemia: A novel PTEN/Ikaros/miR-26b mechanism reveals a critical targetable role for PIK3CD. *Leukemia* **2017**, *31*, 2355–2364. [[CrossRef](#)]
30. Freeman, D.J.; Li, A.G.; Wei, G.; Li, H.-H.; Kertesz, N.; Lesche, R.; Whale, A.D.; Martínez-Díaz, H.; Rozenfurt, N.; Cardiff, R.D.; et al. PTEN tumor suppressor regulates p53 protein levels and activity through phosphatase-dependent and -independent mechanisms. *Cancer Cell* **2003**, *3*, 117–130. [[CrossRef](#)]
31. Tang, Y.; Weng, X.; Liu, C.; Li, X.; Chen, C. Hypoxia Enhances Activity and Malignant Behaviors of Colorectal Cancer Cells through the STAT3/MicroRNA-19a/PTEN/PI3K/AKT Axis. *Anal. Cell. Pathol.* **2021**, *2021*, 4132488. [[CrossRef](#)] [[PubMed](#)]
32. Liang, T.; Gao, E.; Chen, J. Role of PTEN-less in cardiac injury, hypertrophy and regeneration. *Cell Regen.* **2021**, *10*, 25. [[CrossRef](#)] [[PubMed](#)]
33. Zhang, Z.; Yao, L.; Yang, J.; Wang, Z.; Du, G. PI3K/Akt and HIF-1 signaling pathway in hypoxia-ischemia (Review). *Mol. Med. Rep.* **2018**, *18*, 3547–3554. [[CrossRef](#)] [[PubMed](#)]
34. Bizouarne, N.; Denis, V.; Legrand, A.; Monsigny, M.; Kieda, C.; Bizourne, N. A SV-40 immortalized murine endothelial cell line from peripheral lymph node high endothelium expresses a new α -L-fucose binding protein. *Biol. Cell* **1993**, *79*, 209–218. [[CrossRef](#)]
35. Ran, F.A.; Hsu, P.D.; Wright, J.; Agarwala, V.; Scott, D.A.; Zhang, F. Genome engineering using the CRISPR-Cas9 system. *Nat. Protoc.* **2013**, *8*, 2281–2308. [[CrossRef](#)]
36. Fusco, N.; Sajjadi, E.; Venetis, K.; Gaudioso, G.; Lopez, G.; Corti, C.; Rocco, E.G.; Criscitello, C.; Malapelle, U.; Invernizzi, M. PTEN Alterations and Their Role in Cancer Management: Are We Making Headway on Precision Medicine? *Genes* **2020**, *11*, 719. [[CrossRef](#)]
37. The AACR Project GENIE Consortium AACR Project GENIE: Powering Precision Medicine through an International Consortium. *Cancer Discov.* **2017**, *7*, 818–831. [[CrossRef](#)]
38. Khouzam, R.A.; Rao, S.P.; Venkatesh, G.H.; Zeinelabdin, N.A.; Buart, S.; Meylan, M.; Nimmakayalu, M.; Terry, S.; Chouaib, S. An Eight-Gene Hypoxia Signature Predicts Survival in Pancreatic Cancer and Is Associated with an Immunosuppressed Tumor Microenvironment. *Front. Immunol.* **2021**, *12*, 435. [[CrossRef](#)]
39. Sørensen, B.S.; Knudsen, A.; Witttrup, C.F.; Nielsen, S.; Aggerholm-Pedersen, N.; Busk, M.; Horsman, M.; Høyer, M.; Bouchelouche, P.N.; Overgaard, J.; et al. The usability of a 15-gene hypoxia classifier as a universal hypoxia profile in various cancer cell types. *Radiother. Oncol.* **2015**, *116*, 346–351. [[CrossRef](#)]
40. Kong, F.; Ran, W.; Jiang, N.; Li, S.; Zhang, D.; Sun, D. Identification and characterization of differentially expressed miRNAs in HepG2 cells under normoxic and hypoxic conditions. *RSC Adv.* **2019**, *9*, 16884–16891. [[CrossRef](#)]
41. Bertero, T.; Rezzonico, R.; Pottier, N.; Mari, B. Impact of MicroRNAs in the Cellular Response to Hypoxia. *Int. Rev. Cell Mol. Biol.* **2017**, *333*, 91–158. [[CrossRef](#)] [[PubMed](#)]
42. Yoshino, H.; Yonemori, M.; Miyamoto, K.; Tatarano, S.; Kofuji, S.; Nohata, N.; Nakagawa, M.; Enokida, H. microRNA-210-3p depletion by CRISPR/Cas9 promoted tumorigenesis through revival of TWIST1 in renal cell carcinoma. *Oncotarget* **2017**, *8*, 20881–20894. [[CrossRef](#)] [[PubMed](#)]
43. Song, B.-W.; Lee, C.Y.; Kim, R.; Kim, W.J.; Lee, H.W.; Lee, M.Y.; Kim, J.; Jeong, J.-Y.; Chang, W. Multiplexed targeting of miRNA-210 in stem cell-derived extracellular vesicles promotes selective regeneration in ischemic hearts. *Exp. Mol. Med.* **2021**, *53*, 695–708. [[CrossRef](#)] [[PubMed](#)]
44. Liu, X.-D.; Cai, F.; Liu, L.; Zhang, Y.; Yang, A.-L. microRNA-210 is involved in the regulation of postmenopausal osteoporosis through promotion of VEGF expression and osteoblast differentiation. *Biol. Chem.* **2015**, *396*, 339–347. [[CrossRef](#)] [[PubMed](#)]
45. Chio, C.-C.; Lin, J.-W.; Cheng, H.-A.; Chiu, W.-T.; Wang, Y.-H.; Wang, J.-J.; Hsing, C.-H.; Chen, R.-M. MicroRNA-210 targets antiapoptotic Bcl-2 expression and mediates hypoxia-induced apoptosis of neuroblastoma cells. *Arch. Toxicol.* **2012**, *87*, 459–468. [[CrossRef](#)] [[PubMed](#)]
46. Lv, J.; Zhou, J.; Tong, R.; Wang, B.; Chen, X.; Zhuang, Y.; Xia, F.; Wei, X. Hypoxia-induced miR-210 contributes to apoptosis of mouse spermatocyte GC-2 cells by targeting Kruppel-like factor 7. *Mol. Med. Rep.* **2018**, *19*, 271–279. [[CrossRef](#)]
47. Kohnoh, T.; Hashimoto, N.; Ando, A.; Sakamoto, K.; Miyazaki, S.; Aoyama, D.; Kusunose, M.; Kimura, M.; Omote, N.; Imaizumi, K.; et al. Hypoxia-induced modulation of PTEN activity and EMT phenotypes in lung cancers. *Cancer Cell Int.* **2016**, *16*, 33. [[CrossRef](#)]
48. Shi, J.; Zhang, D.; Zhong, Z.; Zhang, W. lncRNA ROR promotes the progression of renal cell carcinoma through the miR-206/VEGF axis. *Mol. Med. Rep.* **2019**, *20*, 3782–3792. [[CrossRef](#)]

49. Singh, A.; Pruett, N.; Pahwa, R.; Mahajan, A.P.; Schrupp, D.S.; Hoang, C.D. MicroRNA-206 suppresses mesothelioma progression via the Ras signaling axis. *Mol. Ther. Nucleic Acids* **2021**, *24*, 669–681. [[CrossRef](#)]
50. Liao, M.; Peng, L. MiR-206 may suppress non-small lung cancer metastasis by targeting CORO1C. *Cell. Mol. Biol. Lett.* **2020**, *25*, 22. [[CrossRef](#)]
51. Huang, J.; Sun, C.; Wang, S.; He, Q.; Li, D. microRNA miR-10b inhibition reduces cell proliferation and promotes apoptosis in non-small cell lung cancer (NSCLC) cells. *Mod. Biosyst.* **2015**, *11*, 2051–2059. [[CrossRef](#)] [[PubMed](#)]
52. Sheedy, P.; Medarova, Z. The fundamental role of miR-10b in metastatic cancer. *Am. J. Cancer Res.* **2018**, *8*, 1674–1688. [[PubMed](#)]
53. Kim, J.; Siverly, A.N.; Chen, D.; Wang, M.; Yuan, Y.; Wang, Y.; Lee, H.; Zhang, J.; Muller, W.J.; Liang, H.; et al. Ablation of miR-10b Suppresses Oncogene-Induced Mammary Tumorigenesis and Metastasis and Reactivates Tumor-Suppressive Pathways. *Cancer Res.* **2016**, *76*, 6424–6435. [[CrossRef](#)] [[PubMed](#)]
54. Lin, C.-C.; Liao, W.-T.; Yang, T.-Y.; Lu, H.-J.; Hsu, S.-L.; Wu, C.-C. MicroRNA-10b modulates cisplatin tolerance by targeting p53 directly in lung cancer cells. *Oncol. Rep.* **2021**, *46*, 1–13. [[CrossRef](#)] [[PubMed](#)]
55. Bhandari, V.; PCAWG Consortium; Li, C.H.; Bristow, R.G.; Boutros, P.C. Divergent mutational processes distinguish hypoxic and normoxic tumours. *Nat. Commun.* **2020**, *11*, 737. [[CrossRef](#)] [[PubMed](#)]
56. Wu, K.; Li, J.; Qi, Y.; Zhang, C.; Zhu, D.; Liu, D.; Zhao, S. SNHG14 confers gefitinib resistance in non-small cell lung cancer by up-regulating ABCB1 via sponging miR-206-3p. *Biomed. Pharmacother.* **2019**, *116*, 108995. [[CrossRef](#)]
57. Chen, Z.; Gao, Y.-J.; Hou, R.-Z.; Ding, D.-Y.; Song, D.-F.; Wang, D.-Y.; Feng, Y. MicroRNA-206 facilitates gastric cancer cell apoptosis and suppresses cisplatin resistance by targeting MAPK2 signaling pathway. *Eur. Rev. Med. Pharmacol. Sci.* **2019**, *23*, 171–180.
58. Wang, T.; Dong, X.-M.; Zhang, F.-L.; Zhang, J.-R. miR-206 enhances nasopharyngeal carcinoma radiosensitivity by targeting IGF1. *Kaohsiung J. Med. Sci.* **2017**, *33*, 427–432. [[CrossRef](#)]
59. Nishida, N.; Yamashita, S.; Mimori, K.; Sudo, T.; Tanaka, E.; Shibata, K.; Yamamoto, H.; Ishii, H.; Doki, Y.; Mori, M. MicroRNA-10b is a Prognostic Indicator in Colorectal Cancer and Confers Resistance to the Chemotherapeutic Agent 5-Fluorouracil in Colorectal Cancer Cells. *Ann. Surg. Oncol.* **2012**, *19*, 3065–3071. [[CrossRef](#)]
60. Zhen, L.; Li, J.; Zhang, M.; Yang, K. MiR-10b decreases sensitivity of glioblastoma cells to radiation by targeting AKT. *J. Biol. Res.* **2016**, *23*, 14. [[CrossRef](#)]
61. Pranzirini, E.; Leo, A.; Rappizzi, E.; Ramazzotti, M.; Magherini, F.; Giovannelli, L.; Caselli, A.; Cirri, P.; Taddei, M.L.; Paoli, P. miR-210-3p mediates metabolic adaptation and sustains DNA damage repair of resistant colon cancer cells to treatment with 5-fluorouracil. *Mod. Carcinog.* **2019**, *58*, 2181–2192. [[CrossRef](#)] [[PubMed](#)]
62. Zhuang, H.-Q.; Wang, J.; Yuan, Z.-Y.; Zhao, L.-J.; Wang, P.; Wang, C.-L. The drug-resistance to gefitinib in PTEN low expression cancer cells is reversed by irradiation in vitro. *J. Exp. Clin. Cancer Res.* **2009**, *28*, 123–129. [[CrossRef](#)] [[PubMed](#)]
63. Steelman, L.S.; Navolanic, P.M.; Sokolosky, M.L.; Taylor, J.R.; Lehmann, B.D.; Chappell, W.H.; Abrams, S.L.; Wong, E.W.T.; Stadelman, K.M.; Terrian, D.M.; et al. Suppression of PTEN function increases breast cancer chemotherapeutic drug resistance while conferring sensitivity to mTOR inhibitors. *Oncogene* **2008**, *27*, 4086–4095. [[CrossRef](#)] [[PubMed](#)]
64. Zhang, G.; Wang, W.; Yao, C.; Zhang, S.; Liang, L.; Han, M.; Ren, J.; Qi, X.; Zhang, X.; Wang, S.; et al. Radiation-resistant cancer stem-like cell properties are regulated by PTEN through the activity of nuclear β -catenin in nasopharyngeal carcinoma. *Oncotarget* **2017**, *8*, 74661–74672. [[CrossRef](#)]
65. Fu, X.; Wen, H.; Jing, L.; Yang, Y.; Wang, W.; Liang, X.; Nan, K.; Yao, Y.; Tian, T. MicroRNA-155-5p promotes hepatocellular carcinoma progression by suppressing PTEN through the PI3K/Akt pathway. *Cancer Sci.* **2017**, *108*, 620–631. [[CrossRef](#)]
66. Wang, G.; Chen, L.; Meng, J.; Chen, M.; Zhuang, L.; Zhang, L. Overexpression of microRNA-100 predicts an unfavorable prognosis in renal cell carcinoma. *Int. Urol. Nephrol.* **2013**, *45*, 373–379. [[CrossRef](#)]
67. Nagaraja, A.K.; Creighton, C.J.; Yu, Z.; Zhu, H.; Gunaratne, P.H.; Reid, J.G.; Olokpa, E.; Itamochi, H.; Ueno, N.T.; Hawkins, S.; et al. A Link between miR-100 and FRAP1/mTOR in Clear Cell Ovarian Cancer. *Mol. Endocrinol.* **2010**, *24*, 447–463. [[CrossRef](#)]
68. Guo, Y.; Li, X.; Zheng, J.; Fang, J.; Pan, G.; Chen, Z. Identification of a novel immune-related microRNA prognostic model in clear cell renal cell carcinoma. *Transl. Androl. Urol.* **2021**, *10*, 888–899. [[CrossRef](#)]
69. Shi, J.; Zhang, Y.; Jin, N.; Li, Y.; Wu, S.; Xu, L. MicroRNA-221-3p Plays an Oncogenic Role in Gastric Carcinoma by Inhibiting PTEN Expression. *Oncol. Res. Featur. Preclin. Clin. Cancer Ther.* **2017**, *25*, 523–536. [[CrossRef](#)]
70. Detassis, S.; Grasso, M.; Del Vecovo, V.; Denti, M.A. microRNAs Make the Call in Cancer Personalized Medicine. *Front. Cell Dev. Biol.* **2017**, *5*, 86. [[CrossRef](#)]
71. Wu, X.-G.; Zhou, C.-F.; Zhang, Y.-M.; Yan, R.-M.; Wei, W.-F.; Chen, X.-J.; Yi, H.-Y.; Liang, L.-J.; Fan, L.-S.; Liang, L.; et al. Cancer-derived exosomal miR-221-3p promotes angiogenesis by targeting THBS2 in cervical squamous cell carcinoma. *Angiogenesis* **2019**, *22*, 397–410. [[CrossRef](#)] [[PubMed](#)]
72. Deng, D.; Liang, H. Silencing MEG3 protects PC12 cells from hypoxic injury by targeting miR-21. *Artif. Cells Nanomed. Biotechnol.* **2020**, *48*, 610–619. [[CrossRef](#)] [[PubMed](#)]
73. Kulshreshtha, R.; Ferracin, M.; Wojcik, S.E.; Garzon, R.; Alder, H.; Agosto-Perez, F.J.; Davuluri, R.; Liu, C.-G.; Croce, C.M.; Negrini, M.; et al. A MicroRNA Signature of Hypoxia. *Mol. Cell. Biol.* **2007**, *27*, 1859–1867. [[CrossRef](#)] [[PubMed](#)]
74. Papagiannakopoulos, T.; Shapiro, A.; Kosik, K.S. MicroRNA-21 Targets a Network of Key Tumor-Suppressive Pathways in Glioblastoma Cells. *Cancer Res.* **2008**, *68*, 8164–8172. [[CrossRef](#)] [[PubMed](#)]

75. Zheng, F.; He, K.; Li, X.; Zhao, D.; Sun, F.; Zhang, Y.; Nie, D.; Li, X.; Chu, W.; Sun, Y.; et al. Transient overexpression of TGFBR3 induces apoptosis in human nasopharyngeal carcinoma CNE-2Z cells. *Biosci. Rep.* **2013**, *33*, e00029. [[CrossRef](#)] [[PubMed](#)]
76. Edgar, R.; Domrachev, M.; Lash, A.E. Gene Expression Omnibus: NCBI gene expression and hybridization array data repository. *Nucleic Acids Res.* **2002**, *30*, 207–210. [[CrossRef](#)] [[PubMed](#)]

Supplementary Materials

Commercially available RNA isolates were purchased from TaKaRa, San Jose, CA, USA.

2 independent vials of RNA isolates were used in each experiment.

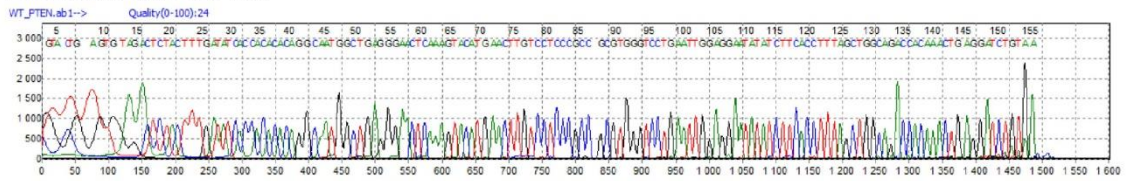
Healthy (#cat 636529 #LOT 1405150A) – normal human kidney pooled from a 40-year-old Caucasian female, cause of death: sudden death

Tumor (cat 636632 #LOT 1102289A) – kidney renal cell carcinoma isolated from a 48-year-old male Caucasian.

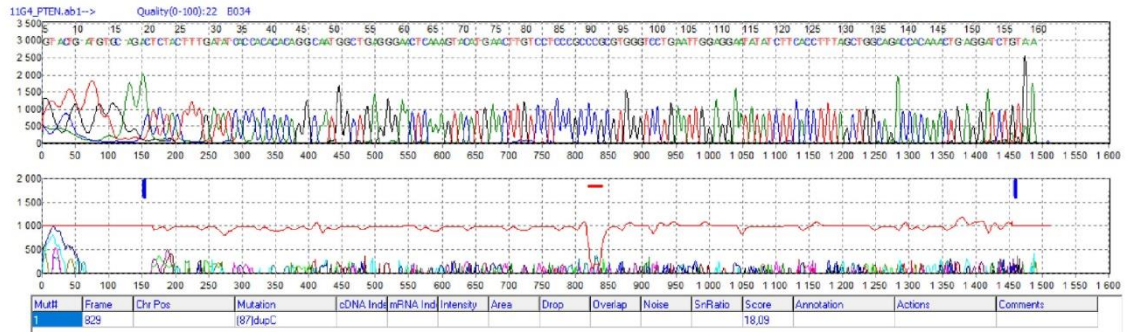
Supplementary Figure S1

Results of sequencing - PTEN knockout clones

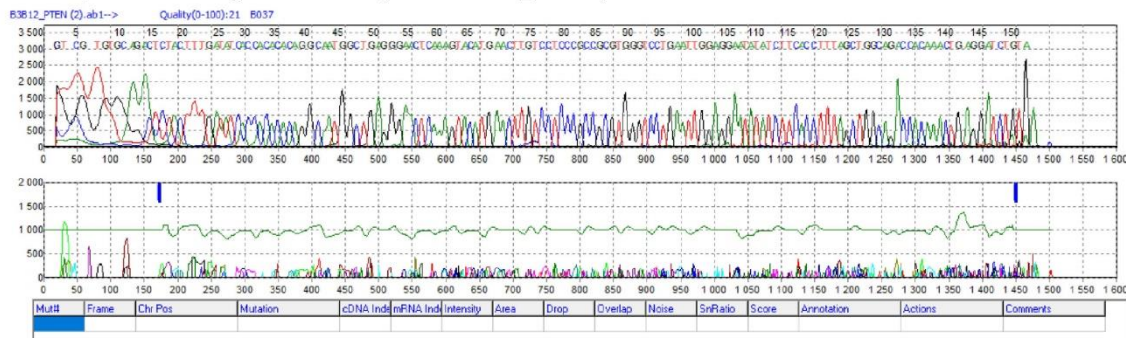
Renca wild-type cell line:



Renca pten/KO (clone 11G4_PTEN):



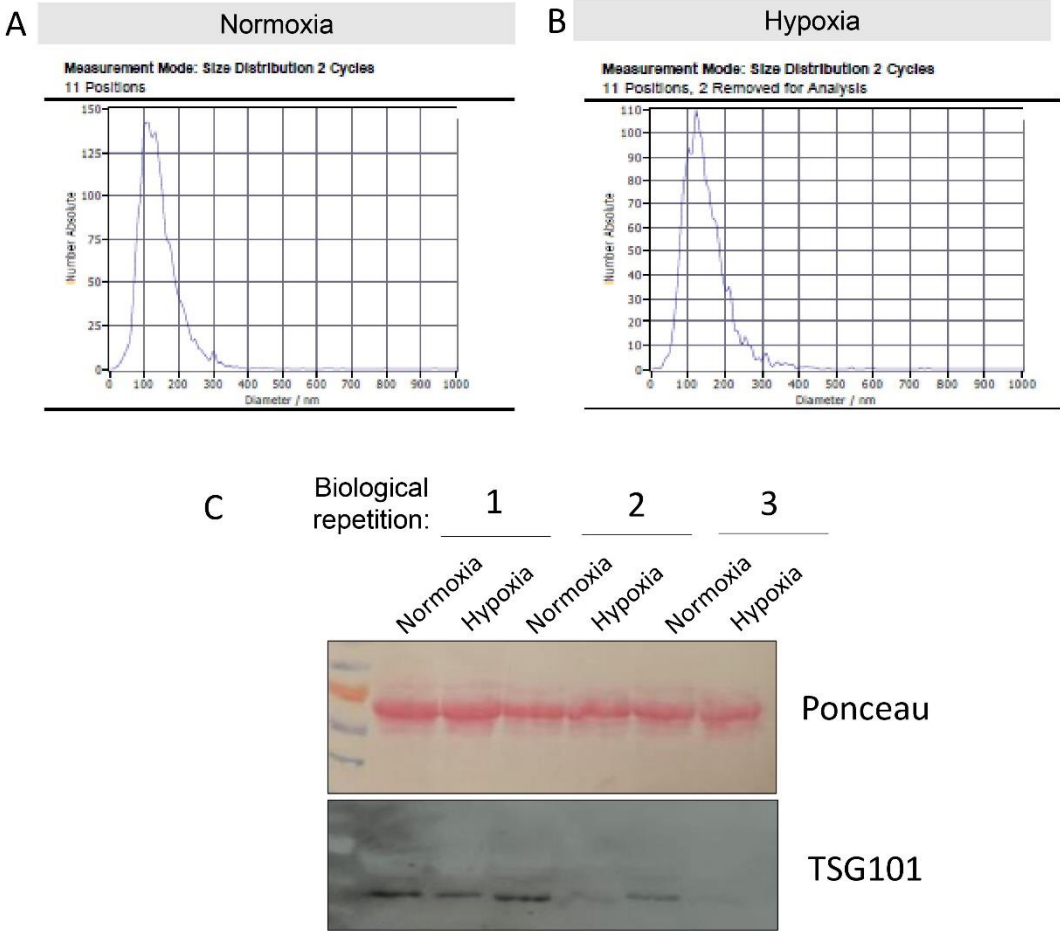
Renca pten/WT – negative control (clone B3B12_PTEN):



No.	Sample File	Reference File	Dir	Gene	Exon	RF	Start	End	Size	Quali	Mut#	Mutation1	Mutation2
2	11G4_PTEN.ab1	WT_PTEN.ab1	1-R	Pten	7	2	57840	57974	135	22	1		57905dupG\$18
3	B3B12_PTEN (2).ab	WT_PTEN.ab1	1-R	Pten	7	2	57841	57973	133	21	0		
4	sequenc_R11_Synth	WT_PTEN.ab1	1-R	Pten	7	2	57840	57974	135	82	0		
4									466	36	0.50	33.3%	33.3%

Supplementary Figure S2

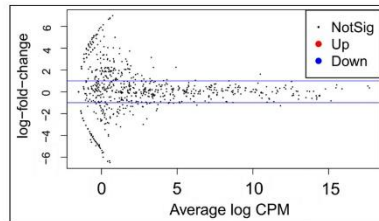
Size of nanoparticles isolated with the ExoQuick Buffer from Renca cells conditioned medium
 A) normoxic B) hypoxic, measured using Zeta Viewer Nanoparticle Analyzer C) level of
 exosomal marker TSG101 in samples of isolated nanoparticles



Supplementary Figure S3

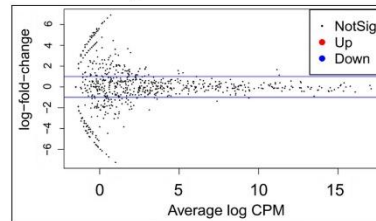
Volcano plots of DE miRNA between Renca pten/WT and pten/KO cell in A) normoxic B) hypoxic conditions. Listed miRNAs significantly changed in pten/KO in vivo samples compared to pten/WT

A Renca pten/WT vs pten/KO normoxic condition



miRNA	logFC	PValue	FDR
mmu-miR-342-3p	4.05	0.06	1,0000
mmu-miR-7115-5p	2.97	0.34	1,0000
mmu-miR-155-5p	2.25	0.00	0,4742
mmu-miR-100-5p	1.62	0.00	0,1777
mmu-miR-3102-3p	1.00	0.06	1,0000
mmu-miR-3068-5p	0.51	0.58	1,0000
mmu-miR-5126	0.00	1.00	1,0000

B Renca pten/WT vs pten/KO hypoxic condition



miRNA	logFC	PValue	FDR
mmu-miR-342-3p	6.91	0.01	1
mmu-miR-100-5p	1.66	0	0.1836
mmu-miR-155-5p	1.58	0.01	1
mmu-miR-3068-5p	0.68	0.51	1
mmu-miR-5126	0.04	0.96	1
mmu-miR-7115-5p	-0.67	0.8	1
mmu-miR-3102-3p	-0.77	0.09	1

4 PODSUMOWANIA I WNIOSKI

Wyniki uzyskane w niniejszej pracy potwierdzają kontrowersje i rozbieżności dotyczące roli PTEN w różnych typach nowotworów. To zróżnicowanie może mieć kluczowe znaczenie w odpowiedzi na stosowane terapie przeciwnowotworowe.

Normalizacja naczyń za pośrednictwem ITPP wydaje się obiecującym podejściem terapeutycznym w modelu czerniaka (B16 F10) [65], jednak w modelu raka nerki (Renca) stosowanie ITPP nie przyniosło oczekiwanych korzyści (Publikacja 1). Pomimo podobnej odpowiedzi na niedotlenienie, związanej ze spadkiem poziomu PTEN i dominacją formy pPTEN w obu testowanych modelach, wykazano różnice aktywności szlaków sygnałowych regulowanych przez PTEN. Tylko w raku nerki obserwowano zmiany aktywności ścieżki p53/MDM2 przy braku akumulacji pAKT, natomiast w czerniaku spadek poziomu PTEN w hipoksji skutkował klasyczną aktywacją PI3K/AKT. Co więcej, komórki Renca wykazywały silny potencjał proangiogeny, szczególnie w niedotlenieniu, który istotnie wpływał na funkcje zarówno dojrzałych komórek śródbłonna, jak i progenitorów (Publikacja 1). Różnice w indukowanych niedotlenieniem zmianach aktywności PTEN i właściwościach proangiogeny obu testowanych modeli mogą przyczyniać się do odmiennej odpowiedzi na leczenie ITPP.

Z wykorzystaniem edycji genomu metodą CRISPR/Cas9 w obu modelach uzyskano linie komórkowe z nokautem *Pten*, co pozwoliło określić jego rolę, z pominięciem innych indukowanych niedotlenieniem zmian. Zarówno w komórkach B16 F10, jak i Renca obserwowano akumulację pAKT, jednak nie odnotowano istotnych zmian w proliferacji komórek *in vitro* i wzroście guzów *in vivo*, co może wskazywać na aktywację mechanizmów kompensujących niedobór PTEN. Wzrost poziomu pAKT w komórkach Renca z nokautem *Pten* jest szczególnie istotny z uwagi na brak takiej odpowiedzi w niedotlenieniu; zatem destabilizacja PTEN w niskim pO_2 jest niewystarczająca do aktywacji ścieżki PI3K/AKT. Na odmienną rolę PTEN w obu typach nowotworów wskazały różnice w oporności na cisplatinę. W komórkach Renca nokaut PTEN indukował oporność na cisplatinę, a w B16 F10 powodował większą wrażliwość. Odmienne regulacje wydzielania inhibitora aktywatora plazminogenu (PAI-1, *ang. plasminogen activator inhibitor*), po nokaucie PTEN w obu badanych modelach, a także różny wpływ na poziom supresora guza p53, mogą być zaangażowane w obserwowane

różnice w zmianie wrażliwości na leczenie. W raku nerki PTEN jest zaangażowany w zmiany fenotypu komórek indukując EMT (Publikacja 2).

W modelu nowotworu nerki zarówno utrata PTEN, jak i niedotlenienie wywołały zmiany ekspresji miRNA. Wśród najbardziej zmienionych miRNA w odpowiedzi na mutacje PTEN odnotowano wzrost ekspresji onkomiru miR-155. Najważniejsze miRNA indukowane niedotlenieniem to miR-210 i miR-221, które jednocześnie mogą być zaangażowane w zależny od hipoksji spadek poziomu PTEN (Publikacja 3).

Wyniki niniejszej pracy dostarczają nowych dowodów dotyczących roli i aktywności PTEN w mikrośrodkowisku mysich modeli raka nerki i czerniaka. Przedstawione różnice, zarówno w aktywności PTEN, jak i odpowiedzi na niedotlenienie, mogą odgrywać kluczową rolę w skuteczności terapii przeciwnowotworowych. Rozważania na temat odmiennej roli PTEN w różnych typach nowotworów skłaniają do promowania terapii personalizowanej, jednak wciąż brakuje wystarczająco szybkich i kompleksowych testów określających rolę PTEN w konkretnych nowotworach.

5 OPINIA KOMISJI ETYCZNEJ

UCHWAŁA NR WAW2/76/2017

z dnia 19 września 2017 r.

II Lokalnej Komisji Etycznej do spraw doświadczeń na zwierzętach w Warszawie

§ 1

Na podstawie art. 48 pkt. 1 ustawy z dnia 15 stycznia 2015 r. o ochronie zwierząt wykorzystywanych do celów naukowych lub edukacyjnych (Dz. U. poz. 266) po rozpatrzeniu wniosku pt.: „Przywracanie fizjoksji w celu naprawy niedotlenionych tkanek - regulacja mikroRNA dla celowanej normalizacji naczyń w nowotworach” z dnia 12 września 2017 r., złożonego przez: Wojskowy Instytut Higieny i Epidemiologii, adres: 01-163 Warszawa, ul. Kozielska 4,¹ zaplanowanego przez Klaudię Brodaczewską², lokalna komisja etyczna:

WYRAŻA ZGODĘ

Na przeprowadzenie doświadczeń na zwierzętach w zakresie wniosku.

§ 2

W wyniku rozpatrzenia wniosku o którym mowa w 1 §, Lokalna Komisja Etyczna ustaliła, że:

1. Wniosek należy przypisać do kategorii: badania podstawowe, onkologia.
2. Najwyższy stopień dotkliwości proponowanych procedur to: umiarkowana.
3. Doświadczenia będą przeprowadzane na gatunkach lub grupach gatunków³:

Gatunek	Wiek/stadium rozwoju	Liczba
Mysz BALB/c	6-8 tygodni	900
Mysz C57Bl/6	6-8 tygodni	486

4. Doświadczenia będą przeprowadzane przez: Klaudia Brodaczewska, Sławomir Lewicki, Katarzyna Krawczak.
5. Doświadczenie będzie przeprowadzane w terminie⁴ od 01.12.2017 do 01.12.2020r.
6. Doświadczenie będzie przeprowadzone w ośrodku⁵: WIHiE, ul. Szaserów 128, 04-141 Warszawa.
7. Doświadczenie będzie przeprowadzone poza ośrodkiem w: nie dotyczy.
8. Użyte do procedur zwierzęta dzikie zostaną odłowione przez: nie dotyczy.
9. Doświadczenie ~~zostanie~~/nie zostanie poddane ocenie retrospektywnej.

¹imię i nazwisko oraz adres i miejsce zamieszkania albo nazwę oraz adres i siedzibę użytkownika, który przeprowadzi to doświadczenie, z tym że w przypadku gdy użytkownikiem jest osoba fizyczna wykonująca działalność gospodarczą, zamiast adresu i miejsca zamieszkania tej osoby – adres i miejsce wykonywania działalności, jeżeli są inne niż adres i miejsce zamieszkania tej osoby;

²imię i nazwisko osoby, która zaplanowała i jest odpowiedzialna za przeprowadzenie doświadczenia

³ Podać liczbę, szczerp/stado, wiek/stadium rozwoju

⁴ Nie dłużej niż 5 lat

⁵ Podać jeśli jest to inny ośrodek niż użytkownik

§ 3

Uzasadnienie:

Komisja oceniła wniosek zgodnie z kryteriami zawartymi w art. 47.1 . ustawy z dnia 15 stycznia 2015 r. o ochronie zwierząt wykorzystywanych do celów naukowych lub edukacyjnych (Dz. U. poz. 266). Po ocenie wniosku komisja stwierdza, że przedstawiony projekt spełnia warunki dopuszczenia doświadczenia na zwierzętach.

Na podstawie art. 107 § 4 ustawy z dnia 14 czerwca 1960 r. – Kodeks postępowania administracyjnego z późniejszymi zmianami (Dz. U. z 2016 poz. 23) odstąpiono od sporządzania uzasadnienia decyzji, gdyż uwzględnia ona w całości żądanie strony.

§ 4

Integralną część niniejszej uchwały stanowi kopia wniosku, o którym mowa w § 1

Szkola Główna Gospodarstwa Wiejskiego
w Warszawie
II Lokalna Komisja Etyczna
ds. Doświadczeń na Zwierzętach
02-786 Warszawa, ul. Ciszewskiego 8
tel. 22 69-35622
(Pieczęć lokalnej komisji etycznej)

PRZEWODNICZĄCA
ds. Doświadczeń na Zwierzętach
Podpis przewodniczącego komisji
Prof. dr hab. Joanna Gromadzka-Ostrowska

Otrzymuje Użytkownik

Pouczenie:

Od niniejszej decyzji komisji można wnieść odwołanie do Krajowej Komisji Etycznej w terminie 14 od dnia otrzymania uchwały.

Użytkownik kopie przekazuje:

- Osoba planująca doświadczenie
- Zespół ds. dobrostanu

6 OŚWIADCZENIA WSPÓLAUTORÓW

WARSZAWA 15.09.2023
(miejsowość, data)

CLAUDINE KIEDA
(imię i nazwisko)

OŚWIADCZENIE

Jako współautor pracy pt. *Comparative analysis of the effect of hypoxia in two different tumor cell models shows the differential involvement of PTEN control of proangiogenic pathways* oświadczam, iż mój własny wkład merytoryczny w przygotowanie, przeprowadzenie i opracowanie badań oraz przedstawienie pracy w formie publikacji stanowi: opracowanie założeń pracy i metodyki, pomoc i nadzorowanie przeprowadzonych eksperymentów, analiza i interpretacja danych, opracowanie manuskryptu.

Mój udział procentowy w przygotowaniu publikacji określam jako **20 %**.

Wkład **Aleksandry Majewskiej** w powstawanie publikacji określam jako **51 %**,

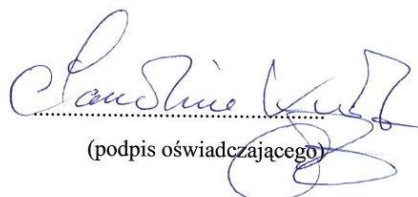
(imię i nazwisko kandydata do stopnia)

obejmował on: opracowanie założeń pracy i metodyki, przeprowadzenie eksperymentów, analizę i interpretację danych oraz opracowanie manuskryptu.

(merytoryczny opis wkładu kandydata do stopnia w powstanie publikacji)*

Jednocześnie wyrażam zgodę na wykorzystanie w/w pracy jako część rozprawy doktorskiej mgr inż. Aleksandry Majewskiej.

(imię i nazwisko kandydata do stopnia)


(podpis oświadczającego)

*w szczególności udziału w przygotowaniu koncepcji, metodyki, wykonaniu badań, interpretacji wyników

WARSZAWA 15.08 2023
(miejsowość, data)

CLAUDINE KIEDA
(imię i nazwisko)

OŚWIADCZENIE

Jako współautor pracy pt. *Pten knockout affects drug resistance differently in melanoma and kidney cancer* oświadczam, iż mój własny wkład merytoryczny w przygotowanie, przeprowadzenie i opracowanie badań oraz przedstawienie pracy w formie publikacji stanowi: opracowanie założeń pracy, analiza i interpretacja danych, krytyczna ocena manuskryptu.

Mój udział procentowy w przygotowaniu publikacji określam jako 12 %.

Wkład **Aleksandry Majewskiej** w powstawanie publikacji określam jako 38 %,

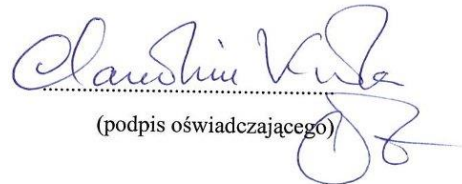
(imię i nazwisko kandydata do stopnia)

obejmował on: opracowanie metodyki, przeprowadzenie eksperymentów, analizę i interpretację danych oraz opracowanie manuskryptu.

(merytoryczny opis wkładu kandydata do stopnia w powstanie publikacji)*

Jednocześnie wyrażam zgodę na wykorzystanie w/w pracy jako część rozprawy doktorskiej mgr inż. Aleksandry Majewskiej.

(imię i nazwisko kandydata do stopnia)


(podpis oświadczającego)

*w szczególności udziału w przygotowaniu koncepcji, metodyki, wykonaniu badań, interpretacji wyników

WARSZAWA.....15.08.2023
(miejsowość, data)

CLAUDINE KIEDA
(imię i nazwisko)

OŚWIADCZENIE

Jako współautor pracy pt. *MiRNA pattern in hypoxic microenvironment of kidney cancer – role of PTEN* oświadczam, iż mój własny wkład merytoryczny w przygotowanie, przeprowadzenie i opracowanie badań oraz przedstawienie pracy w formie publikacji stanowi: opracowanie założeń pracy i metodyki, nadzorowanie przeprowadzonych eksperymentów, analiza i interpretacja danych, krytyczna ocena manuskryptu.

Mój udział procentowy w przygotowaniu publikacji określam jako 15 %.

Wkład **Aleksandry Majewskiej** w powstawanie publikacji określam jako 51 %,

(imię i nazwisko kandydata do stopnia)

obejmował on: opracowanie założeń pracy i metodyki, przeprowadzenie eksperymentów, analizę i interpretację danych oraz opracowanie manuskryptu.

(merytoryczny opis wkładu kandydata do stopnia w powstanie publikacji)*

Jednocześnie wyrażam zgodę na wykorzystanie w/w pracy jako część rozprawy doktorskiej mgr inż. Aleksandry Majewskiej.

(imię i nazwisko kandydata do stopnia)


.....
(podpis oświadczającego)
Claudine Kieda

*w szczególności udziału w przygotowaniu koncepcji, metodyki, wykonaniu badań, interpretacji wyników

14.9.23 Warszawa
(miejscowość, data)

Klaudia Brodeur
(imię i nazwisko)

OŚWIADCZENIE

Jako współautor pracy pt. *Comparative analysis of the effect of hypoxia in two different tumor cell models shows the differential involvement of PTEN control of proangiogenic pathways* oświadczam, iż mój własny wkład merytoryczny w przygotowanie, przeprowadzenie i opracowanie badań oraz przedstawienie pracy w formie publikacji stanowi: opracowanie założeń pracy i metodyki, pomoc i nadzorowanie przeprowadzonych eksperymentów, analiza i interpretacja danych, opracowanie manuskryptu.

Mój udział procentowy w przygotowaniu publikacji określam jako 20 %.

Wkład Aleksandry Majewskiej w powstawanie publikacji określam jako 51 %,

(imię i nazwisko kandydata do stopnia)

obejmował on: opracowanie założeń pracy i metodyki, przeprowadzenie eksperymentów, analizę i interpretację danych oraz opracowanie manuskryptu.

(merytoryczny opis wkładu kandydata do stopnia w powstanie publikacji)*

Jednocześnie wyrażam zgodę na wykorzystanie w/w pracy jako część rozprawy doktorskiej mgr inż. Aleksandry Majewskiej.

(imię i nazwisko kandydata do stopnia)

Adiunkt
Laboratorium Onkologii Molekularnej
i Terapii Innowacyjnych
Wojskowego Instytutu Medycznego
dr (podpis oświadczającego) KA

*w szczególności udziału w przygotowaniu koncepcji, metodyki, wykonaniu badań, interpretacji wyników

13. 9. 2020 r.
(miejsowość, data)

Klaudia Brodaszewska
(imię i nazwisko)

OŚWIADCZENIE

Jako współautor pracy pt. *Pten knockout affects drug resistance differently in melanoma and kidney cancer* oświadczam, iż mój własny wkład merytoryczny w przygotowanie, przeprowadzenie i opracowanie badań oraz przedstawienie pracy w formie publikacji stanowi: opracowanie założeń pracy i metodyki, pomoc i nadzorowanie przeprowadzonych eksperymentów, analiza i interpretacja danych, opracowanie manuskryptu. Mój udział procentowy w przygotowaniu publikacji określam jako **38 %**.

Wkład Aleksandry Majewskiej w powstawanie publikacji określam jako **38 %**,

(imię i nazwisko kandydata do stopnia)

obejmował on: opracowanie metodyki, przeprowadzenie eksperymentów, analizę i interpretację danych oraz opracowanie manuskryptu.

(merytoryczny opis wkładu kandydata do stopnia w powstanie publikacji)*

Jednocześnie wyrażam zgodę na wykorzystanie w/w pracy jako część rozprawy doktorskiej mgr inż. Aleksandry Majewskiej.

(imię i nazwisko kandydata do stopnia)

Adfunkt
Laboratorium Onkologii Molekularnej
i Terapii Innowacyjnych
Wojkowego Instytutu Medycznego

dr. n. biol. Klaudia BRODASZEWSKA

(podpis oświadczającego)

*w szczególności udziału w przygotowaniu koncepcji, metodyki, wykonaniu badań, interpretacji wyników

14.9.2014
Uamnia
(miejscowość, data)

Klaudia Boboczeńska
(imię i nazwisko)

OŚWIADCZENIE

Jako współautor pracy pt. *MiRNA pattern in hypoxic microenvironment of kidney cancer – role of PTEN* oświadczam, iż mój własny wkład merytoryczny w przygotowanie, przeprowadzenie i opracowanie badań oraz przedstawienie pracy w formie publikacji stanowi: opracowanie założeń pracy i metodyki, pomoc i nadzorowanie przeprowadzonych eksperymentów, analiza i interpretacja danych, opracowanie manuskryptu.

Mój udział procentowy w przygotowaniu publikacji określam jako **20 %**.

Wkład Aleksandry Majewskiej w powstawanie publikacji określam jako **51 %**,

(imię i nazwisko kandydata do stopnia)

obejmował on: opracowanie założeń pracy i metodyki, przeprowadzenie eksperymentów, analizę i interpretację danych oraz opracowanie manuskryptu.

(merytoryczny opis wkładu kandydata do stopnia w powstanie publikacji)*

Jednocześnie wyrażam zgodę na wykorzystanie w/w pracy jako część rozprawy doktorskiej mgr inż. Aleksandry Majewskiej.

(imię i nazwisko kandydata do stopnia)

Adiunkt
Laboratorium Onkologii Molekularnej
i Terapii Innowacyjnych
Wojskowego Instytutu Medycznego
dr n. biol. Katarzyna BOBOCZEŃSKA
(podpis oświadczającego)

*w szczególności udziału w przygotowaniu koncepcji, metodyki, wykonaniu badań, interpretacji wyników

Kraków 11/09/23
(miejscowość, data)

Aleksandra Filipiak - Dułbon
(imię i nazwisko)

OŚWIADCZENIE

Jako współautor pracy pt. *Comparative analysis of the effect of hypoxia in two different tumor cell models shows the differential involvement of PTEN control of proangiogenic pathways* oświadczam, iż mój własny wkład merytoryczny w przygotowanie, przeprowadzenie i opracowanie badań oraz przedstawienie pracy w formie publikacji stanowi: opracowanie założeń pracy i metodyki, pomoc i nadzorowanie przeprowadzonych eksperymentów, analiza i interpretacja danych, opracowanie manuskryptu.

Mój udział procentowy w przygotowaniu publikacji określam jako 9 %.

Wkład Aleksandry Majewskiej w powstawanie publikacji określam jako 51 %,

(imię i nazwisko kandydata do stopnia)

obejmował on: przeprowadzenie eksperymentów, analizę i interpretację danych oraz opracowanie manuskryptu.

(merytoryczny opis wkładu kandydata do stopnia w powstanie publikacji)*

Jednocześnie wyrażam zgodę na wykorzystanie w/w pracy jako część rozprawy doktorskiej mgr inż. Aleksandry Majewskiej.

(imię i nazwisko kandydata do stopnia)

Aleksandra Filipiak - Dułbon
(podpis oświadczającego)

*w szczególności udziału w przygotowaniu koncepcji, metodyki, wykonaniu badań, interpretacji wyników

Kraków, 16.08.23

(miejsowość, data)

Aleksandra Filipiak-Deliben
(imię i nazwisko)

OŚWIADCZENIE

Jako współautor pracy pt. *Pten knockout affects drug resistance differently in melanoma and kidney cancer* oświadczam, iż mój własny wkład merytoryczny w przygotowanie, przeprowadzenie i opracowanie badań oraz przedstawienie pracy w formie publikacji stanowi: przeprowadzenie eksperymentów, analiza i interpretacja danych, opracowanie manuskryptu.

Mój udział procentowy w przygotowaniu publikacji określam jako **12 %**.

Wkład Aleksandry Majewskiej w powstawanie publikacji określam jako **38 %**,

(imię i nazwisko kandydata do stopnia)

obejmował on: opracowanie metodyki, przeprowadzenie eksperymentów, analizę i interpretację danych oraz opracowanie manuskryptu.

(merytoryczny opis wkładu kandydata do stopnia w powstanie publikacji)*

Jednocześnie wyrażam zgodę na wykorzystanie w/w pracy jako część rozprawy doktorskiej mgr inż. Aleksandry Majewskiej.

(imię i nazwisko kandydata do stopnia)

Aleksandra Filipiak-Deliben
(podpis oświadczającego)

*w szczególności udziału w przygotowaniu koncepcji, metodyki, wykonaniu badań, interpretacji wyników

Kraków, 16.09.23
(miejsowość, data)

Aleksandra Filipiek-Duliban
(imię i nazwisko)

OŚWIADCZENIE

Jako współautor pracy pt. *MIRNA pattern in hypoxic microenvironment of kidney cancer – role of PTEN* oświadczam, iż mój własny wkład merytoryczny w przygotowanie, przeprowadzenie i opracowanie badań oraz przedstawienie pracy w formie publikacji stanowi: przeprowadzenie eksperymentów, analiza i interpretacja danych, opracowanie manuskryptu.

Mój udział procentowy w przygotowaniu publikacji określam jako 8 %.

Wkład Aleksandry Majewskiej w powstawanie publikacji określam jako 51 %,

(imię i nazwisko kandydata do stopnia)

obejmował on: opracowanie założeń pracy i metodyki, przeprowadzenie eksperymentów, analizę i interpretację danych oraz opracowanie manuskryptu.

(merytoryczny opis wkładu kandydata do stopnia w powstanie publikacji)*

Jednocześnie wyrażam zgodę na wykorzystanie w/w pracy jako część rozprawy doktorskiej mgr inż. Aleksandry Majewskiej.

(imię i nazwisko kandydata do stopnia)

Aleksandra Filipiek-Duliban
(podpis oświadczającego)

*w szczególności udziału w przygotowaniu koncepcji, metodyki, wykonaniu badań, interpretacji wyników

Poznań, 14.09.2023
(miejsowość, data)

Arkadiusz Kajdasz
(imię i nazwisko)

OŚWIADCZENIE

Jako współautor pracy pt. *MiRNA pattern in hypoxic microenvironment of kidney cancer – role of PTEN* oświadczam, iż mój własny wkład merytoryczny w przygotowanie, przeprowadzenie i opracowanie badań oraz przedstawienie pracy w formie publikacji stanowi: analiza i interpretacja danych, krytyczna ocena manuskryptu.

Mój udział procentowy w przygotowaniu publikacji określam jako **6 %**.

Wkład Aleksandry Majewskiej w powstawanie publikacji określam jako **51 %**,

(imię i nazwisko kandydata do stopnia)

obejmował on: opracowanie założeń pracy i metodyki, przeprowadzenie eksperymentów, analizę i interpretację danych oraz opracowanie manuskryptu.

(merytoryczny opis wkładu kandydata do stopnia w powstanie publikacji)*

Jednocześnie wyrażam zgodę na wykorzystanie w/w pracy jako część rozprawy doktorskiej mgr inż. Aleksandry Majewskiej.

(imię i nazwisko kandydata do stopnia)

Arkadiusz
Kajdasz

.....
(podpis oświadczającego)

*w szczególności udziału w przygotowaniu koncepcji, metodyki, wykonaniu badań, interpretacji wyników

7 DOROBEK NAUKOWY

Publikacje:

1. Piasecki, P., **Majewska, A.**, Narloch, J., Maciak, M., Brodaczevska, K., Kuc, M., Was, H., Wierzbicki, M., Brzozowski, K., Ziecina, P., Mazurek, A., Dziuk, M., Iller, E., & Kieda, C. (2021). A new in vitro model applied 90Y microspheres to study the effects of low dose beta radiation on colorectal cancer cell line in various oxygenation conditions. *Scientific reports*, 11(1), 4472. <https://doi.org/10.1038/s41598-021-84000-7>
2. El Hafny-Rahbi, B., Brodaczevska, K., Collet, G., **Majewska, A.**, Klimkiewicz, K., Delalande, A., Grillon, C., & Kieda, C. (2021). Tumour angiogenesis normalized by myo-inositol trispyrophosphate alleviates hypoxia in the microenvironment and promotes antitumor immune response. *Journal of cellular and molecular medicine*, 25(7), 3284–3299. <https://doi.org/10.1111/jcmm.16399>
3. **Majewska, A.**, Wilkus, K., Brodaczevska, K., & Kieda, C. (2021). Endothelial Cells as Tools to Model Tissue Microenvironment in Hypoxia-Dependent Pathologies. *International journal of molecular sciences*, 22(2), 520. <https://doi.org/10.3390/ijms22020520>
4. Filipiak-Duliban, A., Brodaczevska, K., **Majewska, A.**, & Kieda, C. (2022). Spheroid culture models adequately imitate distinctive features of the renal cancer or melanoma microenvironment. *In vitro cellular & developmental biology. Animal*, 58(5), 349–364. <https://doi.org/10.1007/s11626-022-00685-8>
5. Thinard, R., Farkas, A. E., Halasa, M., Chevalier, M., Brodaczevska, K., **Majewska, A.**, Zdanowski, R., Paprocka, M., Rossowska, J., Duc, L. T., Greferath, R., Krizbai, I., Van Leuven, F., Kieda, C., & Nicolau, C. (2022). "Endothelial Antibody Factory" at the Blood Brain Barrier: Novel Approach to Therapy of Neurodegenerative Diseases. *Pharmaceutics*, 14(7), 1418. <https://doi.org/10.3390/pharmaceutics14071418>
6. Maciak, M., Konior, M., Wawszczak, D., **Majewska, A.**, Brodaczevska, K.K., Piasecki, P., Narloch, J., Sady, M., Olszewski, J., Gajewski, Z., Kieda, C., Ziel, T., & Iller, E. (2022). Physical properties and biological impact of 90Y microspheres prepared by sol-gel method for liver radioembolization. *Radiation Physics and Chemistry*. 202, 110506, <https://doi.org/10.1016/j.radphyschem.2022.110506>
7. Siewiera, J., Brodaczevska, K., Jermakow, N., Lubas, A., Kłos, K., **Majewska, A.**, & Kot, J. (2022). Effectiveness of Hyperbaric Oxygen Therapy in SARS-CoV-2 Pneumonia: The Primary Results of a Randomised Clinical Trial. *Journal of clinical medicine*, 12(1), 8. <https://doi.org/10.3390/jcm12010008>
8. Wilkus-Adamczyk, K., Brodaczevska, K., **Majewska, A.**, & Kieda, C. (2023). Microenvironment commits breast tumor ECs to dedifferentiation by micro-RNA-200-b-3p regulation and extracellular matrix remodeling. *Frontiers in cell and developmental biology*, 11, 1125077. <https://doi.org/10.3389/fcell.2023.1125077>
9. Synowiec, A., Brodaczevska, K., Wcisło, G., **Majewska, A.**, Borkowska, A., Filipiak-Duliban, A., Gawrylak, A., Wilkus, K., Piwocka, K., Kominek, A., Waś, H., Lewicki, S., Siewiera, J., Szczylik, C., Szenajch, J., Kubiak, J. Z., & Kieda, C. (2023). Hypoxia, but Not Normoxia, Reduces Effects of Resveratrol on Cisplatin Treatment in A2780 Ovarian Cancer Cells: A Challenge for Resveratrol Use in Anticancer Adjuvant Cisplatin Therapy. *International journal of molecular sciences*, 24(6), 5715. <https://doi.org/10.3390/ijms24065715>

Konferencje:

1. **Majewska A.**, Brodaczewska K., Kieda C., Targeting cancer PTEN for hypoxia related tumor microenvironment, 10th Anniversary international conference of contemporary oncology, 21-23 March 2018, Poznań – Poster
2. **Majewska A.**, Brodaczewska K., Kieda C., Intra-tumor hypoxia as a modulator of endothelial cell activity: in-vitro model of pathological angiogenesis, 44th FEBS Congress, 6-11 July 2019, Krakow – Poster
3. **Majewska A.**, Brodaczewska K., Kieda C., Effects of hypoxia on cancer PTEN activity, 6th LIA Meeting, 4-5 June 2019, Warsaw – Poster
4. **Majewska A.**, Brodaczewska K., Kieda C., PTEN as a target for hypoxia alleviation therapy in melanoma and renal cancer, 6th International Conference of Cell Biology, 6-8 November 2020 online – Prezentacja ustna
5. **Majewska A.**, Brodaczewska K., Kieda C., The role of tumor microenvironment in regulation of Serpine1, EACR 2022 Congress - Translating Biology to Medicine, 20-23 June, Sevilla, Spain – Poster
6. **Majewska A.**, Brodaczewska K., Kieda C. The role of miR-224-5p in kidney cancer progression, V ZJAZD NAUKOWY POLSKIEGO TOWARZYSTWA BIOLOGII MEDYCZNEJ, „Biologia-Medycyna-Terapia”, 15-17.09.2023, Lublin – Poster

8 REFERENCJE

1. Global Burden of Disease Cancer, C., et al., *Cancer Incidence, Mortality, Years of Life Lost, Years Lived With Disability, and Disability-Adjusted Life Years for 29 Cancer Groups From 2010 to 2019: A Systematic Analysis for the Global Burden of Disease Study 2019*. JAMA Oncol, 2022. **8**(3): p. 420-444.
2. Foreman, K.J., et al., *Forecasting life expectancy, years of life lost, and all-cause and cause-specific mortality for 250 causes of death: reference and alternative scenarios for 2016-40 for 195 countries and territories*. Lancet, 2018. **392**(10159): p. 2052-2090.
3. Anderson, N.M. and M.C. Simon, *The tumor microenvironment*. Curr Biol, 2020. **30**(16): p. R921-R925.
4. Theocharis, A.D., et al., *Extracellular matrix structure*. Adv Drug Deliv Rev, 2016. **97**: p. 4-27.
5. Popova, N.V. and M. Jucker, *The Functional Role of Extracellular Matrix Proteins in Cancer*. Cancers (Basel), 2022. **14**(1).
6. Gal, P., et al., *How Signaling Molecules Regulate Tumor Microenvironment: Parallels to Wound Repair*. Molecules, 2017. **22**(11).
7. Shah, L., et al., *Role of stiffness and physico-chemical properties of tumour microenvironment on breast cancer cell stemness*. Acta Biomater, 2022. **152**: p. 273-289.
8. Pandkar, M.R., S.G. Dhamdhere, and S. Shukla, *Oxygen gradient and tumor heterogeneity: The chronicle of a toxic relationship*. Biochim Biophys Acta Rev Cancer, 2021. **1876**(1): p. 188553.
9. Hancock, R.L., et al., *Epigenetic regulation by histone demethylases in hypoxia*. Epigenomics, 2015. **7**(5): p. 791-811.
10. Carreau, A., et al., *Why is the partial oxygen pressure of human tissues a crucial parameter? Small molecules and hypoxia*. J Cell Mol Med, 2011. **15**(6): p. 1239-53.
11. Muz, B., et al., *The role of hypoxia in cancer progression, angiogenesis, metastasis, and resistance to therapy*. Hypoxia (Auckl), 2015. **3**: p. 83-92.
12. Slemc, L. and T. Kunej, *Transcription factor HIF1A: downstream targets, associated pathways, polymorphic hypoxia response element (HRE) sites, and initiative for standardization of reporting in scientific literature*. Tumour Biol, 2016. **37**(11): p. 14851-14861.
13. Zimna, A. and M. Kurpisz, *Hypoxia-Inducible Factor-1 in Physiological and Pathophysiological Angiogenesis: Applications and Therapies*. Biomed Res Int, 2015. **2015**: p. 549412.
14. Lin, Q., X. Cong, and Z. Yun, *Differential hypoxic regulation of hypoxia-inducible factors 1alpha and 2alpha*. Mol Cancer Res, 2011. **9**(6): p. 757-65.
15. Kim, W.Y. and W.G. Kaelin, *Role of VHL gene mutation in human cancer*. J Clin Oncol, 2004. **22**(24): p. 4991-5004.
16. Ma, X., et al., *VHL gene alterations in renal cell carcinoma patients: novel hotspot or founder mutations and linkage disequilibrium*. Oncogene, 2001. **20**(38): p. 5393-400.
17. Kim, B.J., et al., *Prognostic and predictive value of VHL gene alteration in renal cell carcinoma: a meta-analysis and review*. Oncotarget, 2017. **8**(8): p. 13979-13985.
18. Batie, M. and S. Rocha, *Gene transcription and chromatin regulation in hypoxia*. Biochem Soc Trans, 2020. **48**(3): p. 1121-1128.
19. Lugano, R., M. Ramachandran, and A. Dimberg, *Tumor angiogenesis: causes, consequences, challenges and opportunities*. Cell Mol Life Sci, 2020. **77**(9): p. 1745-1770.
20. Zhao, X., et al., *Endothelial progenitor cells promote tumor growth and progression by enhancing new vessel formation*. Oncol Lett, 2016. **12**(2): p. 793-799.
21. Klimkiewicz, K., et al., *A 3D model of tumour angiogenic microenvironment to monitor hypoxia effects on cell interactions and cancer stem cell selection*. Cancer Lett, 2017. **396**: p. 10-20.

22. Gao, D., et al., *Bone marrow-derived endothelial progenitor cells contribute to the angiogenic switch in tumor growth and metastatic progression*. *Biochim Biophys Acta*, 2009. **1796**(1): p. 33-40.
23. Collet, G., et al., *Endothelial precursor cell-based therapy to target the pathologic angiogenesis and compensate tumor hypoxia*. *Cancer Lett*, 2016. **370**(2): p. 345-57.
24. Yuan, H.F. and X.T. Pei, *[The application of endothelial progenitor cells (EPC) in the cellular and gene therapy of cardiovascular-disease]*. *Sheng Li Ke Xue Jin Zhan*, 2003. **34**(2): p. 165-8.
25. Kolesnichenko, O.A., et al., *Therapeutic Potential of Endothelial Progenitor Cells in Pulmonary Diseases*. *Am J Respir Cell Mol Biol*, 2021. **65**(5): p. 473-488.
26. Thinard, R., et al., *"Endothelial Antibody Factory" at the Blood Brain Barrier: Novel Approach to Therapy of Neurodegenerative Diseases*. *Pharmaceutics*, 2022. **14**(7).
27. Wechman, S.L., et al., *Vascular mimicry: Triggers, molecular interactions and in vivo models*. *Adv Cancer Res*, 2020. **148**: p. 27-67.
28. Maniotis, A.J., et al., *Vascular channel formation by human melanoma cells in vivo and in vitro: vasculogenic mimicry*. *Am J Pathol*, 1999. **155**(3): p. 739-52.
29. Ricci-Vitiani, L., et al., *Tumour vascularization via endothelial differentiation of glioblastoma stem-like cells*. *Nature*, 2010. **468**(7325): p. 824-8.
30. Williamson, S.C., et al., *Vasculogenic mimicry in small cell lung cancer*. *Nat Commun*, 2016. **7**: p. 13322.
31. Maj, E., D. Papiernik, and J. Wietrzyk, *Antiangiogenic cancer treatment: The great discovery and greater complexity (Review)*. *Int J Oncol*, 2016. **49**(5): p. 1773-1784.
32. Quintero-Fabian, S., et al., *Role of Matrix Metalloproteinases in Angiogenesis and Cancer*. *Front Oncol*, 2019. **9**: p. 1370.
33. Naito, H., T. Iba, and N. Takakura, *Mechanisms of new blood-vessel formation and proliferative heterogeneity of endothelial cells*. *Int Immunol*, 2020. **32**(5): p. 295-305.
34. Azzi, S., J.K. Hebda, and J. Gavard, *Vascular permeability and drug delivery in cancers*. *Front Oncol*, 2013. **3**: p. 211.
35. Wilkus, K., et al., *Distinctive Properties of Endothelial Cells from Tumor and Normal Tissue in Human Breast Cancer*. *Int J Mol Sci*, 2021. **22**(16).
36. Morikawa, S., et al., *Abnormalities in pericytes on blood vessels and endothelial sprouts in tumors*. *Am J Pathol*, 2002. **160**(3): p. 985-1000.
37. Baluk, P., et al., *Abnormalities of basement membrane on blood vessels and endothelial sprouts in tumors*. *Am J Pathol*, 2003. **163**(5): p. 1801-15.
38. Edgar, L.T., et al., *Extracellular matrix density regulates the rate of neovessel growth and branching in sprouting angiogenesis*. *PLoS One*, 2014. **9**(1): p. e85178.
39. Bordeleau, F., et al., *Matrix stiffening promotes a tumor vasculature phenotype*. *Proc Natl Acad Sci U S A*, 2017. **114**(3): p. 492-497.
40. Folkman, J., *Tumor angiogenesis: therapeutic implications*. *N Engl J Med*, 1971. **285**(21): p. 1182-6.
41. Ellis, L.M., *Mechanisms of action of bevacizumab as a component of therapy for metastatic colorectal cancer*. *Semin Oncol*, 2006. **33**(5 Suppl 10): p. S1-7.
42. Hurwitz, H., et al., *Bevacizumab plus irinotecan, fluorouracil, and leucovorin for metastatic colorectal cancer*. *N Engl J Med*, 2004. **350**(23): p. 2335-42.
43. Al-Husein, B., et al., *Antiangiogenic therapy for cancer: an update*. *Pharmacotherapy*, 2012. **32**(12): p. 1095-111.
44. Hermosilla, J., et al., *Comprehensive biophysical and functional study of ziv-aflibercept: characterization and forced degradation*. *Sci Rep*, 2020. **10**(1): p. 2675.
45. Kelly, R.J., C. Darnell, and O. Rixe, *Target inhibition in antiangiogenic therapy a wide spectrum of selectivity and specificity*. *Cancer J*, 2010. **16**(6): p. 635-42.
46. Hu-Lowe, D.D., et al., *Nonclinical antiangiogenesis and antitumor activities of axitinib (AG-013736), an oral, potent, and selective inhibitor of vascular endothelial growth factor receptor tyrosine kinases 1, 2, 3*. *Clin Cancer Res*, 2008. **14**(22): p. 7272-83.
47. Popescu, A. and R.M. Anghel, *Tyrosine-kinase Inhibitors Treatment in Advanced Malignant Melanoma*. *Maedica (Bucur)*, 2017. **12**(4): p. 293-296.

48. Giantonio, B.J., et al., *Bevacizumab in combination with oxaliplatin, fluorouracil, and leucovorin (FOLFOX4) for previously treated metastatic colorectal cancer: results from the Eastern Cooperative Oncology Group Study E3200*. J Clin Oncol, 2007. **25**(12): p. 1539-44.
49. Van der Veldt, A.A., et al., *Rapid decrease in delivery of chemotherapy to tumors after anti-VEGF therapy: implications for scheduling of anti-angiogenic drugs*. Cancer Cell, 2012. **21**(1): p. 82-91.
50. Llovet, J.M., et al., *Sorafenib in advanced hepatocellular carcinoma*. N Engl J Med, 2008. **359**(4): p. 378-90.
51. Ratain, M.J., et al., *Phase II placebo-controlled randomized discontinuation trial of sorafenib in patients with metastatic renal cell carcinoma*. J Clin Oncol, 2006. **24**(16): p. 2505-12.
52. Escudier, B., et al., *Sorafenib for treatment of renal cell carcinoma: Final efficacy and safety results of the phase III treatment approaches in renal cancer global evaluation trial*. J Clin Oncol, 2009. **27**(20): p. 3312-8.
53. Motzer, R.J., et al., *Overall survival and updated results for sunitinib compared with interferon alfa in patients with metastatic renal cell carcinoma*. J Clin Oncol, 2009. **27**(22): p. 3584-90.
54. Paez-Ribes, M., et al., *Antiangiogenic therapy elicits malignant progression of tumors to increased local invasion and distant metastasis*. Cancer Cell, 2009. **15**(3): p. 220-31.
55. Jain, R.K., *Normalizing tumor vasculature with anti-angiogenic therapy: a new paradigm for combination therapy*. Nat Med, 2001. **7**(9): p. 987-9.
56. Moserle, L., G. Jimenez-Valerio, and O. Casanovas, *Antiangiogenic therapies: going beyond their limits*. Cancer Discov, 2014. **4**(1): p. 31-41.
57. Maione, F., et al., *Semaphorin 3A is an endogenous angiogenesis inhibitor that blocks tumor growth and normalizes tumor vasculature in transgenic mouse models*. J Clin Invest, 2009. **119**(11): p. 3356-72.
58. Shimizu, K., et al., *Gene regulation of a novel angiogenesis inhibitor, vasohibin, in endothelial cells*. Biochem Biophys Res Commun, 2005. **327**(3): p. 700-6.
59. Kern, J., et al., *Vasohibin inhibits angiogenic sprouting in vitro and supports vascular maturation processes in vivo*. BMC Cancer, 2009. **9**: p. 284.
60. Mazzone, M., et al., *Heterozygous deficiency of PHD2 restores tumor oxygenation and inhibits metastasis via endothelial normalization*. Cell, 2009. **136**(5): p. 839-851.
61. Duarte, C.D., et al., *myo-Inositol trispyrophosphate: a novel allosteric effector of hemoglobin with high permeation selectivity across the red blood cell plasma membrane*. Chembiochem, 2010. **11**(18): p. 2543-8.
62. Kieda, C., et al., *Suppression of hypoxia-induced HIF-1alpha and of angiogenesis in endothelial cells by myo-inositol trispyrophosphate-treated erythrocytes*. Proc Natl Acad Sci U S A, 2006. **103**(42): p. 15576-81.
63. Evans, B.A., et al., *Modulation of red blood cell oxygen affinity with a novel allosteric modifier of hemoglobin is additive to the Bohr effect*. Blood Cells Mol Dis, 2021. **87**: p. 102520.
64. Okninska, M., et al., *New potential treatment for cardiovascular disease through modulation of hemoglobin oxygen binding curve: Myo-inositol trispyrophosphate (ITPP), from cancer to cardiovascular disease*. Biomed Pharmacother, 2022. **154**: p. 113544.
65. Kieda, C., et al., *Stable tumor vessel normalization with pO(2) increase and endothelial PTEN activation by inositol trispyrophosphate brings novel tumor treatment*. J Mol Med (Berl), 2013. **91**(7): p. 883-99.
66. Arahamian, M., et al., *Myo-InositolTrisPyroPhosphate treatment leads to HIF-1alpha suppression and eradication of early hepatoma tumors in rats*. Chembiochem, 2011. **12**(5): p. 777-83.
67. Grgic, I., et al., *Tumor Oxygenation by Myo-Inositol Trispyrophosphate Enhances Radiation Response*. Int J Radiat Oncol Biol Phys, 2021. **110**(4): p. 1222-1233.

68. Fornvik, K., et al., *ITPP Treatment of RG2 Glioblastoma in a Rat Model*. *Anticancer Res*, 2016. **36**(11): p. 5751-5755.
69. Iyengar, S. and D. Schwartz, *Failure of Inositol Trispyrophosphate to Enhance Highly Effective Radiotherapy of GL261 Glioblastoma in Mice*. *Anticancer Res*, 2017. **37**(3): p. 1121-1125.
70. El Hafny-Rahbi, B., et al., *Tumour angiogenesis normalized by myo-inositol trispyrophosphate alleviates hypoxia in the microenvironment and promotes antitumor immune response*. *J Cell Mol Med*, 2021. **25**(7): p. 3284-3299.
71. Grzymajlo, K., B. El Hafny-Rahbi, and C. Kieda, *Tumour suppressor PTEN activity is differentially inducible by myo-inositol phosphates*. *J Cell Mol Med*, 2023. **27**(6): p. 879-890.
72. Steck, P.A., et al., *Identification of a candidate tumour suppressor gene, MMAC1, at chromosome 10q23.3 that is mutated in multiple advanced cancers*. *Nat Genet*, 1997. **15**(4): p. 356-62.
73. Li, J., et al., *PTEN, a putative protein tyrosine phosphatase gene mutated in human brain, breast, and prostate cancer*. *Science*, 1997. **275**(5308): p. 1943-7.
74. Bononi, A. and P. Pinton, *Study of PTEN subcellular localization*. *Methods*, 2015. **77-78**: p. 92-103.
75. Orozco-Garcia, E., et al., *Endothelial plasticity across PTEN and Hippo pathways: A complex hormetic rheostat modulated by extracellular vesicles*. *Transl Oncol*, 2023. **31**: p. 101633.
76. Bazzichetto, C., et al., *PTEN as a Prognostic/Predictive Biomarker in Cancer: An Unfulfilled Promise?* *Cancers (Basel)*, 2019. **11**(4).
77. Masson, G.R. and R.L. Williams, *Structural Mechanisms of PTEN Regulation*. *Cold Spring Harb Perspect Med*, 2020. **10**(3).
78. Kwabi-Addo, B., et al., *Haploinsufficiency of the Pten tumor suppressor gene promotes prostate cancer progression*. *Proc Natl Acad Sci U S A*, 2001. **98**(20): p. 11563-8.
79. Ngeow, J., K. Sesock, and C. Eng, *Clinical Implications for Germline PTEN Spectrum Disorders*. *Endocrinol Metab Clin North Am*, 2017. **46**(2): p. 503-517.
80. Tan, M.H., et al., *Lifetime cancer risks in individuals with germline PTEN mutations*. *Clin Cancer Res*, 2012. **18**(2): p. 400-7.
81. Smirnov, V.E. and V.Z. Makhovskii, [*Multiple primary cancer of the large intestine associated with chemical burn of the rectum*]. *Klin Khir (1962)*, 1985(2): p. 47-8.
82. Bermudez Brito, M., E. Goulielmaki, and E.A. Papakonstanti, *Focus on PTEN Regulation*. *Front Oncol*, 2015. **5**: p. 166.
83. Kohnoh, T., et al., *Hypoxia-induced modulation of PTEN activity and EMT phenotypes in lung cancers*. *Cancer Cell Int*, 2016. **16**: p. 33.
84. Rascio, F., et al., *The Pathogenic Role of PI3K/AKT Pathway in Cancer Onset and Drug Resistance: An Updated Review*. *Cancers (Basel)*, 2021. **13**(16).
85. Murugan, A.K., *mTOR: Role in cancer, metastasis and drug resistance*. *Semin Cancer Biol*, 2019. **59**: p. 92-111.
86. Chibaya, L., et al., *Mdm2 phosphorylation by Akt regulates the p53 response to oxidative stress to promote cell proliferation and tumorigenesis*. *Proc Natl Acad Sci U S A*, 2021. **118**(4).
87. Datta, S.R., et al., *Akt phosphorylation of BAD couples survival signals to the cell-intrinsic death machinery*. *Cell*, 1997. **91**(2): p. 231-41.
88. Alzahrani, A.S., *PI3K/Akt/mTOR inhibitors in cancer: At the bench and bedside*. *Semin Cancer Biol*, 2019. **59**: p. 125-132.
89. Papa, A. and P.P. Pandolfi, *The PTEN(-)PI3K Axis in Cancer*. *Biomolecules*, 2019. **9**(4).
90. Tamura, M., et al., *PTEN interactions with focal adhesion kinase and suppression of the extracellular matrix-dependent phosphatidylinositol 3-kinase/Akt cell survival pathway*. *J Biol Chem*, 1999. **274**(29): p. 20693-703.
91. Gu, J., M. Tamura, and K.M. Yamada, *Tumor suppressor PTEN inhibits integrin- and growth factor-mediated mitogen-activated protein (MAP) kinase signaling pathways*. *J Cell Biol*, 1998. **143**(5): p. 1375-83.

92. Vogelmann, R., et al., *TGFbeta-induced downregulation of E-cadherin-based cell-cell adhesion depends on PI3-kinase and PTEN*. J Cell Sci, 2005. **118**(Pt 20): p. 4901-12.
93. Perumal, E., et al., *PTEN inactivation induces epithelial-mesenchymal transition and metastasis by intranuclear translocation of beta-catenin and snail/slug in non-small cell lung carcinoma cells*. Lung Cancer, 2019. **130**: p. 25-34.
94. Shen, W.H., et al., *Essential role for nuclear PTEN in maintaining chromosomal integrity*. Cell, 2007. **128**(1): p. 157-70.
95. Ming, M. and Y.Y. He, *PTEN in DNA damage repair*. Cancer Lett, 2012. **319**(2): p. 125-129.
96. Brandmaier, A., S.Q. Hou, and W.H. Shen, *Cell Cycle Control by PTEN*. J Mol Biol, 2017. **429**(15): p. 2265-2277.
97. Li, A.G., et al., *Mechanistic insights into maintenance of high p53 acetylation by PTEN*. Mol Cell, 2006. **23**(4): p. 575-87.
98. Chen, Z.H., et al., *PTEN interacts with histone H1 and controls chromatin condensation*. Cell Rep, 2014. **8**(6): p. 2003-2014.
99. Putz, U., et al., *PTEN secretion in exosomes*. Methods, 2015. **77-78**: p. 157-63.
100. Hopkins, B.D., et al., *A secreted PTEN phosphatase that enters cells to alter signaling and survival*. Science, 2013. **341**(6144): p. 399-402.
101. Song, X., et al., *Hypoxic Microenvironment-Induced Reduction in PTEN-L Secretion Promotes Non-Small Cell Lung Cancer Metastasis through PI3K/AKT Pathway*. Evid Based Complement Alternat Med, 2022. **2022**: p. 6683104.
102. Vidotto, T., et al., *Emerging role of PTEN loss in evasion of the immune response to tumours*. Br J Cancer, 2020. **122**(12): p. 1732-1743.
103. Song, M., et al., *PTEN loss increases PD-L1 protein expression and affects the correlation between PD-L1 expression and clinical parameters in colorectal cancer*. PLoS One, 2013. **8**(6): p. e65821.
104. Parsa, A.T., et al., *Loss of tumor suppressor PTEN function increases B7-H1 expression and immunoresistance in glioma*. Nat Med, 2007. **13**(1): p. 84-8.
105. Maxwell, P.J., et al., *Potentiation of inflammatory CXCL8 signalling sustains cell survival in PTEN-deficient prostate carcinoma*. Eur Urol, 2013. **64**(2): p. 177-88.
106. Peng, W., et al., *Loss of PTEN Promotes Resistance to T Cell-Mediated Immunotherapy*. Cancer Discov, 2016. **6**(2): p. 202-16.
107. Conciatori, F., et al., *PTEN Function at the Interface between Cancer and Tumor Microenvironment: Implications for Response to Immunotherapy*. Int J Mol Sci, 2020. **21**(15).
108. Ma, J., et al., *PTEN regulates angiogenesis through PI3K/Akt/VEGF signaling pathway in human pancreatic cancer cells*. Mol Cell Biochem, 2009. **331**(1-2): p. 161-71.
109. Serra, H., et al., *PTEN mediates Notch-dependent stalk cell arrest in angiogenesis*. Nat Commun, 2015. **6**: p. 7935.
110. Mithal, P., et al., *PTEN loss in biopsy tissue predicts poor clinical outcomes in prostate cancer*. Int J Urol, 2014. **21**(12): p. 1209-14.
111. Li, S., et al., *Loss of PTEN expression in breast cancer: association with clinicopathological characteristics and prognosis*. Oncotarget, 2017. **8**(19): p. 32043-32054.
112. Hu, T.H., et al., *Expression and prognostic role of tumor suppressor gene PTEN/MMAC1/TEP1 in hepatocellular carcinoma*. Cancer, 2003. **97**(8): p. 1929-40.
113. Martins, F.C., et al., *Clinical and pathological associations of PTEN expression in ovarian cancer: a multicentre study from the Ovarian Tumour Tissue Analysis Consortium*. Br J Cancer, 2020. **123**(5): p. 793-802.
114. Bucheit, A.D., et al., *Complete loss of PTEN protein expression correlates with shorter time to brain metastasis and survival in stage IIIB/C melanoma patients with BRAFV600 mutations*. Clin Cancer Res, 2014. **20**(21): p. 5527-36.
115. Whiteman, D.C., et al., *Nuclear PTEN expression and clinicopathologic features in a population-based series of primary cutaneous melanoma*. Int J Cancer, 2002. **99**(1): p. 63-7.

116. Que, W.C., et al., *PTEN in kidney cancer: A review and meta-analysis*. Clin Chim Acta, 2018. **480**: p. 92-98.
117. Tang, L., et al., *Phosphatase and tensin homolog (PTEN) expression on oncologic outcome in renal cell carcinoma: A systematic review and meta-analysis*. PLoS One, 2017. **12**(7): p. e0179437.
118. Chang, L., et al., *PI3K/Akt/mTOR pathway inhibitors enhance radiosensitivity in radioresistant prostate cancer cells through inducing apoptosis, reducing autophagy, suppressing NHEJ and HR repair pathways*. Cell Death Dis, 2014. **5**(10): p. e1437.
119. Fischer, T., et al., *PTEN mutant non-small cell lung cancer require ATM to suppress pro-apoptotic signalling and evade radiotherapy*. Cell Biosci, 2022. **12**(1): p. 50.
120. Wu, H., et al., *Effect of tumor suppressor gene PTEN on the resistance to cisplatin in human ovarian cancer cell lines and related mechanisms*. Cancer Lett, 2008. **271**(2): p. 260-71.
121. Zhang, H., et al., *Oncogenic Y68 frame shift mutation of PTEN represents a mechanism of docetaxel resistance in endometrial cancer cell lines*. Sci Rep, 2019. **9**(1): p. 2111.
122. Zhou, M., et al., *PTEN reverses MDM2-mediated chemotherapy resistance by interacting with p53 in acute lymphoblastic leukemia cells*. Cancer Res, 2003. **63**(19): p. 6357-62.
123. Sekino, Y., et al., *PTEN Is Involved in Sunitinib and Sorafenib Resistance in Renal Cell Carcinoma*. Anticancer Res, 2020. **40**(4): p. 1943-1951.
124. Paraiso, K.H., et al., *PTEN loss confers BRAF inhibitor resistance to melanoma cells through the suppression of BIM expression*. Cancer Res, 2011. **71**(7): p. 2750-60.
125. Qi, Z., et al., *Overcoming resistance to immune checkpoint therapy in PTEN-null prostate cancer by intermittent anti-PI3Kalpha/beta/delta treatment*. Nat Commun, 2022. **13**(1): p. 182.
126. Wightman, B., I. Ha, and G. Ruvkun, *Posttranscriptional regulation of the heterochronic gene lin-14 by lin-4 mediates temporal pattern formation in C. elegans*. Cell, 1993. **75**(5): p. 855-62.
127. Lee, Y., et al., *MicroRNA genes are transcribed by RNA polymerase II*. EMBO J, 2004. **23**(20): p. 4051-60.
128. Lee, Y., et al., *The nuclear RNase III Drosha initiates microRNA processing*. Nature, 2003. **425**(6956): p. 415-9.
129. Nguyen, T.A., et al., *Functional Anatomy of the Human Microprocessor*. Cell, 2015. **161**(6): p. 1374-87.
130. Wilson, R.C., et al., *Dicer-TRBP complex formation ensures accurate mammalian microRNA biogenesis*. Mol Cell, 2015. **57**(3): p. 397-407.
131. He, B., et al., *miRNA-based biomarkers, therapies, and resistance in Cancer*. Int J Biol Sci, 2020. **16**(14): p. 2628-2647.
132. Gulyaeva, L.F. and N.E. Kushlinskiy, *Regulatory mechanisms of microRNA expression*. J Transl Med, 2016. **14**(1): p. 143.
133. Lewis, B.P., C.B. Burge, and D.P. Bartel, *Conserved seed pairing, often flanked by adenosines, indicates that thousands of human genes are microRNA targets*. Cell, 2005. **120**(1): p. 15-20.
134. Valinezhad Orang, A., R. Safaralizadeh, and M. Kazemzadeh-Bavili, *Mechanisms of miRNA-Mediated Gene Regulation from Common Downregulation to mRNA-Specific Upregulation*. Int J Genomics, 2014. **2014**: p. 970607.
135. Vishnoi, A. and S. Rani, *MiRNA Biogenesis and Regulation of Diseases: An Overview*. Methods Mol Biol, 2017. **1509**: p. 1-10.
136. Hill, M. and N. Tran, *miRNA interplay: mechanisms and consequences in cancer*. Dis Model Mech, 2021. **14**(4).
137. Hata, A. and R. Kashima, *Dysregulation of microRNA biogenesis machinery in cancer*. Crit Rev Biochem Mol Biol, 2016. **51**(3): p. 121-34.
138. Karube, Y., et al., *Reduced expression of Dicer associated with poor prognosis in lung cancer patients*. Cancer Sci, 2005. **96**(2): p. 111-5.
139. Nowak, I. and A.A. Sarshad, *Argonaute Proteins Take Center Stage in Cancers*. Cancers (Basel), 2021. **13**(4).

140. Makarova, J., et al., *Extracellular miRNAs and Cell-Cell Communication: Problems and Prospects*. Trends Biochem Sci, 2021. **46**(8): p. 640-651.
141. Yu, X., M. Odenthal, and J.W. Fries, *Exosomes as miRNA Carriers: Formation-Function-Future*. Int J Mol Sci, 2016. **17**(12).
142. Turchinovich, A., et al., *Characterization of extracellular circulating microRNA*. Nucleic Acids Res, 2011. **39**(16): p. 7223-33.
143. Wilkus-Adamczyk, K., et al., *Microenvironment commits breast tumor ECs to dedifferentiation by micro-RNA-200-b-3p regulation and extracellular matrix remodeling*. Front Cell Dev Biol, 2023. **11**: p. 1125077.
144. Volinia, S., et al., *A microRNA expression signature of human solid tumors defines cancer gene targets*. Proc Natl Acad Sci U S A, 2006. **103**(7): p. 2257-61.
145. Gaur, A.B., et al., *Downregulation of Pcd4 by mir-21 facilitates glioblastoma proliferation in vivo*. Neuro Oncol, 2011. **13**(6): p. 580-90.
146. Dong, J., et al., *Bcl-2 upregulation induced by miR-21 via a direct interaction is associated with apoptosis and chemoresistance in MIA PaCa-2 pancreatic cancer cells*. Arch Med Res, 2011. **42**(1): p. 8-14.
147. Yan, L.X., et al., *Knockdown of miR-21 in human breast cancer cell lines inhibits proliferation, in vitro migration and in vivo tumor growth*. Breast Cancer Res, 2011. **13**(1): p. R2.
148. Kong, W., et al., *Upregulation of miRNA-155 promotes tumour angiogenesis by targeting VHL and is associated with poor prognosis and triple-negative breast cancer*. Oncogene, 2014. **33**(6): p. 679-89.
149. Kandell, W.M., et al., *MicroRNA-155 governs SHIP-1 expression and localization in NK cells and regulates subsequent infiltration into murine AT3 mammary carcinoma*. PLoS One, 2020. **15**(2): p. e0225820.
150. Jin, H.M., et al., *MicroRNA-155 as a proinflammatory regulator via SHIP-1 down-regulation in acute gouty arthritis*. Arthritis Res Ther, 2014. **16**(2): p. R88.
151. Bayraktar, R. and K. Van Roosbroeck, *miR-155 in cancer drug resistance and as target for miRNA-based therapeutics*. Cancer Metastasis Rev, 2018. **37**(1): p. 33-44.
152. Chirshhev, E., et al., *Let-7 as biomarker, prognostic indicator, and therapy for precision medicine in cancer*. Clin Transl Med, 2019. **8**(1): p. 24.
153. Calin, G.A., et al., *MiR-15a and miR-16-1 cluster functions in human leukemia*. Proc Natl Acad Sci U S A, 2008. **105**(13): p. 5166-71.
154. Shen, J., et al., *miR-15b and miR-16 induce the apoptosis of rat activated pancreatic stellate cells by targeting Bcl-2 in vitro*. Pancreatology, 2012. **12**(2): p. 91-9.
155. Hou, Z., et al., *MicroRNA-146a is down-regulated in gastric cancer and regulates cell proliferation and apoptosis*. Med Oncol, 2012. **29**(2): p. 886-92.
156. Fernandez, S., et al., *miR-340 inhibits tumor cell proliferation and induces apoptosis by targeting multiple negative regulators of p27 in non-small cell lung cancer*. Oncogene, 2015. **34**(25): p. 3240-50.
157. Wu, Z.-s., et al., *miR-340 inhibition of breast cancer cell migration and invasion through targeting of oncoprotein c-Met*. Cancer, 2011. **117**(13): p. 2842-2852.
158. Peng, X., et al., *The interplay between HIF-1alpha and noncoding RNAs in cancer*. J Exp Clin Cancer Res, 2020. **39**(1): p. 27.
159. Kulshreshtha, R., et al., *A microRNA signature of hypoxia*. Mol Cell Biol, 2007. **27**(5): p. 1859-67.
160. Nallamshetty, S., S.Y. Chan, and J. Loscalzo, *Hypoxia: a master regulator of microRNA biogenesis and activity*. Free Radic Biol Med, 2013. **64**: p. 20-30.
161. McCormick, R.I., et al., *miR-210 is a target of hypoxia-inducible factors 1 and 2 in renal cancer, regulates ISCU and correlates with good prognosis*. Br J Cancer, 2013. **108**(5): p. 1133-42.
162. Hermeking, H., *The miR-34 family in cancer and apoptosis*. Cell Death Differ, 2010. **17**(2): p. 193-9.
163. Kim, T., et al., *p53 regulates epithelial-mesenchymal transition through microRNAs targeting ZEB1 and ZEB2*. J Exp Med, 2011. **208**(5): p. 875-83.

164. Caruso, P., et al., *Dynamic changes in lung microRNA profiles during the development of pulmonary hypertension due to chronic hypoxia and monocrotaline*. *Arterioscler Thromb Vasc Biol*, 2010. **30**(4): p. 716-23.
 165. Rupaimoole, R., et al., *Hypoxia-mediated downregulation of miRNA biogenesis promotes tumour progression*. *Nat Commun*, 2014. **5**: p. 5202.
 166. Wu, C., et al., *Hypoxia potentiates microRNA-mediated gene silencing through posttranslational modification of Argonaute2*. *Mol Cell Biol*, 2011. **31**(23): p. 4760-74.
 167. Li, W., et al., *Regulation of PTEN expression by noncoding RNAs*. *J Exp Clin Cancer Res*, 2018. **37**(1): p. 223.
 168. Ding, S., et al., *MiR-21/PTEN signaling modulates the chemo-sensitivity to 5-fluorouracil in human lung adenocarcinoma A549 cells*. *Int J Clin Exp Pathol*, 2019. **12**(6): p. 2339-2352.
 169. Lou, Y., et al., *MicroRNA-21 promotes the cell proliferation, invasion and migration abilities in ovarian epithelial carcinomas through inhibiting the expression of PTEN protein*. *Int J Mol Med*, 2010. **26**(6): p. 819-27.
 170. Yang, Y., J.X. Guo, and Z.Q. Shao, *miR-21 targets and inhibits tumor suppressor gene PTEN to promote prostate cancer cell proliferation and invasion: An experimental study*. *Asian Pac J Trop Med*, 2017. **10**(1): p. 87-91.
 171. Cao, L.Q., et al., *Exosomal miR-21 regulates the TETs/PTENp1/PTEN pathway to promote hepatocellular carcinoma growth*. *Mol Cancer*, 2019. **18**(1): p. 148.
 172. Li, J., et al., *miR-221 Promotes Epithelial-Mesenchymal Transition through Targeting PTEN and Forms a Positive Feedback Loop with beta-catenin/c-Jun Signaling Pathway in Extra-Hepatic Cholangiocarcinoma*. *PLoS One*, 2015. **10**(10): p. e0141168.
 173. Wei, H., et al., *miR-130a Deregulates PTEN and Stimulates Tumor Growth*. *Cancer Res*, 2017. **77**(22): p. 6168-6178.
 174. Egawa, H., et al., *The miR-130 family promotes cell migration and invasion in bladder cancer through FAK and Akt phosphorylation by regulating PTEN*. *Sci Rep*, 2016. **6**: p. 20574.
 175. Ye, L., et al., *MiR-130 exerts tumor suppressive function on the tumorigenesis of human non-small cell lung cancer by targeting PTEN*. *Am J Transl Res*, 2017. **9**(4): p. 1856-1865.
 176. Tian, F., et al., *Upregulation of microrna-451 increases the sensitivity of A549 cells to radiotherapy through enhancement of apoptosis*. *Thorac Cancer*, 2016. **7**(2): p. 226-31.
 177. Ghafouri-Fard, S., et al., *Regulatory role of microRNAs on PTEN signaling*. *Biomed Pharmacother*, 2021. **133**: p. 110986.
 178. Dart, D.A., P. Uysal-Onganer, and W.G. Jiang, *Prostate-specific PTen deletion in mice activates inflammatory microRNA expression pathways in the epithelium early in hyperplasia development*. *Oncogenesis*, 2017. **6**(12): p. 400.
-